A loss-of-function approach to investigate the role of cholesterol in prion replication

A thesis submitted in partial fulfilment for the degree of

Doctor of Philosophy to University College London

by

Billy West

MSci (Hons) University of Nottingham

Declaration

I, Billy West, confirm that the work presented in this thesis is my own. Where information has been derived from other sources, I confirm that this has been indicated in the thesis.

Acknowledgements

Although this thesis only has my name at the front the truth is a hell of a lot of people helped me get everything together so I could get my PhD. My supervisors Peter Klöhn and Parmjit Jat have been invaluable over the past 4 years in helping shape my research and develop my scientific skills. Elsewhere in the Klöhn lab Anna Harvey was instrumental in helping me adjust to working in molecular biology, whilst my fellow PhD students Masue Marbiah and Lucy Sheytanova have quite simply been fantastic to work alongside.

A great part of my life whilst working towards my PhD has been spent in the company of the students and staff of the Institute of Neurology. In particular (but no particular order) I want to thank Mike F, Luci D, Xun C, Charlotte R, Matt R, Laura P, Dan W, Sav B, Jamie R, Rabea B, Toby C, Olivia S, Chris M, Steph C, Andy T, Rosie B-S, Justin T, Jess S, Adam W, Rachele S and Craig B for generally being awesome and making my time here pretty damn fun. For those of us in the student room who were playing our little game, my word was 'diddle' and it's been awkwardly shoehorned in on page 133.

No thesis acknowledgements section would be complete without thanking family and this one is no different. So thanks to Mum, Dad, Ro and J for supporting me whilst I've been working towards this and pretending to be interested/understand what I'm talking about when I've sometimes brought my work on holiday with me.

Automation of the Scrapie Cell Assay has allowed me to screen so many treatments for effects on prion propagation. Thanks are due to the Robot team (past and present) at the MRC prion unit, with particular note going to Christian Schmidt who has headed the team during my time here and proved to be a valuable ally. Filipin labelling played a key part in confirming the effects of several genes in this study. Michael Duchen kindly allowed us to use his microscope to visualise filipin as other microscopes available to us did not have the required laser lines required for excitation. An exciting model for some of my later

experiments was primary neurons. I would like to thank Silvia Purro for providing me with viable preparations of mouse cortical neurons which gave me a reliable source of samples when I was rushed trying to collect the final data for my thesis.

- ***Randall Munroe, XKCD***

Abstract

Prions, the infectious agents of prion diseases, are abnormal conformational variants of the host-encoded prion protein (PrP^C) and are thought to replicate by template-directed conversion of native PrP^C. There are multiple prion strains thought to arise from different conformations of PrP; of particular interest to this thesis different prion strains are differently able to propagate in cultured cell lines.

This PhD focused on two main projects. Firstly, as PrP^C segregates into cholesterol-rich rafts at the plasma membrane, the question arises whether cholesterol affects the conversion of PrP^C to prions. Using transcriptional gene silencing we investigated whether downregulation of genes with a role in biosynthesis and trafficking of cholesterol affect the rate of prion replication. Silencing of *Hmgcr* and *Dhcr24*, two genes that encode for enzymes of cholesterol biosynthesis, reduced the total cholesterol levels by about 50% whilst increasing PrP conversion rates by two-fold, suggesting an inhibitory role of cholesterol.

Interestingly, perturbation of cholesterol trafficking by knockdown of *Npc1* and *Npc2,* which causes accumulation of cholesterol in late endosomes/lysosomes, led to diametrically opposing effects on prion conversion. Silencing of *Npc1* in N_2a cells decreased, while *Npc2* loss of function increased, conversion rates. Notably, *Npc1* knockdown led to a dramatic loss of surface PrP^C expression, a phenotype that was absent upon *Npc2* silencing, suggesting that the *Npc1*-associated decrease in conversion rates is cholesterol-independent and accounted for by decreased PrP^C, the substrate for conversion.

A secondary project focused on identifying cellular factors underlying selective propagation of prion strains. We subcloned the CAD5 cell line, susceptible to both RML and 22L prion strains, and showed selective prion strain propagation in a small number of isolated clones.

Selective propagation could not be stably obtained and this project was halted in favour of further investigation into the role of cholesterol in prion replication.

Table of Contents

List of Tables and Figures

List of Acronyms and Abbreviations

ABCA1	ATP-Binding Cassette Transporter A1
ACAT	Acetyl-CoA acetyl transferase
Acetyl CoA	Acetyl coenzyme A
AP	Alkaline Phosphatase
ApoA1	Apolipoprotein A1
ApoE	Apolipoprotein E
ApoER2	Apolipoprotein E Receptor 2 (see LRP8)
APP	Amyloid Precursor Protein
Arf6	Adenosine diphosphate-ribolysation factor 6
ATP	Adenosine Triphosphate
Aβ	Amyloid beta
BGS	Bovine Growth Serum
BODIPY	boron dipyrromethene difluoride
CAD5	Murine Catecholaminergic Neuroblastoma cells
CD1	Inbred laboratory mouse strain
CD81	Cluster of differentiation 81
cDNA	Complementary DNA
CJD	Creutzfeldt-Jakob Disease
CMII	Conditioned Medium II for primary murine cultures
CNS	Central Nervous System
CtxB	Cholera toxin beta subunit
CtxB-555	Alexa-Fluor 555 conjugated CtxB
CtxB-b	Biotinylated CtxB
CYP46A1	cytochrome P450, family 46, subfamily A, polypeptide 1
DAPI	4',6-diamidino-2-phenylindole
Dhcr24	3β-hydroxysteroid-Δ24 reductase

DICER	endoribonuclease Dicer
DIV	Days in vitro
DMEM	Dublecco's Modified Medium Eagle
DMSO	Dimethyl sulfoxide
DNA	Deoxyribonucleic Acid
dNTPs	deoxyribonucleoside triphosphates
DRM	Detergent Resistant Membrane Domain
DsiRNA	DICER-substrate short interfering RNA
ECM	Extracellular Matrix
EDTA	ethylene diamine tetra-acetic acid
EGFR	Epidermal Growth Factor Receptor
Elispot	Enzyme Linked Immunospot Assay
ER	Endoplasmic Reticulum
FAM	6-carboxyfluorescein
FB1	Fumonisin B1
FBS	Foetal Bovine Serum
FD	Fold Difference
g	Acceleration due to gravity
GM1	Glycosphingolipid ganglioside
GPI	glycosylphosphatidylinositol
GSS	Gerstmann-Sträussler-Scheinker
GTC	Guanidine Thiocyanate
GWAS	Genome Wide Association Study
HDL	High Density Lipoprotein
HEPES	4-(2-hydroxyethyl)-1-piperazineethanesulfonic acid
HMG-CoA	3-hydroxy-3-methylglutaryl CoA
Hmgcr	3-hydroxy-3-methylglutaryl CoA reductase

HRP	Horse Radish Peroxidase
HSPG	Heparan Sulfate Proteoglycan
iS7	RML-infected S7 cells
kDa	kiloDalton
Lamp1	Lysosome associated membrane protein 1
LD9	Murine fibroblast cells
LDS	Lipoprotein Deficient Serum
LIPA	Gene encoding lysosomal acid lipase
LRP	Low density lipoprotein receptor related protein
LRRK2	Leucine rich repeat kinase 2
LXR	Liver X receptor
MEME	Modified Essential Medium Eagle
MRC	Medical Research Council
MSC	Microbiological Safety Cabinet
MβCD	Methyl beta cyclodextrin
N2a	Murine Neuroblastoma 2a cells
Npc1	Niemann-Pick type C gene 1
Npc2	Niemann-Pick type C gene 2
OBGS	OptiMEM supplemented 10% BGS + 1% PenStrep
OFCS	OptiMEM supplemented 10% FBS + 1% PenStrep
PBS	Phosphate Buffered Saline
PBST	Phosphate Buffered Saline with Tween
PCR	Polymerase Chain Reaction
PDMP	1-phenyl-2-(decanoyl-amino)-3-morpholino-1-propanol
PE	phosphatidylethanolamine
PFA	Paraformaldehyde
PIPLC	phosphatidylinositol specific phospholipase C

PK	Proteinase K
PK1	N2a cell prion susceptible subclone
PMCA	Protein Misfolding Cyclic Amplification
Prnp	Prion protein gene
PrP	Prion Protein
PrP^{27-30}	Protease-resistant core of PrP^{Sc}
PrP^{C}	Cellular Prion Protein
PrP^{d}	Disease-associated deposits of PrP
PrP^{Sc}	Scrapie (disease isoform, PK resistant) Prion Protein
PVDF	Polyvinylidene fluoride
qPCR	Quantitative PCR
R33	N2a prion resistant subclone 33 cells
RI	Response Index
RML	Rocky Mountain Laboratory prion strain
RNA	Ribonucleic acid
rpm	Revolutions per minute
RT	Reverse Transcription
S7	N2a-PK1 prion susceptible subclone 7 cells
SCA	Scrapie Cell Assay
sCJD	Sporadic Creutzfeldt-Jakob Disease
ScN2a	Scrapie infected N2a cells
SDS	sodium dodecyl sulphate
SDS-PAGE	sodium dodecyl sulphate polyacrylamide gel electrophoresis
SH-SY5Y	Human Neuroblastoma cells
Srepb2	Sterol Regulatory Element-Binding Protein 2
SS	Selectivity Score
TBST	Tris-buffered saline with Tween

TE	Tris-EDTA
TGN	Trans-Golgi Network
TNET	Tris-EDTA Sodium chloride and TX100 buffer
TSE	Transmissible Spongiform Encephalopathy
TX100	Triton X-100
UCL	University College London
UV	Ultraviolet
v/v	Volume per volume
vCJD	Variant Creutzfeldt-Jakob Disease
w/v	Weight per volume
WHO	World Health Organisation
ZEN-IBFQ	ZEN-Iowa Black Fluorescence Quencher
βCD	Beta cyclodextrin

CHAPTER 1 INTRODUCTION

1.1 Prion disease

Transmissible Spongiform Encephalopathies (TSEs), also known as prion diseases, are invariably fatal neurodegenerative diseases which are known to affect (among others) humans, cattle and mice. Prion diseases present long disease incubation times followed by rapid neurodegeneration (Collinge, 2005), and are often identified post-mortem by characteristic deposition of misfolded prion protein in brain and other tissues including spleen and lymph nodes (Kimberlin and Walker, 1979, 1989, Ramasamy et al., 2003). Clinically prion diseases typically present with ataxia, dementia and psychiatric disorders such as depression (Collinge, 2001), while both human and animal disease pathology includes spongiform change, neuronal loss, astrocytosis, and amyloid plaque formation (Jeffrey et al, 1995). Prion diseases such as Creutzfeldt-Jakob disease (CJD) and Gerstmann-Sträussler-Scheinker (GSS) can be inherited (Brown et al., 1991, Hsiao et al., 1991, Collinge et al., 1993) while other forms of prion diseases such as variant CJD (vCJD) can be spread by transfer of infectious prion protein (Hill et al., 1997, Weber and Aguzzi, 1997). Prion diseases were first identified in sheep and goats as Scrapie in 1732 (Plummer, 1946) and rose to prominence in the 1990s with the outbreak of Bovine Spongiform Encephalopathy (BSE) in European cattle. The BSE crisis notably demonstrated the potential for cross species transmission of prions with BSE, itself thought to be derived from sheep Scrapie prions (Hope et al, 1989), causing variant CJD (vCJD) in infected humans (Hill et al, 1997). Although the spread of BSE was effectively halted by mass culls of cattle the after effects of the crisis are still felt today, the USA for example still prohibits blood donation from people resident in the UK for 6 months or more between 1980 and 1996 (FDA recommendation, 1999). In recent history the increased incidence of chronic wasting disease (CWD) in cervids has driven a large part of prion disease research in North America (Robinson et al, 2012, Saunders et al, 2012, Davenport et al, 2015).

Sporadic Creutzfeldt-Jakob disease (sCJD) now accounts for the majority of human prion disease cases occurring at a rate of 1 person per million per year (WHO Surveillance Data). Recent findings suggest sub-clinical cases of vCJD in the UK may occur at a much higher rate of 1:2000 as a result of the outbreak of BSE in the 1990s (Gill et al., 2013). Inherited prion diseases have similarly rare incidences, with GSS thought to affect less than 2 in 100 million people per year while fatal familial insomnia (FFI) is rarer still (Ghetti et al, 1995). Both FFI and familial CJD include a mutation in codon 178 of *PRNP* which substitutes asparagine for aspartic acid, but can be differentiated genetically by the presence of methionine at codon 129 in FFI patients and valine in those with familial CJD (Gambetti et al, 2003). The causative mutation in GSS is thought to be a proline to leucine substitution at codon 102 which has been found in the majority of GSS cases (Hsaio et al, 1989). The MRC Prion Unit has devoted considerable resources to characterising Kuru in the indigenous tribes of Papua New Guinea, a form of prion disease thought to be spread by ritual consumption of family members as part of funeral rites (Liberski et al, 2012).

1.1.1 The Prion protein

The Prion protein (PrP) is a 231 amino acid protein of indeterminate function encoded by *PRNP* in humans (*Prnp* in mice) (Oesch et al., 1985, Hornemann et al., 1997, Yusa et al., 2012) and incorporated into detergent resistant domains (DRMs, also known as lipid rafts) in the cell membrane by virtue of its C-terminal glycosylphosphatidylinositol (GPI) anchor (Stahl et al., 1987, Baron and Caughey, 2003). PrP contains two glycosylation sites at residues Asn 181 and Asn 197 (human numbering) and as such can exist as un-, mono- and di-glycosylated forms (Ermonval et al., 2003). The prion protein is synthesised in the Endoplasmic Reticulum (Atkinson, 2004) and undergoes several post-translational modifications, including addition of N-linked oligosaccharide chains, the formation of a disulphide bond and the attachment to the GPI anchor (Taylor and Hooper, 2006), before the mature protein is expressed on the cell surface in lipid rafts. The cellular form of the prion protein is termed PrP^C and is required

for prion replication (Oesch et al., 1985, Prusiner et al., 1987). PrP^{C} contains three α-helices and a two-strand antiparallel β-sheet, whilst the disease associated isoform, PrP^{Sc}, incorporates a greater proportion of β-sheet in its secondary structure (Pan et al, 1993). The second and third helices of PrP^{C} contain a disulphide bond between residues Cys179 and Cys214 (Linden et al, 2008). The folded protein contains a central hydrophobic region between residues 106-126 and work by Jobling and colleagues using a clone incorporating this region suggest the core is involved in the toxicity of PrP^{Sc} (Jobling et al, 1999). The unstructured N-terminus of PrP includes 5 octapeptide repeats of sequence PHGGGWGQ which confer metal binding ability, thus far demonstrated for copper, zinc, manganese and nickel (Prcina et al, 2015). A schematic of the prion protein is shown in **Figure 1.1**.

Figure 1.1 A schematic of key regions of interest in the prion protein

The Prion protein (PrP) is a 231 amino acid protein of indeterminate function encoded by PRNP in humans. The N-terminal end of PrP is unstructured and contains a signal peptide (black) and a series of 5 octapeptide tandem repeats between residues 51 and 90 (sequence PHGGGWGQ, orange). In the structure region of PrP residues 106-126 form a hydrophobic core (purple) while the remainder of the structure includes three α-helices (green). A two-strand anti-parallel β-sheet (blue) is formed either side of the first helix, while the second and third helices are linked by a disulphide bond between Cys residues 179 and 214. PrP can by glycosylated at residues 181 and 197 (red) and is modified to include a C-terminal GPI-anchor (dark blue) which incorporates the mature protein in lipid rafts.

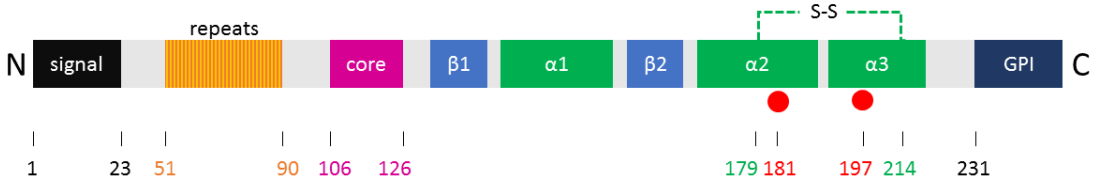

Host-encoded PrP^C exerts an as yet unknown physiological function in cells and indeed may be multi-functional (Passet et al., 2013, Onodera et al., 2014). Growing evidence suggests that PrP may function in cell signalling and maintenance of synaptic junctions (Re et al., 2006). Several studies support a function of PrP in homeostasis of metals including iron (Singh et al., 2013), zinc (Watt et al., 2012) and copper (Zhou and Millhauser, 2012). Binding of copper ions causes rapid internalisation of PrP^C in neuronal cells (Pauly and Harris, 1998, Haigh et al., 2005). It is possible that disrupted metal balance following prion infection could underlie toxicity in prion disease (Kawahara et al., 2011). Recently PrP has been implicated in Alzheimer's disease (Nygaard and Strittmatter, 2009) and may in part contribute to neuronal death through excitotoxicity (Thellung et al., 2013).

Work by several groups suggests that PrP is a ligand for the low density lipoprotein receptor-related protein LRP1. LRP1 is known to act as a receptor for Apolipoprotein E (ApoE) (Liu et al., 2007) which implies a role for PrP in regulation of lipid import. LRP1 is required for clathrin-mediated endocytosis of PrP^C (Taylor and Hooper, 2007) and functions to anchor PrP^C to clathrin coated pits following departure from lipid rafts (Hooper et al., 2008). Moreover work by Roger Morris and colleagues has demonstrated that LRP1 expression is required for recycling of PrP^C back to neuronal membranes (Parkyn et al., 2008), while work by Taylor and colleagues indicates LRP1 is required for copper ion-mediated endocytosis of PrP^C (Taylor and Hooper, 2007). Further work in the Morris group has shown a requirement of LRP1 for internalisation of PrP^{Sc}, albeit with altered intracellular trafficking as PrP^{Sc} is directed towards lysosomes in place of recycling to the cell surface (Jen et al., 2010).

1.1.2 The protein-only hypothesis

The protein only hypothesis was first proposed by Griffith in 1967 and later refined by Prusiner and colleagues (Griffith, 1967, Prusiner, 1982). According to the widely accepted protein only hypothesis prions, the infectious agents of prion diseases, consist solely of

misfolded prion protein. PrP^{Sc} multiplies by catalysing the conversion of PrP^{C} into a copy of the PrP^{Sc} conformer (Weissmann and Bueler, 2004). As a result of this conversion the predominantly alpha-helical PrP^{C} undergoes a conformational change to PrP^{Sc} and incorporates a higher proportion of beta sheet into its secondary structure (Pan et al., 1993, Huang et al., 2013). PrP^{C} is protease sensitive whilst PrP^{Sc} is proteinase K (PK) resistant which allows for experimental differentiation between PrP^{C} and PrP^{Sc} (Borchelt et al., 1990, Caughey and Raymond, 1991). Due to differences in glycosylation PK-digested PrP^{Sc} displays distinct migration patterns when run through gel electrophoresis.

Following the discovery that a 27-30 kDa protease resistant core of PrP^{Sc}, termed $PrP^{27\text{-}30}$, was the infectious agent in Hamster scrapie (Oesch et al., 1985) Charles Weissmann and others later showed that PrP^{Sc} was encoded by a host gene named *Prnp* (Basler et al., 1986, Kretzschmar et al., 1986). Ablation of *Prnp* has been shown to prevent prion disease (Bueler et al., 1993) however the expression of *Prnp* is not sufficient to cause prion disease without the introduction of PrP^{Sc} unless the expressed gene contains mutations associated with spontaneous prion generation (Hsiao et al., 1990). Expression of hamster *Prnp* in *Prnp*-knockout mice, which are resistant to infection with mouse prions, has been shown to be sufficient for propagation of hamster prions following inoculation with infected hamster brain homogenate (Bueler et al., 1993). Furthermore, depletion of PrP^{C} in mice following prion infection reduces both toxicity and spread of prion disease (G et al., 2003).

More recent investigations using cell free conversion assays suggest prion replication is promoted by cofactors such as polyanions (Deleault et al, 2003) and lipids (Baron and Caughey, 2003, Deleault et al 2005). Although not a requirement for prion conversion (Baron and Caughey, 2003, Lewis et al., 2006, Raymond et al., 2012) the GPI anchor is found in both PrP^{C} and PrP^{Sc} and is sensitive to cleavage by phosphatidylinositol specific phospholipase C (PIPLC) (Stahl et al., 1987). It is possible that GPI-anchoring increases the proximity of PrP^{C}

and PrP^{Sc} in lipid rafts, an idea discussed in greater detail in section 1.2.2 below. Notably, although recombinant prions formed in the absence of mammalian cofactors remained infectious, inclusion of RNA and lipids in cell free conversion assays greatly increased the infectivity of prions produced (Deleault et al, 2007, Wang et al, 2010). It is possible that detergents used to extract prion seeds could form an interface similar to lipid rafts in cofactor-free assays, and remarkably recombinant prion fibrils produced using detergent-free methods are insufficient to cause disease in animals (Ma, 2012).

1.1.3 Prion strains

Whilst all prions are infectious they can be divided into strains which can be characterised by distinct disease incubation times and pattern of brain lesions and deposition of abnormal PrP (Fraser and Dickinson, 1973, Bruce, 1993). Prion strains can be further characterised by differences in the migration of the protease-resistant protein on Western blots which varies according to the degree of glycosylation of the strain (Collinge et al., 1996). Prion strains can be stably passaged *in vivo* (Bruce, 1993) which has allowed for relatively high scale production of mouse brain homogenates infected with prion strains such as RML. Differences between prion strains do not appear to be due to differences in amino acid sequence as multiple strains can be propagated on the same form of PrP^{C} (Hope et al., 1986, Collinge and Clarke, 2007). Differences between strains may be determined by the conformation of PrP^{Sc}, and studies in [PS1+] yeast prions have demonstrated different strain properties of different conformers (Tanaka et al., 2006). Prions strains have been suggested to be quasispecies of different conformational variants of PrP (Collinge, 2010), and it is thought that a dominant subspecies within each strain may give rise to the characteristic differences between prion strains (Peretz et al., 2001). Prion strains have shown changes in strain characteristics when propagated in different cell and tissue types (Li et al., 2010) which may follow adaptation as

a recessive conformer outcompetes the dominant conformer in a new environment (Mahal et al., 2010). These adaptations are discussed in greater detail below.

1.1.2 (a) The species barrier

Differences in the primary structure of PrP between different species are thought to contribute to a 'species barrier' which limits transmission of prions between species. It is likely that differences in conformation of PrP between species also contribute to the species barrier. Zoonotic transmission of prion disease still occurs as seen in the spread of vCJD from BSE-infected beef in 1990s Britain (Hill et al., 1997) and it is possible for prion strains to overcome the species barrier experimentally (Nakamura et al., 2000, Shi et al., 2012). Given the Quasispecies hypothesis, which states that prion strains contain a pool of PrP^{Sc} conformers, it is possible that breaches in the species barrier are due to conformers which are replication-competent with similar PrP primary structures (Hagiwara et al., 2013). This theory predicts that different prion strains may spread more readily across species due to the presence of different PrP^{Sc} conformers.

1.1.2 (b) Selective propagation of prion strains in vitro

There is a marked discrepancy between susceptibility to different prion strains in *in vivo* and *in vitro* models. Whilst many prion strains of a given species can be propagated in rodents, like mice or bank voles (Bruce, 1993, Watts et al., 2014), cultured cells often propagate prion strains selectively (Mahal et al., 2007, Li et al., 2010). Previous work in our group has shown that some cell lines are heterogeneous with regard to strain selectivity and prion replication, with subcloning of N2a cells yielding both highly susceptible and prion resistant subclones (Klohn et al., 2003). We have recently reported that genes involved in extracellular matrix (ECM) remodelling regulate susceptibility to prion replication (Marbiah et al., 2014) in these cells and it is possible that cellular factors may also underlie susceptibility to different prion strains.

Some cell lines propagate prion strains promiscuously, although at different rates (Mahal et al., 2007). Interestingly, the work of Mahal and colleagues also demonstrated that prion strains which are readily propagated in one cell line may not be replicated in a different cell line, irrespective of its general susceptibility to other prion strains. This suggests that cellular factors not only determine the susceptibility to prion infection, but also to prion strains. One potential explanation for this in light of the quasispecies theory of prion strains is that different cellular factors alter or interact with conformational variants of PrP^C, which could limit their ability to replicate.

1.1.2 (c) Darwinian strain selection

An elegant study by Charles Weissmann and colleagues (Li et al., 2010) provided experimental evidence for adaptations within a prion strain passaged in both mouse brain and immortalised cells. A 'cell-adapted' form of the initial prion strain outcompeted its 'brain-adapted' counterpart when tested in cultured cells, whilst the opposite was true when the same strains were used to infect mouse brain. Remarkably, by applying selection pressure by incubating cells with the glycosylation inhibitor swainsonine in a separate experiment, the researchers were able to isolate a resistant sub-strain which altered the characteristics of the prion strain. Swainsonine-resistant prions were outcompeted by swainsonine-susceptible species in the absence of the drug, which suggests prion strains are capable of adapting to environmental pressure. Working in the Weissmann lab Mahal et al (2010) contributed to this work, showing that isolated clones of prion-infected R33 cells yielded prion strains with altered characteristics. In the same study the authors also demonstrated that differentially adapted prion strains exhibited different conformational stabilities of PK-resistant PrP similar to the work of Peretz et al (2001), who showed that different prion strains were differentially susceptible to denaturation by guanidine. These experiments lend evidence to the theory that prion strains exist as quasispecies, containing a mix of various PrP conformers of which one or more are dominant and confer the strain

characteristics (Collinge, 2010). In response to environmental pressure it is possible that a non-dominant conformer is able to replicate faster and out-compete the dominant conformer thus changing the strain characteristics. There is also evidence for competition between stable prion strains. Work by Kimberlin and Walker has demonstrated that the 22A prion strain blocks infection of the 22C strain (Kimberlin and Walker, 1985). This effect was prevented by denaturing 22A with urea, suggesting that an infectious blocking strain is required to limit propagation of a second prion strain. It is possible that established infection with 22A prions, which were inoculated into mice 105 days prior to 22C, converted PrP^{C} more efficiently that 22C and so depleted potential substrate for 22C propagation. A hypothetical example of quasispecies selection and prion strain selection is shown in **Figure 1.2** (reproduced from Collinge, 2010).

Although the species barrier which prevents zoonotic transmission of prions is largely thought to be due to differences in the primary structure of PrP between species (Vanik et al., 2004, Kurt et al., 2015) strain adaptation, and by extension selection of prion quasispecies, may help to explain why species barriers are occasionally breached. In particular some PrP^{Sc} conformations may be more readily able to convert on a variety of host species than other strains due to a favourable conformation for replication (Torres et al., 2014). Prion strains which have been adapted to other species show increased infectivity following multiple passages (Plinston et al., 2011) suggesting that the prion strain adapts to propagate more efficiently in a new host species.

Figure 1.2 Prion strain selection and mutation due to environmental pressure (reproduced from Collinge, 2010)

A *A prion strain may contain multiple PrP^{Sc} conformers. A given prion strain may be readily transmitted between host species which express similar conformations of PrP^{C} such as species I and II. Transmission barriers may arise when there is no overlap between PrP conformations such as with species I and III.* ***B*** *Host factors maintain selection pressure on prion strains. Transmission within a species expressing the same PrP^{C} conformers maintains strain characteristics (a) whilst the availability of different PrP conformations in the same or different species may alter strain characteristics (b, c). Barriers to transmission arise between different species which express different PrP conformers (d) although these can be overcome with mutation.*

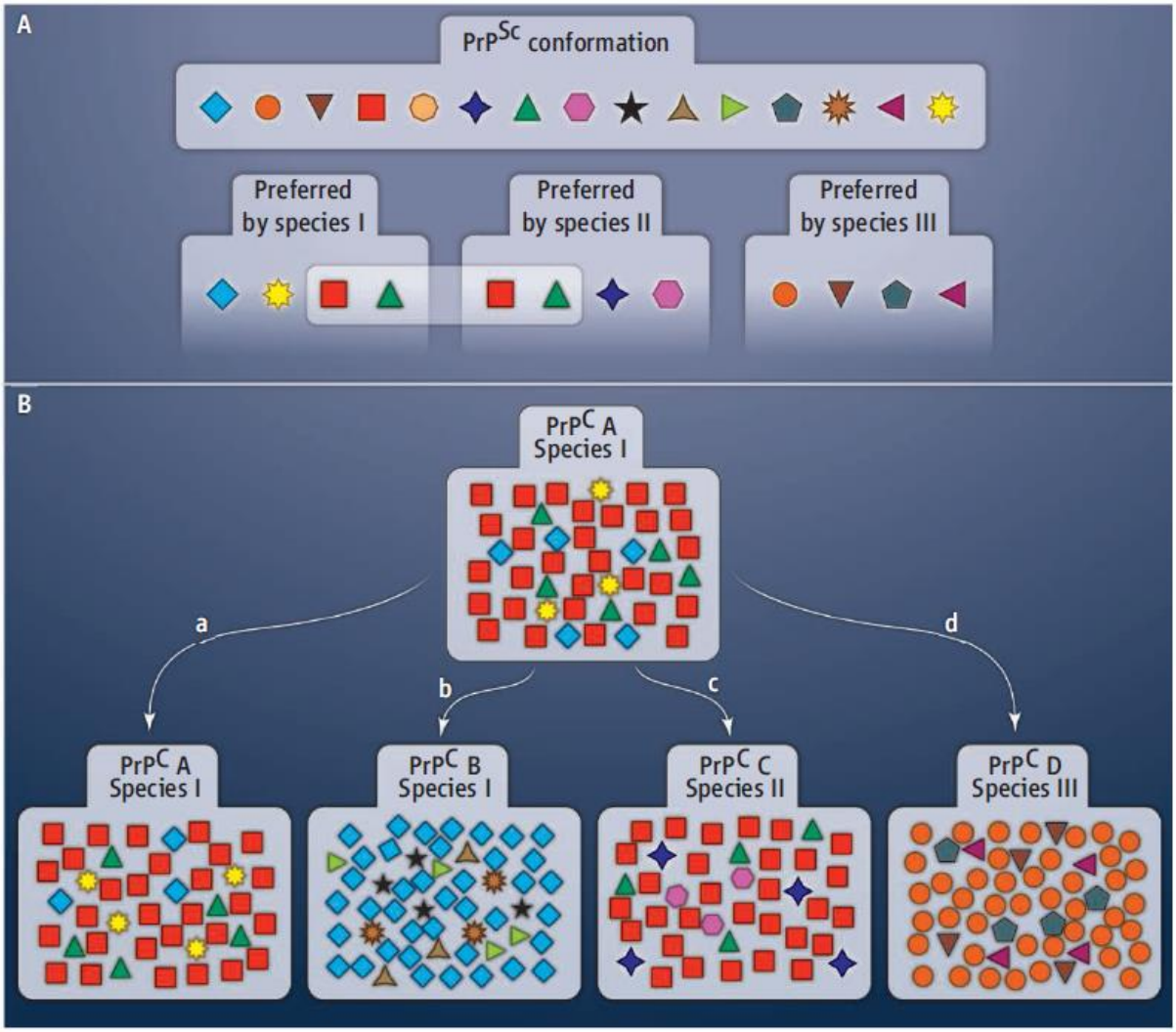

1.1.4 PrP^{Sc} as a marker of infectivity

PrP^{Sc} has been widely accepted as a biomarker of prion infection (Oesch et al., 1985, Caughey and Raymond, 1991) but there is uncertainty regarding prion toxicity with some suggesting that an unknown toxic species causes neuronal death in prion disease (Ashe and Aguzzi, 2013). Some infectious prions remain sensitive to PK (Tzaban et al., 2002) which may be due to altered stability of different PrP conformers in prion strains. Ongoing work in the MRC Prion Unit indicates that prions themselves are not the toxic species but instead induce the formation of toxic species (Sandberg et al., 2011).

In this thesis PK-resistant PrP^{Sc} is used as a measure of prion propagation. This definition follows the biochemical definition of the infectious agent of prion disease outlined by the Protein-Only hypothesis (Oesch et al., 1985). This definition is key to our chosen means of determining prion propagation in cells: the Scrapie Cell Assay (SCA). The endpoint of the SCA is the Elispot assay which determines the number of PrP^{Sc}-positive cells in a given sample by PK-digestion of PVDF membrane-bound cells followed by detection of PK-resistant PrP by immunohistochemistry (Klohn et al., 2003).

1.1.5 PrP^{C} trafficking

The prion protein is not wholly resident in the plasma membrane, and it has been suggested that prion conversion occurs during intracellular trafficking of PrP^{C}. Both PrP^{C} and PrP^{Sc} leave lipid rafts prior to internalisation, however the mechanism of internalisation remains unclear. Internalisation of PrP through caveolae has been shown in Chinese hamster ovary cells (Vey *et al.*, 1996; Peters *et al.*, 2003), whereas immunogold detection suggests internalisation through clathrin-coated pits in neuronal cells (Shyng *et al.*, 1994; Shyng *et al.*, 1995; Sunyach *et al.*, 2003). When trafficked internally PrP is initially present in early endosomes, before being sorted for recycling in the endosomal recycling compartment (ERC)

or redirected to lysosomes for degradation (Maxfield and Mcgraw, 2004, Jen et al., 2010). PrP^{C} trafficked in endosomes is recycled to lipid rafts in the plasma membrane (Morris et al., 2006). Work by Chiara Zurzolo and colleagues suggests cholesterol may partially determine the degree to which PrP is recycled – in normal function the majority of PrP was recycled to the cholesterol-rich ERC, however treatment with 4- hydroxytamoxifen to induce cholesterol accumulation in late endosomes increased trafficking of PrP^{Sc} to lysosomes (Browman and Zurzolo, 2013). Kinetic studies indicate fairly rapid turnover of PrP^{C} with a half-life of less than 5 hours in neuronal cell membranes (Caughey et al., 1989, Borchelt et al., 1990). Recycling of PrP^{C} from lipid rafts and through endosomes is summarised in **Figure 1.3**. There is some evidence that the endosomal/lysosomal compartment is the site of conversion of PrP^{C} to PrP^{Sc} (Borchelt et al., 1992, Marijanovic et al., 2009, Yim et al., 2015). Multiple cell-free assays demonstrate that acidic environments are required for formation of PrP^{Sc} (Kocisko et al., 1995, Alonso et al., 2001, Qi et al., 2012). Notably a recent study suggests that the low pH in lysosomes facilitates fibrilisation of misfolded PrP (Qi et al., 2012). In 1992 Laszlo et al showed accumulation of high levels of PrP^{Sc} in lysosomes and suggested that this represented rapid conversion of PK-resistant PrP in these organelles (Laszlo et al., 1992). A clear rebuttal to this theory is of course that lysosomes act to degrade incorrectly folded proteins (Liu et al., 2012) and PrP^{Sc} is known to be trafficked to lysosomes in prion-infected cells (Goold et al., 2013). As such the accumulation seen by Laszlo et al may be the result of increased trafficking of PrP to the lysosome in a cellular attempt to clear PrP^{Sc}.

Figure 1.3 PrP^C leaves lipid rafts for intracellular trafficking (Adapted from Linden et al, 2008 and Browman and Zurzolo, 2013)

PrP^C (red) resides in lipid rafts (green) in the plasma membrane. Prior to internalisation PrP leaves lipid rafts and is endocytosed through either clathrin-coated pits or caveolae being trafficked through the endosomal (blue) system. In normal function the majority of PrP is recycled back to the plasma membrane with a small amount targeted for degradation in lysosomes (yellow). If cholesterol is redirected from the endosomal recycling compartment (green) towards late endosomes (not shown) PrP^{Sc} trafficking has been shown to redirect to lysosomes (Browman and Zurzolo, 2013).

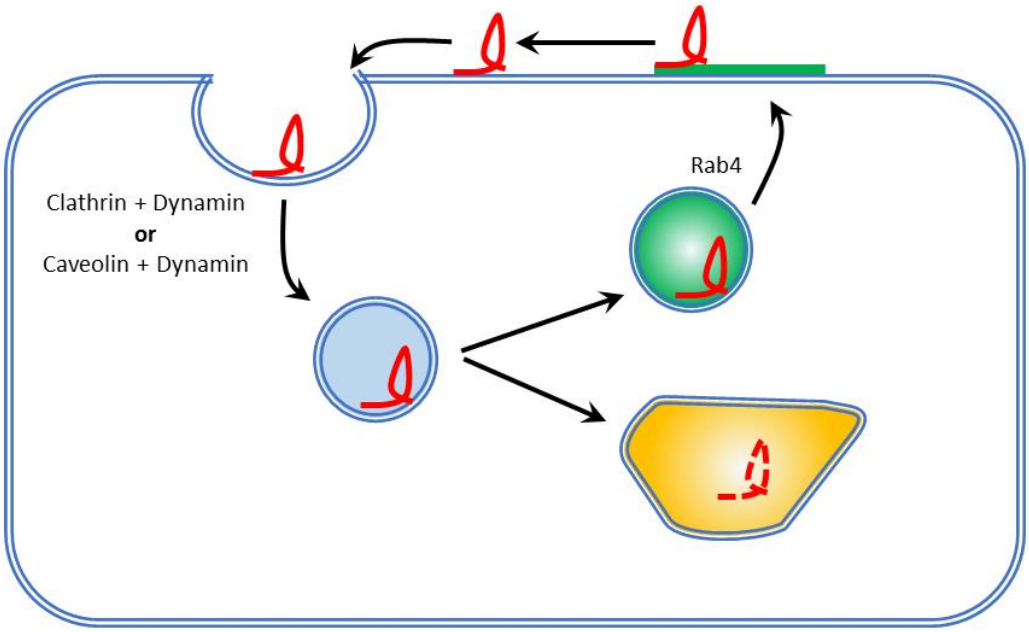

1.2 Lipid rafts

The cell plasma membrane is continuous and incorporates a mosaic of lipid and protein structures which support various cellular functions. Lipid rafts, also known as detergent resistant membrane domains (DRMs), are lipid-rich regions of the cell membrane which display a more ordered structure than the surrounding membrane (Simons and Ikonen, 1997) and facilitate attachment and internalisation of GPI anchored membrane proteins such as PrP (Brown and Rose, 1992). Lipid rafts typically include 3-5-fold greater cholesterol than surrounding plasma membrane, which acts as an interstitial 'glue' between other lipids (Korade and Kenworthy, 2008). The amphipathic nature of cholesterol and sphingomyelin means they are able to pack closely together in rafts and imbed their hydrophobic tails within the plasma membrane (Fantini et al, 2004). Cholesterol interacts preferentially with sphingolipids in rafts, and due to the rigid nature of its sterol group partitions to the more rigid, more saturated acyl chains of sphingolipids where its conical shape allows it to pack tightly into gaps between sphingolipids (Rietveld and Simons, 1998). Acyl chains are thought to be straighter and more saturated in clustered rafts, forming a so-called 'lipid ordered state' (Lingwood and Simons, 2007). Lipid rafts demonstrate resistance to non-ionic detergents at low temperatures, an effect thought to be mediated by cholesterol (Naslavsky et al, 1997). It is likely that the tight packing of lipids in rafts mean hydrophobic regions are less accessible to detergents, and so resist a low level of detergent which solubilises the surrounding plasma membrane allowing for raft extraction (Brown and London, 1998).

Lipid rafts can be further divided into planar rafts, which are continuous with the plasma membrane and incorporate flotillin proteins, and caveolae which are widely expressed in the nervous system and cause detectable deformation of the plasma membrane (Allen et al, 2007). It has been speculated that the different properties of planar rafts and caveolae segregate signalling molecules and play an important role in neurotransmission (Masserini

et al, 1999, Owen et al, 2012). PrP is enriched in cholesterol-sphingolipid lipid rafts which have previously been suggested to both facilitate and inhibit prion replication by various researchers.

1.2.1 Controversy of lipid rafts

Although becoming more widely accepted the very existence of lipid rafts remains debatable (Hawkes and Mak, 2006). Lipid rafts remain difficult to visualise by conventional microscopy (Owen et al., 2012) and have required indirect methods of observation to investigate (Jacobson et al., 2007). These difficulties have led some to suggest that rafts may be an artefact of detergents used in their extraction (Chamberlain, 2004). More recent studies provide continuing evidence for the existence of lipid rafts including detection by atomic force microscopy (Lawrence et al., 2003), super-resolution microscopy (Owen et al., 2012), and the replication of lipid-ordered domains across model cell membranes (Dietrich et al., 2001). Growing evidence suggests that lipid rafts are formed in the Golgi following sphingolipid synthesis and are then trafficked to cell membranes (Simons and Van Meer, 1988). Regardless of this debate growing evidence suggests multiple roles for ordered lipid-rich domains in membranes in cellular functions (Chu et al., 2004, Zhu et al., 2006). Proteins including PrP have consistently been found in lipid-rich fractions of the cell membrane (Crameri et al., 2006, Taylor et al., 2009) with some studies suggesting lipids such as cholesterol are required for cell surface presentation of PrP^{C} (Gilch et al., 2005). Lipid rafts are implicated in the entry of several viruses into cells (Ikeda et al., 2006, Zhu et al., 2012) and may act as a site of conversion of PrP^{C} to PrP^{Sc}.

1.2.2 Association of GPI-anchored proteins with lipid rafts

PrP and other membrane proteins such as Thy1 incorporate into lipid rafts by virtue of their GPI-anchors (Stahl et al., 1987, Paulick and Bertozzi, 2008). Incorporation into lipid rafts is a

requirement for cell surface expression of PrP (Gilch et al., 2005, Caputo et al., 2009) and some have suggested that lipid rafts are a potential site for prion propagation (Fantini et al., 2002, Cui et al., 2014). In this model rafts act as substrates by increasing the proximity of PrP^{C} and PrP^{Sc} and thereby increasing the likelihood of prion conversion. In contrast, lipid raft association has been shown to stabilise PrP^{C} (Sarnataro et al., 2004) which may impair misfolding. The GPI anchor is added to PrP^{C} post-translationally (Stahl et al., 1987) and anchoring of PrP^{C} into lipid rafts is likely to be important for the function of mature PrP^{C} (Lewis and Hooper, 2011). Some evidence suggests that PrP^{C} is incorporated into rafts early in the secretory pathway (Naslavsky et al., 1997, Sarnataro et al., 2004), indicating that lipid raft association is required for correct trafficking of PrP.

In 2005, Sabine Gilch and colleagues reported that cholesterol is required for cell surface presentation of PrP (Gilch et al., 2005), putatively as a result of GPI-directed incorporation of PrP into cholesterol-rich lipid rafts which cannot form in the absence of cholesterol. Both PrP^{C} and PrP^{Sc} reside in lipid rafts (Vey et al., 1996, Naslavsky et al., 1997), fuelling early suggestions that rafts are the site of prion conversion. Despite these findings the site(s) of prion replication remain unknown, and more recent evidence indicates that conversion may occur once PrP^{C} leaves lipid rafts (Marijanovic et al., 2009, Yim et al., 2015). Lipid rafts are also involved in intracellular trafficking of PrP (Vey et al., 1996) and have been shown to facilitate PrP internalisation via caveolae (Peters et al., 2003, Sarnataro et al., 2009). Multiple sources suggest that PrP is endocytosed via clathrin coated-pits (Shyng et al., 1995, Sunyach et al., 2003, Taylor and Hooper, 2007) although a clathrin-independent pathway has also been shown (Kang et al., 2009). Evidence suggests that PrP^{C} leaves rafts for clathrin-mediated internalisation (Sunyach et al., 2003) and is recycled back to the plasma membrane via early endosomes (Magalhaes et al., 2002). It appears likely that PrP^{C} is internalised through multiple pathways even in the same cell (Lewis and Hooper, 2011) and there is evidence that PrP can also be taken up directly via caveolae (Taylor and Hooper, 2006). Whilst lipid raft

disruption and inhibition of clathrin-mediated endocytosis both reduce uptake of PrP, it was recently shown that PrP internalisation is only completely abolished by inhibiting both pathways (Sarnataro et al., 2009).

1.2.3 The composition of PrP-containing lipid rafts

Seminal work by Naslavsky and colleagues demonstrated that cholesterol and sphingolipids form the principal components of lipid rafts containing PrP (Naslavsky et al., 1997). Cholesterol in particular has been shown to be required for cell-surface expression of PrP (Gilch et al., 2005). The ganglioside GM1 is a sphingolipid component of lipid rafts which can be isolated in PrP-containing fractions of cell lysates run on sucrose gradients (Naslavsky et al., 1997, Crameri et al., 2006, Annaba et al., 2008). A sphingolipid binding domain similar to the V3 loop of HIV envelope protein has been identified in PrP (Mahfoud et al., 2002). Interestingly this domain includes the site of the E200K mutation which is associated with familial CJD (Prusiner, 1998); suggesting sphingolipid binding may be involved in prion formation. Aside from sphingolipids and cholesterol lipid rafts can contain multiple proteins which require rafts for cell surface localisation (Loertscher and Lavery, 2002, Suzuki et al., 2007). A recent review by Nigel Hooper (2011) explored the association between PrP-containing lipid rafts and the heparin sulphate proteoglycan (HSPG) glypican-1. Glypican-1 may facilitate association of PrP^C with lipid rafts and depletion of glypican-1 impaired prion replication (Taylor et al., 2009).

1.3 Suggested roles of lipids in prion conversion

The role of lipids in prion replication is unclear and controversially discussed in the literature. Cell-free models such as Protein Misfolding Cyclic Amplification (PMCA) suggest certain lipids may be required as co-factors for prion replication (Wang et al., 2010). The close association of PrP with lipid rafts would suggest that these lipids act as the required co-factors. However

in direct contrast to this, cell-based models, which provide a full complement of regulatory genes for lipid metabolism, suggest PrP is stabilised in lipid rafts (Sarnataro et al., 2004) which would be expected to inhibit prion replication.

1.3.1 Lipids as co-factors for prion propagation

Early evidence for the requirement of lipids in prion replication comes from Stanley Prusiner's lab where it was demonstrated that the cholesterol synthesis inhibitor lovastatin decreased PrP^{Sc} in infected cells (Taraboulos et al., 1995), putatively by disrupting the association between PrP and lipid rafts. Indeed more recently statin treatment has been shown to prolong lifespan in prion-infected mice (Mok et al., 2006, Kempster et al., 2007, Haviv et al., 2008). However, these studies also indicate that increased lifespan may be a pleiotropic effect of statins as neither levels of cholesterol or PrP^{Sc} were found to be reduced by statin treatment. Studies in whole-cell and artificial membrane models complicate this picture, suggesting that lipid rafts stabilise PrP^{C} and so may limit prion replication (Eberl et al., 2004, Sarnataro et al., 2004, Hicks et al., 2006).

Protein Misfolding Cyclic Amplification (PMCA), first developed by Gabriela Sarborio in Claudio Soto's group (Saborio et al., 2001), is a key cell-free assay in the study of prion disease. PMCA reproducibly produces PK resistant PrP forms, albeit with low infectious titres (Timmes et al., 2013), through multiple rounds of incubation and sonication of a PrP^{Sc} 'seed' in presence of excess PrP^{C}. In the incubation phase PrP^{C} is incorporated into oligomers following template conversion to PrP^{Sc}, whilst the sonication phase is thought to disrupt oligomeric structures producing further PrP^{Sc} seeds for subsequent rounds of incubation (Saborio et al., 2001). More recent developments in PMCA have revealed the minimal requirements for PrP^{Sc} amplification include lipids which can be synthetic such as POPG (1-palmitoyl-2-oleoylphosphatidylglycerol) (Wang et al., 2010). In many PMCA experiments seeds are derived from infected brain homogenate and purified for seeding into recombinant

PrP^C (Panza et al., 2010, Luers et al., 2013), essentially by removing all lipid components from the system. Work in the lab of Surachi Supattapone shows that phosphatidylethanolamine (PE) is often co-purified with seeds and acts as a co-factor for prion replication, with synthetic PE being sufficient for formation of PrP^{Sc} from recombinant PrP in PMCA (Deleault et al., 2012). In light of early findings that cell-free prion replication required insertion of PrP^{Sc} into model membranes (Baron et al., 2002) some have suggested that lipids provide a substrate to increase the proximity of PrP^C and PrP^{Sc} and so aids conversion (Fantini et al., 2002). Due to differences between cell-free and cell-based models, it is possible that whilst lipids may be required for prion replication in PMCA and other cell-free models this may not be the case in host cells.

1.3.2 Lipids as inhibitors of prion propagation

Chiara Zurzolo and colleagues have demonstrated that association with cholesterol-rich rafts stabilises immature PrP^C (Sarnataro et al., 2004). This work showed that immature PrP^C initially associates with cholesterol-rich rafts in the endoplasmic reticulum, and that cholesterol depletion slows PrP maturation and can lead to misfolding. Interestingly, these effects could not be replicated by depleting sphingolipids, indicating cholesterol is sufficient to stabilise PrP^C in lipid rafts. It stands to reason that if cholesterol stabilises immature PrP^C against misfolding, it may also protect against template-induced conversion into PrP^{Sc}. In a cell-free model of prion conversion Baron and Caughey demonstrated that PrP^C linked to cholesterol and sphingolipid rich raft-like liposomes by a GPI anchor resisted conversion into PrP^{Sc} (Baron and Caughey, 2003). Interestingly, this resistance was overcome by treating samples with PIPLC to cleave the GPI anchor, suggesting that binding to lipid rafts prevented the use of PrP^C as a substrate for prion conversion.

It is likely that lipids other than cholesterol influence prion propagation. Indeed oligodendrocytes, which contain high levels of sphingolipids, are resistant to prion infection

(Prinz et al., 2004) whilst both neurons and astrocytes are susceptible. In 1999 Naslavsky and colleagues demonstrated that the rate of prion replication is inversely proportional to the sphingomyelin content of cultured prion-infected neuroblastoma cells (Naslavsky et al., 1999). Treatment of cells with fumosin B1, which inhibits ceramide synthase and thus the production of several sphingolipids, decreased both sphingomyelin and GM1 whilst increasing levels of PrP^{Sc}. Further study in the same report showed that treatment with sphingomyelinase to selectively deplete sphingomyelin produced a similar increase in PrP^{Sc} without altering GM1 level. In these experiments there was little or no change observed in PrP^{C} production or turnover. The authors noted that this result was in direct contrast to the work of Albert Taraboulos and colleagues which demonstrated reduced PrP^{Sc} in cells following inhibition of cholesterol synthesis using lovastatin (Taraboulos et al., 1995).

1.3.3 The role of cholesterol in neurodegenerative diseases

Perturbations in cholesterol metabolism have been shown to affect neurodegenerative diseases other than prion disease. Cholesterol may be neuroprotective in Alzheimer's disease (Crameri et al., 2006) whilst impaired cholesterol trafficking gives rise to progressive neurodegeneration in Niemann-Pick type C (NPC) disease (Sturley et al., 2004). The major genetic risk factor currently known for Alzheimer's disease is the ε4 allele of the gene encoding Apolipoprotein E (ApoE) (Corder et al., 1993, Strittmatter et al., 1993, Liu et al., 2015). ApoE transports cholesterol between cells and is discussed along with key players in cholesterol metabolism in greater detail below (**section 1.4**). Other cholesterol-related genes have been implicated in Alzheimer's disease, possibly as a result of altered membrane lipid composition altering cleavage of APP (Malnar et al., 2012, Maulik et al., 2013). Some research suggests that treatment with statins, which lower cholesterol, may protect against neurodegeneration (Fassbender et al., 2001, Haag et al., 2009) however there is evidence that this may be a result of reduction in co-morbid hypercholesterolemia-induced non-Alzheimer's vascular dementia (Kalback et al., 2004, Wollmer, 2010). Conversely expression

of *DHCR24*, which encodes a key enzyme for cholesterol synthesis, has been found to correlate with protection against Alzheimer's disease and indeed limits disease-associated processing of APP (Crameri et al., 2006).

Impaired cholesterol trafficking through lysosomes underlies neurodegeneration in NPC disease. Cholesterol efflux from lysosomes is mediated by Npc1 and Npc2 and loss of function of either gene leads to a characteristic accumulation of cholesterol in lysosomes (Sturley et al., 2004). Similarly ablation of Npc1 has been shown to cause accumulation of GM1 in lysosomes (Sugimoto et al., 2001) which may indicate disrupted recycling of lipid rafts. Npc1 is a large transmembrane protein which accepts cholesterol from Npc2, a small soluble protein in the lysosomal lumen (Carstea et al., 1997, Naureckiene et al., 2000). The vast majority of Niemann-Pick type C cases are caused by loss of Npc1 function, with Npc2 deficiency accounting for approximately 5% of all cases (Vance, 2006). Defective trafficking by Npc1 and Npc2 is associated with several other phenotypes alongside lysosomal cholesterol accumulation, including impaired autophagy (Sarkar et al., 2013) and altered processing and localisation of APP (Runz et al., 2002, Kosicek et al., 2010, Malnar et al., 2012). In 2006 Npc1-deficiency was shown to impair processing of glypican-1 leading to production of reactive oxygen species (Mani et al., 2006). Altered processing of glypican-1 following loss of Npc1 function may further contribute to lipid raft disruption alongside cholesterol accumulation.

1.4 Cholesterol metabolism

As the principal component of PrP-associated lipid rafts cholesterol is a prime target for examining the role of cholesterol in prion replication. Cholesterol metabolism is involved in numerous diseases including atherosclerosis (Libby et al., 2011) and Alzheimer's disease (Refolo et al., 2000) and as such is widely studied. We were able to translate the many tools

already in use in cholesterol research to modulate intracellular cholesterol in our models of prion replication.

1.4.1 Cholesterol Synthesis

Cholesterol synthesis is complex and tightly regulated, presenting opportunities as well as challenges for drug and gene induced changes to cellular cholesterol levels. There is a distinct separation between brain and peripheral cholesterol as lipoprotein molecules which transport cholesterol between cells do not easily cross the blood-brain barrier (Dietschy, 2009). The brain accounts for approximately 25% of total body cholesterol which is nearly entirely synthesised locally (Pfrieger, 2003). In the central nervous system (CNS) the majority of cholesterol is synthesised in glia and is exported to lipoproteins at the cell membrane allowing for extracellular trafficking of lipoprotein-bound cholesterol to neurons (Hayashi, 2011). The vast majority of cholesterol in the CNS is in the form of unesterified free cholesterol, a key component of neuronal and astrocyte membranes (Pfrieger and Ungerer, 2011) as well as myelin sheaths of oligodendrocytes (Saher et al., 2005). During development CNS cholesterol is produced rapidly, with the rate of production declining in adult brains as an efficient recycling system maintains cholesterol homeostasis (Dietschy, 2009). Following synthesis cholesterol is transported to cell membranes via the Golgi and Trans-Golgi complex (Simons and Ikonen, 2000), where it incorporates into both raft and non-raft domains (Ikonen, 2008).

Cholesterol is synthesised in the Endoplasmic Reticulum (ER) from acetyl-CoA (Goldstein and Brown, 1990). The mevalonate pathway, which produces cholesterol, is highly complex (Yeganeh et al., 2014) and produces many physiologically required metabolites including ubiquinones (Bentinger et al., 2010) and prenylated proteins (Sinensky and Lutz, 1992). Isoprenoids, produced from a non-cholesterogenic branch of the mevalonate pathway (Chang et al., 2013), are known to be affected by prion propagation (Guan et al., 1996).

Nordström et al demonstrated that treatment with forskolin, an isoprenoid derivative, increased the levels of PrP^{Sc} in prion-infected GT1-1 cells (Nordstrom et al., 2009). Thus disrupting the mevalonate pathway has the potential to perturb prion replication and so care is required to ensure observed effects can be attributed to cholesterol. A non-exhaustive version of the mevalonate pathway which highlights key genes targeted in this study is shown in **Figure 1.4**. Cholesterol synthesis is tightly regulated by transcriptional feedback to the rate-limiting enzyme 3-hydroxy-3-methylglutaryl CoA reductase (HMGCR) encoded by the *Hmgcr* gene. Statins, a classical family of cholesterol-lowering drugs inhibit HMGCR activity (Farmer, 1998) and have been shown to reduce the PrP^{Sc} load in prion infected neuronal cells. Ina Vorberg and colleagues have shown that chronic prion propagation in cells gives rise to increased expression of cholesterogenic genes, including the sterol regulatory element binding protein (*Srebp2*) (Bach et al., 2009) which suggests that prions may disrupt the cholesterol metabolism. Downstream of HMGCR, the mevalonate pathway branches after the production of farnesyl diphosphate to form several non-sterol molecules (Nurenberg and Volmer, 2012). Past research has supplemented cells with mevalonate following HMGCR inhibition to provide for these non-steroidal pathways (Taraboulos et al., 1995). However as mevalonate is produced directly from acetoacetyl CoA by HMGCR (Goldstein and Brown, 1990) the net change in cholesterol caused by these treatments remains unclear.

During the final stages the cholesterol synthesis pathway branches with the final enzymes acting in an indeterminate sequence (Zerenturk et al., 2013). Cholesterol synthesis culminates with the action of 3β-hydroxysteroid-Δ24 reductase which is encoded by *Dhcr24* and catalyses the conversion of desmosterol to cholesterol by reduction of the Δ24 double bond (Waterham et al., 2001). Silencing *Dhcr24* has been shown to cause desmosterolosis, a severe developmental disorder characterised by increased plasma desmosterol (Waterham et al., 2001, Zerenturk et al., 2013). Although principally involved in cholesterol synthesis,

Dhcr24 has also been shown to have a neuroprotective role in ER stress (Lu et al., 2014) and is known to regulate Ras-induced senescence (Wu et al., 2004). *Dhcr24* was originally described as a neuroprotective factor in Alzheimer's disease, *Seladin-1,* and was found to be downregulated in brain areas susceptible to Alzheimer's disease (Greeve et al., 2000, Peri and Serio, 2008). It is possible given the nature of protein aggregation in both Alzheimer's and prion diseases that perturbed cholesterol synthesis could affect these diseases in similar ways. *Dhcr24* expression increases dose-dependently after incubation with simvastatin (Ramos et al., 2012) which may indicate an adaptive response to impaired cholesterol synthesis. Dhcr24 activity can be inhibited by triparanol (Spann et al., 2012) which shows some non-specific activity and also inhibits Hedgehog pathway signalling (Bi et al., 2012). Gene silencing of Dhcr24 with multiple effective siRNAs provides a relatively clean method of reducing cholesterol in cells by excluding the possibility of off-target effects.

Figure 1.4 Cholesterol is synthesised in the Mevalonate Pathway

Cholesterol is synthesised from Acetyl CoA by a tightly regulated multistep pathway. Dashed arrows indicate multiple steps not shown here. HMG-CoA: *3-hydroxy-3 -methylglutaryl CoA,* HMGCR: *3-hydroxy-3-methylglutaryl CoA reductase,* DHCR24: *3β-hydroxysteroid-Δ24 reductase. Black text denotes a metabolite and blue an enzyme. Branched pathway at DHCR24 denotes multiple steps which occur in indeterminate order (parallel Bloch and Kandutsch-Russell pathways) but culminate with action of DHCR24. Adapted from (Goldstein and Brown, 1990, Zerenturk et al., 2013, Yeganeh et al., 2014)*

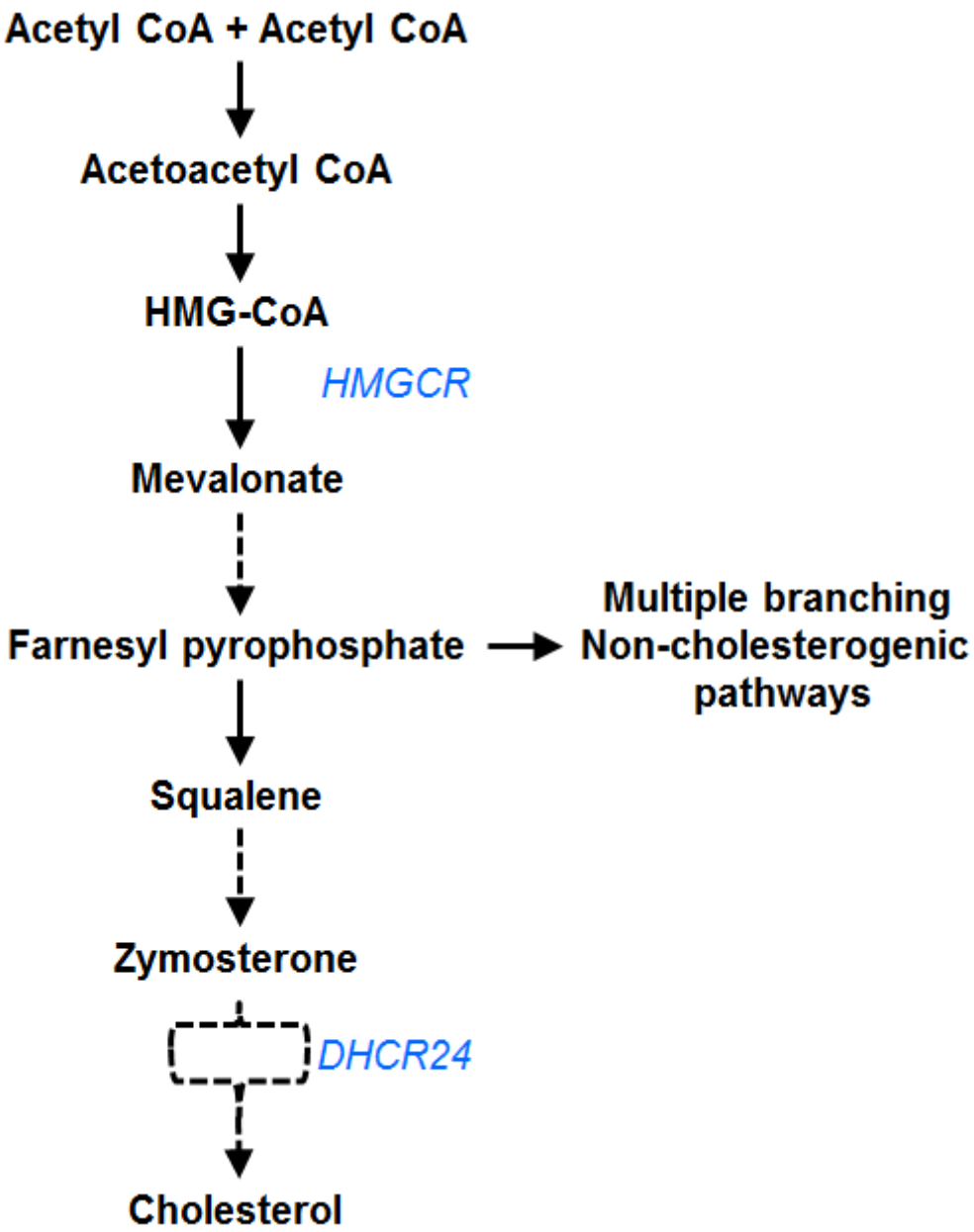

1.4.2 Cholesterol Import

Cholesterol in neurons is predominantly imported via a lipoprotein-based shuttle system (Hayashi, 2011, Pfrieger and Ungerer, 2011). An attractive method of cholesterol depletion in cultured cells is to use lipoprotein-deficient serum in place of Foetal Bovine Serum (Narita et al., 1997, Hawes et al., 2010). Notably reduced fat serum (an early form of lipoprotein-deficient serum) was required to show effects of HMGCR inhibition on PrP^{Sc} levels in the work of Tarabolous et al (1995). Given the reliance of neurones in the CNS on glial cells for cholesterol lipoprotein-deficient serum may have serious adverse effects in cell culture but remains a common method for cholesterol depletion *in vitro*. The half-life of free cholesterol in the periphery is fairly short compared to cholesterol in the CNS (Andersson et al., 1990) and in most cases cholesterol will instead be associated with lipoproteins for transport between cells (Hayashi, 2011).

The ε4 allele of ApoE is widely accepted as the major genetic risk factor for Alzheimer's disease (Corder et al., 1993, Strittmatter et al., 1993, Liu et al., 2015). ApoE acts as a shuttle and transports cholesterol between cell membranes, typically acting in the brain to deliver cholesterol from glia to neurones (Rapp et al., 2006). The activity of ApoE is particularly important in the brain as other key apolipoproteins are almost entirely absent (Poirier et al., 1995). ApoE4 differs from the 'wild type' ApoE3 allele only by a single cysteine to arginine amino acid change at position 112 (Hauser and Ryan, 2013), but binds cholesterol with much greater affinity (Li et al., 2013). Whilst no direct causative link has been described for ApoE4 in prion diseases a genome wide association study (GWAS) performed by Calero et al (2011) indicated that sCJD patients exhibited a higher occurrence of ApoE4 than a control population, suggesting that perturbed cholesterol trafficking is a risk for prion disease. Cholesterol and other lipoprotein components are imported into cells via low-density lipoprotein receptor-related proteins (LRPs) in the cell membrane (Zerbinatti and Bu, 2005). The principal receptors for ApoE are LRP1 and LRP8 (Jaeger and Pietrzik, 2008), although

several other LRPs have been identified with similar functions (May et al., 2007). Growing evidence suggests that LRPs are involved in signal transduction (Bao et al., 2012, Ren et al., 2013) and Roger Morris and others have suggested that LRP1 may act as a receptor for PrP (Taylor and Hooper, 2007, Parkyn et al., 2008). Indeed, recent evidence suggests that lipid rafts and LRP1 are required for prion-mediated toxicity of amyloid β oligomers (Rushworth et al., 2013). Multiple studies have used lipoprotein-deficient serum to 'starve' cultured cells and so reduce cholesterol levels (Narita et al., 1997, Hawes et al., 2010). Models of cholesterol depletion show disruption of cell membranes (Hao et al., 2001, Yang et al., 2012) and increased shedding of membrane proteins into the extracellular matrix and culture medium (Murai et al., 2011). Furthermore, limiting the availability of exogenous cholesterol can alter cell adhesion and motility by disrupting lipid rafts which contributes to loss of adhesion proteins (Jeon et al., 2010, Baumgartner et al., 2014).

The LRPs constitute a family of receptors with multiple functions united by binding of lipoproteins (Strickland et al., 1995, Ye et al., 2012). Of note, LRP6 is involved in Caveolin-1 signalling and regulates activity of Wnt-β-catenin (Tahir et al., 2013). This interaction is reinforced by the binding of LRP6 to Leucine rich repeat kinase 2 (LRRK2) which may help explain why LRRK2 mutations produce neurodegeneration in Parkinson's disease (Berwick and Harvey, 2012). Interactions between LRP6 and Wnt are also implicated in tumorigenesis (Li et al., 2004) with increased LRP6 expression promoting cell proliferation. Similar to LRP1, LRP8 acts as a canonical receptor for ApoE and was previously known as ApoE Receptor 2 (ApoER2) (Jaeger and Pietrzik, 2008). LRP8 is predominantly expressed in the brain (Kim et al., 1996) and mutations in LRP8 have been identified in Alzheimer's disease patients (Carter, 2007).

1.4.3 Intracellular cholesterol trafficking and storage

Following endocytosis via clathrin-coated pits cholesterol is trafficked through the endosomal-lysosomal system. Excess cholesterol is esterified in the Endoplasmic Reticulum (ER) by the action of acyl-CoA: cholesterol acyltransferase (ACAT) enzymes and stored as cytoplasmic lipid droplets and in lysosomes (Tabas, 1995, Chang et al., 1997). When additional cholesterol is required esters are hydrolysed by lysosomal acid lipase, encoded by *LIPA* (Goldstein et al., 1975, Koch et al., 1981), and exported from lysosomes by the sequential action of Npc1 and Npc2 (Vance, 2010). Loss of function of either Npc1 or Npc2 causes accumulation of cholesterol in lysosomes, with the gene names deriving from their pivotal role in invariably fatal Niemann-Pick type C neurodegenerative disease (Sturley et al., 2004). Following export from lysosomes free cholesterol is transported to either the Trans Golgi Network (TGN) (Coxey et al., 1993), from where it is subsequently recycled to the plasma membrane or the ER (Ikonen, 2006). Cholesterol is also trafficked to mitochondria (Kennedy et al., 2012) where it is used for specialised tissue dependent processes including production of bile acids (Li and Chiang, 2014) and steroid hormones (Issop et al., 2013). Recent evidence indicates that accumulation of cholesterol in mitochondria may influence progression of Alzheimer's disease (Barbero-Camps et al., 2014).

Perturbations of intracellular cholesterol trafficking have been previously studied in prion disease. Notably, work by Clive Bate and Alun Williams has demonstrated that ACAT inhibitors increased toxicity in prion infected GT1 cells (Bate et al., 2008), whilst work by Gilch et al has shown that knockdown of Npc1 in prion-infected N2a cells decreased levels of PrP^{Sc} (Gilch et al., 2009). Expression of the GTPase Arf6 (ADP-ribolysation factor 6) has been shown to alleviate both cholesterol and sphingolipid accumulation following Npc1 ablation (Schweitzer et al., 2009) and functions in endosomal recycling. Arf6 is thought to be involved

in clathrin-independent endocytosis of PrP^C (Kang et al., 2009), although expression of constitutively active Arf6 led to accumulation of PrP^C in large intracellular vacuoles.

1.4.4 Cholesterol export and degradation

Cholesterol does not readily cross the blood brain barrier and instead a highly efficient recycling system operates in the CNS to maintain cholesterol levels (Dietschy, 2009). Cholesterol has a half-life of approximately six months in the brain (Andersson et al., 1990) and is eventually metabolised and excreted across the blood brain barrier for degradation in the liver (Pfrieger, 2003). Levels of CNS cholesterol metabolites in the periphery may be of use as indicators of neurological disease (Hughes et al., 2013).

High levels of cholesterol activate nuclear liver X receptors (LXRs), transcription factors which regulate multiple aspects of cholesterol homeostasis in response to increased levels of sterol metabolites (Peet et al., 1998). Two LXRs are currently known, LXRα which is a canonical oxysterol sensor in the liver (Pawar et al., 2003) and LXRβ first discovered in the lab of Jan-Åke Gustafsson which is found in the brain and other tissues (Warner and Gustafsson, 2015). LXRs act to prevent cellular accumulation of cholesterol (Ulven et al., 2004) and activate several pathways to induce cholesterol efflux (Gabbi et al., 2014). Of particular interest to this project LXRs regulate the expression of ATP-Binding Cassette Transporter A1 (ABCA1) which in turn exports cholesterol from cells (Jasmin et al., 2014). Expression of ABCA1 is stimulated not only by LXRs but also retinoic acid receptors and peroxisome proliferator-activated receptors which can form an amplification loop for ABCA1 expression (Jiang et al., 2012). Negative regulation of ABCA1 occurs following serum depletion and is mediated by several molecules including SREBP2 (Zeng et al., 2004), unsaturated fatty acids (Mauerer et al., 2009), and the non-sterol mevalonate pathway intermediate geranylgeranyl pyrophosphate (Gan et al., 2001). A deficit in ABCA1 expression and activity is associated with impaired vesicular traffic from the Golgi to the plasma membrane (Zha et al., 2003, Lin

et al., 2009). Although not itself located in lipid rafts (Oram and Heinecke, 2005) ABCA1 dissociates cholesterol from rafts allowing for transport across cell membranes to external acceptors including Apolipoprotein A1 (ApoA1) (Boadu et al., 2012). Cholesterol efflux to ApoA1 enables the formation of high density lipoprotein molecules (HDL) (Plump et al., 1994) and impaired ApoA1 function can be disease causing in blood vessels (Plump et al., 1997, Smith, 2010). ApoA1 is not synthesised in the CNS, but can cross the blood brain barrier to incorporate into CNS lipoproteins (Pitas et al., 1987, Karten et al., 2006). In a mouse model lacking neuronal ABCA1 Karasinska et al demonstrated decreased brain cholesterol alongside increased cholesterol uptake from plasma HDL (Karasinska et al., 2009) potentially indicating perturbed tight junctions in the blood brain barrier. Prion infection is known to increase ABCA1 expression in infected cells which in turn may increase levels of PrP^{C} and PrP^{Sc} (Kumar et al., 2008). This effect is intriguing as the cholesterogenic transcription factor SREBP2 is upregulated following prion infection (Bach et al., 2009) yet has been shown to negatively regulate transcription of ABCA1 in response to sterol depletion (Zeng et al., 2004). Recent work from the lab of Andy Hill shows that increased ABCA1 expression following prion infection was associated with reduced cholesterol efflux from cells and enhanced internalisation of ABCA1 (Cui et al., 2014). These effects could be reversed by increasing expression of ABCA1 and loading cells with cholesterol suggesting that prion replication may be inversely tied to cholesterol metabolism.

Cholesterol can be experimentally depleted from cell membranes using small molecules. The bacteria-derived polyene antibiotic filipin III binds tightly to cholesterol and has been shown to disrupt lipid rafts (Schnitzer et al., 1994). Treating prion infected cells with filipin has been shown to impair PrP endocytosis and induce cellular PrP release, effectively 'curing' prion infection (Marella et al., 2002). The authors attributed the curing effect to release of PrP^{C} which deprived PrP^{Sc} of a substrate for replication. Furthermore this study underscored the importance of cholesterol-rich raft domains for PrP trafficking and surface presentation.

Cyclodextrins are macrocyclic molecules which contain an internal pocket (Lopez et al., 2011). Cyclodextrins exhibit various properties which has led to intensive research into their potential use for drug delivery (Gidwani and Vyas, 2014). In the context of this thesis the term cyclodextrins refers to hydrophilic molecules with a highly hydrophobic binding pocket. Cyclodextrins sequester cholesterol from plasma membranes into the hydrophobic pocket (Lopez et al., 2011) and methyl-β cyclodextrin (MβCD) is frequently used experimentally to deplete cellular cholesterol (Nicholson and Ferreira, 2009, Onodera et al., 2013). In 2009 cyclodextrin analogues were demonstrated to exert anti-prion effects (McEvoy and McMahon, 2009). Interestingly these effects were not attributed to cholesterol depletion and the authors instead suggested that cyclodextrins may act as chaperones to ensure correct folding of PrP^{C}. Similarities in the mechanism of action of the cyclodextrins used and heparin were also highlighted. Heparin and other glycosaminoglycans have been previously shown to exert anti-prion activity (Bazar et al., 2011, Vieira et al., 2014) putatively by interfering with interactions between PrP and the cell membrane. Although growing evidence suggests lipid rafts are not the site of prion conversion (Borchelt et al., 1992, Marijanovic et al., 2009) the availability of PrP^{C} as a substrate for prion replication remains tightly linked to membrane cholesterol. Altered cholesterol efflux, whether mediated by small molecules or gene silencing, would be expected to influence prion replication.

Excess CNS cholesterol is metabolised to allow for secretion to the periphery. The brain-specific enzyme CYP46A1 converts excess cholesterol to 24S-OH cholesterol allowing for excretion across the blood brain barrier (Russell et al., 2009). Sterol metabolites are then transported to the liver for degradation to bile salts (Li and Chiang, 2014). The presence of sterol metabolites in plasma has drawn interest as an indicator of Alzheimer's disease (Ogundare et al., 2010, Zuliani et al., 2011) and disrupted CNS cholesterol metabolism may provide a potential early biomarker of prion disease which could be detected before blood-borne PrP^{Sc}.

1.5 Rationale and Aims

A growing body of literature indicates that host-encoded cellular factors influence prion propagation. In this thesis I will describe my work characterising the effects of cholesterol on prion replication and outline a potential mechanism for these effects. Primarily this work is focused on the effects of silencing *Hmgcr, Dhcr24, Npc1* and *Npc2*. These genes allow for examination of both the effects of disrupted cholesterol synthesis and trafficking on prion replication. Beyond effects on levels of PrP^{Sc} we also examined the association of PrP^{C} with lipid rafts in order to investigate a potential mechanism through which cholesterol perturbation affects prion replication. The aim of this project is to investigate the effect of depletion of *Hmgcr, Dhcr24, Npc1* and *Npc2*; and subsequent changes in cholesterol, on prion propagation.

I will also outline a pilot study designed to identify cellular factors underlying susceptibility of cultured cells to different prion strains. Subcloning the CAD5 cell line, which propagates both RML and 22L prions, yields rare variant clones which exclusively propagate a single prion strain. This project aimed to identify cellular factors underlying cellular susceptibility to different prion strains by isolation of rare variant subclones and subsequent analysis of these subclones. As a pilot study this work establishes methods for high throughput screening of subclones and gives an indication of the cohort size required to examine differences between rare variant subclones propagating different prion strains.

CHAPTER 2 METHODS

2.1 Cell lines and culture

Our primary cell line for experimental use is N2a-PK1-S7 (S7). This cell line was derived from the N2a parent line, is highly susceptible to infection with RML prions, and has been used to generate the chronically infected cell line N2a-PK1-IPKS7 (iS7) (Klohn et al., 2003). LD9 cells were derived from the murine fibroblast cell line L929 (Mahal et al., 2007). CAD5 cells were derived from mouse neuroblastoma tissue (Qi et al., 1997). A summary of cell lines and culture conditions is shown in **Table 2.1**. OptiMEM is supplemented with 10% Foetal Calf Serum and 1% Pen/Strep (OFCS,Gibco). Alternatively OptiMEM was supplemented with 10% Bovine Growth Serum (HyClone) and 1% Pen/Strep (OBGS). Minimum Essential Medium (Sigma) is supplemented with 10% Foetal Calf Serum and 1% Pen/Strep (MEME). Dulbecco's Modified Essential Medium (Gibco) is supplemented with 10% Foetal Calf Serum and 1% Pen/Strep (DMEM).

Table 2.1 A summary of cell lines used in this project.

Name	**Species**	**Culture conditions**
N2a-PK1-S7 ('S7')	Mouse	OFCS, 37°C 5% CO_2
N2a-PK1-IPKS7 ('iS7', RML infected)	Mouse	OFCS, 37°C 5% CO_2
N2a-PK1-11 ('PK1-11')	Mouse	OFCS, 37°C 5% CO_2
N2a-PK1-R33 ('R33')	Mouse	OFCS, 37°C 5% CO_2
CAD5	Mouse	OBGS, 37°C 5% CO_2
L929-LD9 ('LD9')	Mouse	MEME, 37°C 5% CO_2, requires trypsin to split
RetroPack PT67	Mouse	DMEM, 37°C 5% CO_2, viral packaging cells

2.2 Scrapie Cell Assay

The Scrapie Cell Assay (SCA) is a method for detecting infectious prion titres in cultured cells (Klohn et al., 2003). The SCA has been previously used to characterise the response of cell lines to different prion strains (Mahal et al., 2007). Multiple splits are used to induce propagation and infection can be determined through an Enzyme Linked ImmunoSpot Assay (Elispot). The SCA has been fully automated and allows for high throughput determination of infectious titres.

The SCA is performed in 96-well plates. Twenty thousand cells per well were plated in 300µl of the normal culture medium for the cell type (see **Table 1**), allowed to adhere for 16 hours at normal culture conditions (37°C, 5.0% CO_2) and then media was replaced with 300µl of prion-containing sample (infected brain homogenate diluted in culture media). A 10^{-3} dilution of homogenate typically saturated the elispot assay necessitating the use of lower concentrations. In the automated version of the SCA assay, a 10^{-5} dilution was used for each homogenate. Control cells were treated with uninfected media. Cells were passaged once every three days at a 1:8 split (cells were resuspended in wells and 40µl was transferred to a new well containing 260µl of new media). Following growth to confluence after the 3rd split the PrP^{Sc} content of cells was assessed using the Elispot protocol. A schematic of the SCA is shown in **Figure 2.1**.

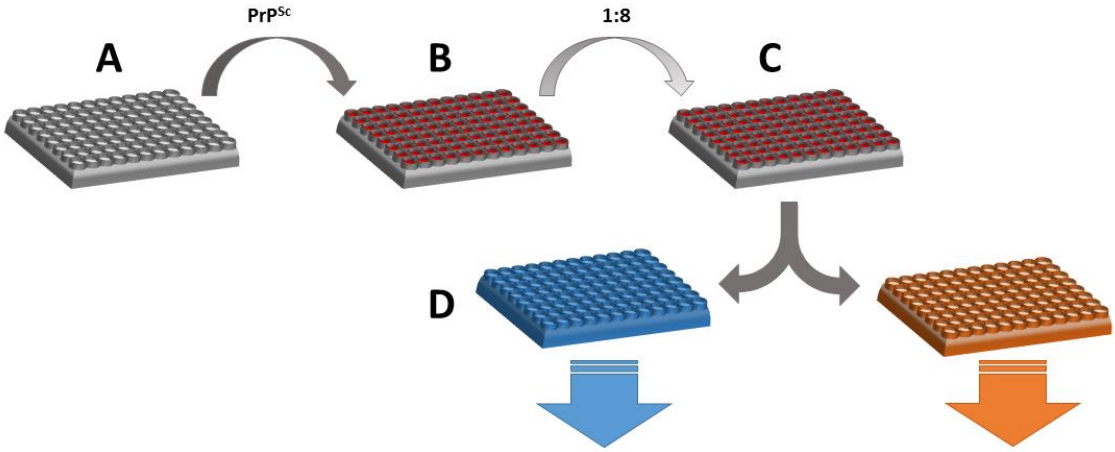

Figure 2.1 The Scrapie Cell Assay

Cells were plated in 96-well plates as described above (part A). After 16 hours growth cell culture medium was removed and replaced with prion brain homogenate diluted in cell culture media (typically to 10^{-5} of the stock concentration) and cells were allowed to continue growing for a further 2 days (3 days total after initial plating, part B). Cells were passaged every 3 days in 1:8 split ratios (part C), and samples collected for Elispot (orange, see section 2.2.1) and Trypan Blue (blue, see section 2.2.1 (b)) assays at predetermined points (part D). Passage and sample collection was performed at multiple points, typically at the post-3rd and post 4th passages. Each subsequent split diluted out the initial prion homogenate while allowing cells to grow and propagate PrP^{Sc} without reaching confluence.

2.2.1 Elispot determination of PrP^{Sc}-positive cells

The Elispot protocol assesses the PrP^{Sc} content of cells in a 96-well PVDF membrane plate (Corning) format. Plates were activated with 70% ethanol, washed twice with PBS and fluids were removed by applying a vacuum. Cells were then seeded onto the plates at a density of 20000 cells per well unless indicated otherwise. When fewer cells were seeded, non-infected control cells were added to a total of 20000 cells. Plates were then dried for one hour at 50°C and stored in the fridge (2-8°C) until further use. Plates were incubated with 60µl Proteinase K (PK, Roche), diluted to 10^{-4} in lysis buffer (50mM Tris.HCl, 150mM NaCl, 0.5% Na deoxycholate, 0.5% Triton X-100 in dH_2O, pH 7.4) for 1 hour at 37°C then washed twice with PBS. PK digest was stopped by 120µl of 1mM phenylmethanesulfonylfluoride (PMSF) for 10 minutes. Tris-guanidinium thiocyanate (GTC, 3M, 120µl/well) was then added and plates incubated for 20 minutes. GTC denaturation was followed by seven washes with PBS, discarding each wash into 2M NaOH. To block unspecific binding sites, wells were incubated with 120µl superblock (Pierce) for 1 hour. Plates were incubated at room temperature for 1 hour with 60µl primary antibody (mouse anti-PrP ICSM18, D-GEN, 1:5000 in TBST (10mM Tris-HCl, 150mM NaCl, 0.1% Tween 20 (v/v)), pH 7.4/1% non-fat milk powder). Plates were then washed five times with TBST and incubated with 60µl secondary antibody (goat anti-mouse-IgG1 AP, Cambridge Bioscience, 1:8000 in 1xTBST/1% non-fat milk powder) for 1 hour at room temperature. Wells were washed five times with TBST, the underdrain of the plates removed and membranes dried. Plates were then incubated with 54µl of alkaline phosphatase colour reaction (BioRad) for approximately 30 minutes at room temperature before rinsing with dH_2O twice and drying. Plates were analysed using plate reader software (Bio-Sys) to quantify the number of infected cells as mean and standard deviation. Individual wells of a 96-well plate were counted as technical repeats, 12 technical repeats were performed for each biological repeat. At least 3 biological repeats were performed for each condition tested.

2.2.1 (a) Chronically prion infected cell Elispot

In addition to examining prion infection in the SCA the Elispot assay can be used to determine prion replication in chronically infected cells. Unlike in the SCA a population of chronically infected cells is expected to be uniformly infected and as such a lower cell seeding density was required to prevent plate reader saturation (20000 spots is far beyond the capabilities of our current system). Typically plates were seeded with 1000 or 2500 chronically infected cells per well buffered to 20000 cells per well total with uninfected cells. In experiments where the buffer cells were omitted the concentration of PK in the Elispot assay was reduced by half to 1/20000 in lysis buffer to prevent over-digestion of PrP^{Sc}.

2.2.1 (b) Trypan Blue assay

As cell counting and dilution carries an inherent error the Trypan Blue assay was used to determine the number of cells seeded per Elispot. A volume approximately equal to 1000 cells was seeded on elispot plates as per the PrP^{Sc} quantification assay above. Dry plates were washed with 0.04% Trypan Blue in PBS and immediately vacuumed, then washed twice again on the vacuum with PBS. Plates were then dried in a hood and read using a Bio-Sys plate reader as above.

2.3 Confocal microscopy

Images were captured using a Leica 710 confocal microscope and Zen software; where required co-localisation and quantification was assessed using Volocity software. Cells were grown to near confluence in 4- or 8-well chamber slides (Corning) and fixed for immunolabeling as described below.

2.3.1 Fixation conditions

Cells were incubated with 4% paraformaldehyde (PFA) for 20 minutes, washed with PBS and incubated with 0.04% Triton X-100 for 15 minutes to permeabilise cells. Cells were washed and stored in PBS. Alternative permeabilisation conditions were used to improve the

detection of PrP deposits in fixed cells. Incubation of fixed cells for one minute at room temperature with acetone (Ac) solubilises and strips neutral lipids (Urist et al., 1997) and reveals previously unseen PrP deposits on the basement adherent membrane of cells (Marbiah et al., 2014). To reveal prion infection associated PrP deposits (PrP^d) cells were fixed with 4% PFA for 12 minutes, incubated with pre-chilled acetone for 30 seconds, washed with PBS, and then incubated with 3M guanidinium thiocyanate (GTC) for 10 minutes to denature proteins within fixed cells to better facilitate antibody binding. Slides were then washed three times with PBS before a further two washes with fresh sterile PBS to avoid GTC cross-contamination which could denature antibodies. Alternatively, five minutes incubation with 100µg/ml digitonin was used to permeabilise BODIPY and filipin treated cells in place of Triton X-100 or acetone/GTC (see below). The fixation and permeabilisation used for each image is given in the relevant figure legend.

2.3.2 Immunofluorescence

Secondary antibodies conjugated to Alexa Fluor 488, 568 and 633 were obtained from Molecular Probes. Highly cross-adsorbed preparations of these antibodies were used for dual labelling experiments. Primary antibodies were purchased from D-Gen, Sigma Aldrich, CST and Santa Cruz.

Following permeabilsation cells were incubated overnight with primary antibody in sterile filtered PBS:Superblock (4:1) at 4°C. Primary antibody concentrations were typically ranged between 1:500 and 1:2000 dilutions of the manufacturers stock. Slides were washed once with sterile PBS and incubated with the relevant secondary antibodies and DAPI (1:10000 dilution of 4µg/ml stock) in PBS:Superblock for 1 hour at room temperature in the dark. Labelled slides were washed once with PBS and stored at 4°C in 0.1% sodium azide (v/v) in PBS until microscopy.

2.3.3 Tracking cholesterol trafficking with BODIPY FL cholesterol

BODIPY FL cholesterol (Molecular Probes), a cholesterol analogue, was used to investigate lipid trafficking. Live cells were incubated with 1 μM BODIPY FL cholesterol in their normal growth media and cells were then fixed using PFA/digitonin as described above and antibody labelled as necessary. Although 1 hour incubations with BODIPY FL cholesterol have been previously used (Sankaranarayanan et al., 2011) we found more evident and specific staining using overnight incubation (~16 hours) under normal culture conditions (37°C, 5.0% CO_2).

2.3.4 Filipin labelling

Although BODIPY FL cholesterol is a useful tool to track cholesterol trafficking it does not provide information on cholesterol levels within cells. Filipin is a sterol-binding protein and so can act as a direct measure of cholesterol levels in cells. Due to artefacts in fixed cells with our standard fixation and permeabilisation protocols fixation to visualise filipin required re-optimisation. Fixation was optimised to a 10 minute fix with 4% PFA followed by 10 minutes incubation with 50μg/ml digitonin to permeabilise cells. Fixed permeabilised cells were incubated for 1 hour with 20μg/ml filipin in the dark at room temperature. Labelled cells were washed once with PBS and then imaged with a Zeiss 510 confocal using ultraviolet excitation and a long pass bandwidth filter.

2.3.5 Live cell imaging

Lysosensor Green DND-189 ('Lysosensor', Life Technologies) was used to identify changes in intracellular pH in live cells. Cells were incubated with 100nM Lysosensor in growth media for 30 minutes at 37°C with 5% CO_2, before replacing with media containing 10mM HEPES (pH 7.4) immediately prior to imaging to preserve pH in the absence of CO_2. Imaging sessions were limited to 30 minutes at which point cells lost viability. To label the endocytotic pathway Dextran Texas Red (Life Technologies) was used. Cells were incubated overnight (>16 hours) with 100μg/ml Dextran Texas Red before washing once with growth media and

incubating with Lysosensor as above. Overnight incubation ensured Dextran Texas Red accumulated in lysosomes prior to imaging (Jaiswal et al., 2002).

2.4 Assessment of target manipulation on cells

Pharmacological and genetic methods were used to perturb lipid pathways and assess resulting effects on PrP^{Sc} in cells.

2.4.1 Small inhibitor/drug treatment

Various small inhibitors and biologically active molecules were used to deplete cholesterol from cells. Where stock concentrations were made in DMSO stocks were made at 1000-fold the highest working dilution to reduce the likelihood of off-target vehicle effects. Cells were seeded in 96 well plates at a density of 15000 cells/well and grown overnight. Media was removed and replaced with a serial dilution of drug treatment in normal cell media. After 3 days growth cells were harvested for their intended use. Stocks of Lovastatin (Santa Cruz) and Simvastatin (Sigma) were made in DMSO and used to inhibit cholesterol synthesis. Methyl-β cyclodextrin (MβCD, Sigma) is a highly hydrophilic molecule which sequesters cholesterol from cell membranes (Kilsdonk et al., 1995, Lopez et al., 2011) and was diluted directly in cell culture medium.

2.4.1 (a) Determination of cell viability

Cell viability following drug treatment was assessed using the CellTitre Glo assay (Promega) which measures ATP levels in cells by mono-oxygenation of luciferase. Media was removed from cells treated in 96 well plates as above and replaced with 80µl CellTitre reagent mixture prepared according to the manufacturer's instructions. The plate was then transferred to a Tecan plate reader and incubated at room temperature for 10 minutes, shaken at 1mm amplitude for 2 minutes and then luminescence recorded. Luminescence was normalised to vehicle treated cells to give percentage cell viability relative to control.

2.4.2 siRNA screening

Custom DICER substrate siRNA (DsiRNA) were purchased from Integrated DNA Technologies (IDT). DsiRNAs are double-stranded RNA molecules that were delivered to cells using DharmaFECT lipid transfection. At least 3 DsiRNAs were designed per target and tested for efficacy of gene knockdown. Silencing RNA duplexes are summarised in **Table 2.2**. Knockdown of target expression was quantified using qPCR (see below). Reverse transfection of cells with DsiRNAs and DharmaFECT 3 (D3, Thermo Fisher) was established as a standard gene silencing protocol. DsiRNA and D3 were mixed in 100µl OptiMEM and incubated at room temperature for 20 minutes. OFCS was then added and the reagents mixed 1:1 with a $1x10^5$ cells/ml cells suspension to give a final DsiRNA concentration of 20nM and D3 concentration of 0.13% for N2a-derived cell lines. 300µl of this mix was plated per well of a 96 well plate whilst 550µl was plated per well of an 8 well chamber slide (Corning). Control cells were treated with NC1 non-silencing DsiRNA (IDT). Cells were grown for 3 days, at which point we observed greatest gene silencing as assessed by qPCR, and then fixed/infected as described above depending on intended use.

Where gene knockdown was required for longer periods, such as to ensure protein turnover prior to confocal imaging, cells were subject to double knockdown. Here cells were split into media containing the same proportion of DsiRNA/D3 mix following the initial 3 day incubation. Cells were then grown for a further 3 days before being used as per the single knockdown protocol outlined above.

2.4.2 (a) Transient gene knockdown in primary cortical neuron cultures

Preparations of E17 primary mouse cortical neurons were kindly provided by Dr Silvia Purro. Due to key differences in culture technique between primary cultures and cell lines our siRNA transfection protocol required adaptation. Primary neurons seeded at $5x10^5$ cells per well in 6 well plates (Corning) were transfected at 8 days in *vitro* (DIV) by replacing culture medium

(CMII, Neurobasal medium containing 2% B27, 1mM pyruvate, 2mM glutamine and 1% Pen/Strep, all Life Technologies) for 6 hours with 2ml conditioned medium containing siRNA-Dharmafect 4 complexes prepared as above at a final concentration of 2µl/ml siRNA and 0.7µl/ml Dharmafect 4. Culture medium was replaced after 6 hours with 2ml fresh conditioned media. Conditioned media was CMII obtained from 10cm dishes of untransfected primary neurons. The effect of gene silencing was assessed 3 days later at 11DIV. For Western blotting and Optiprep gradients (see below) cells were lysed on ice for 20 minutes with 250µl TNET buffer containing 1µl/ml protease inhibitor cocktail (Pierce) per well.

Table 2.2 DsiRNA designs. *Multiple DsiRNA duplexes were designed per target for experimental control purposes.*

Target	DsiRNA	Sense sequence	Antisense sequence
Npc1	1	5'-rGrCrArGrCrArGrGrCrUrCrCrUrGrGrUrGrGrArUrUrCrUAA	5’-rUrUrArGrArArUrCrCrArCrCrArGrGrArGrCrCrUrGrCrUrGrCrArG
	2	5'-rCrCrArArUrArCrArUrGrCrCrUrGrUrCrArUrUrCrArCrGTG	5'-rCrArCrGrUrGrArArUrGrArCrArGrGrCrArUrGrUrArUrUrGrGrUrU
	3	5'-rCrUrArCrCrArGrArGrArGrArUrGrArGrCrGrUrCrUrUrCAG	5'-rCrUrGrArArGrArCrGrCrUrCrArUrCrUrCrUrCrUrGrGrUrArGrGrU
	4	5'-rGrGrArGrUrArCrUrUrUrGrArCrArArGrCrArCrUrUrUrGGG	5'-rCrCrCrArArArGrUrGrCrUrUrGrUrCrArArArGrUrArCrUrCrCrUrU
	5	5'-rCrCrGrUrGrArCrArCrUrGrCrArGrGrArCrArUrCrUrGrUGT	5'-rArCrArCrArGrArUrGrUrCrCrUrGrCrArGrUrGrUrCrArCrGrGrUrU
	6	5'-rCrCrArGrUrArGrArArArCrCrUrCrArUrCrUrUrGrGrGrUAC	5'-rGrUrArCrCrCrArArGrArUrGrArGrGrUrUrUrCrUrArCrUrGrGrUrA
Npc2	*1*	5'-rCrCrArCrCrArCrCrUrArGrCrArCrCrArCrUrUrGrArGrGAG	5'-rCrUrCrCrUrCrArArGrUrGrGrUrGrCrUrArGrGrUrGrGrUrGrGrUrU
	2	5'-rGrGrArGrArGrGrGrArGrGrArArGrArGrGrCrUrGrUrGrGCT	5'-rArGrCrCrArCrArGrCrCrUrCrUrUrCrCrUrCrCrCrUrCrUrCrCrUrU
	3	5'-rGrCrCrArUrArUrGrArUrGrArArCrArGrArArUrUrUrCrAAG	5'-rCrUrUrGrArArArUrUrCrUrGrUrUrCrArUrCrArUrArUrGrGrCrArC
	4	5'-rGrGrArUrGrGrCrUrUrCrCrCrArGrArGrUrCrUrUrCrUrGGC	5'-rGrCrCrArGrArArGrArCrUrCrUrGrGrGrArArGrCrCrArUrCrCrUrU
	1	5'-rGrArArGrGrArGrUrUrGrCrCrUrUrGrGrArGrUrUrUrCrACC	5'-rGrGrUrGrArArArCrUrCrCrArArGrGrCrArArCrUrCrCrUrUrCrArU
	2	5'-rGrGrCrArGrArArArUrCrArCrCrUrCrArUrCrCrArUrUrUrGGC	5'-rGrCrCrArArArArUrGrGrArUrGrArGrGrUrGrArUrUrCrUrGrCrCrUrU
	3	5'-rCrArArGrCrArUrGrGrUrGrUrUrCrUrGrGrGrUrCrCrCrAGC	5'-rGrCrUrGrGrGrArCrCrCrArGrArArCrArCrCrArUrGrCrUrUrGrGrA
	4	5'-rCrUrArGrArArArGrCrUrGrArArUrUrGrGrCrUrGrUrUrGCT	5'-rArGrCrArArCrArGrCrCrArArUrUrCrArGrCrUrUrUrCrUrArGrCrC

Dhcr24	5	5'-rCrCrArArGrArUrCrUrCrCrCrUrCrCrUrGrArArGrCrUrGAC	5'-rGrUrCrArGrCrUrUrCrArGrGrArGrGrGrArGrArUrCrUrUrGrGrGrA
	6	5'-rGrCrArUrGrArGrGrCrArGrCrUrGrGrArGrArArGrUrUrUGT	5'-rArCrArArArCrUrUrCrUrCrCrArGrCrUrGrCrCrUrCrArUrGrCrArG
	7	5'-rGrGrGrArGrArUrGrArArGrCrArGrArGrCrUrCrUrArCrGTG	5'rCrArCrGrUrArGrArGrCrUrCrUrGrCrUrUrCrArUrCrUrCrCrCrUrU
	8	5'-rCrCrUrCrUrArGrArGrUrCrCrArCrUrGrArGrUrCrArCrAAT	5'-rArUrUrGrUrGrArCrUrCrArGrUrGrGrArCrUrCrUrArGrArGrGrArG
	9	5'-rGrUrCrUrUrArArGrArCrGrUrUrGrGrGrArArArGrCrCrUCG	5'-rCrGrArGrGrCrUrUrUrCrCrCrArArCrGrUrCrUrUrArArGrArCrArG
	10	5'-rCrArArGrArArGrArCrCrCrArUrArArGrGrArArCrArUrCrATG	5'-rCrArUrGrArUrGrUrUrCrUrUrArUrGrGrGrUrCrUrUrCrUrUrGrUrA
	11	5'-rCrUrCrUrGrArGrGrUrCrCrUrUrCrUrGrCrCrUrUrGrUrUGA	5'-rUrCrArArCrArArGrGrCrArGrArArGrGrArCrCrUrCrArGrArGrGrC
	12	5'-rGrUrCrArCrArUrUrArGrCrCrUrCrArGrGrUrUrArGrUrGTT	5'-rArArCrArCrUrArArCrCrUrGrArGrGrCrUrArArUrGrUrGrArCrUrC
Hmgcr	1	5'-rCrCrArArUrGrUrCrArUrCrUrUrGrCrUrArArArUrUrCrATG	5’-rCrArUrGrArArUrUrUrArGrCrArArGrArUrGrArCrArUrUrGrGrUrU
	2	5'-rGrCrArUrArUrCrCrCrArGrCrUrUrArCrArArArUrUrGrGAA	5’-rUrUrCrCrArArUrUrUrGrUrArArGrCrUrGrGrGrArUrArUrGrCrUrU
	3	5'-rGrGrArCrUrArArCrArUrGrCrArArUrCrUrGrUrGrArArUTA	5'-rUrArArUrUrCrArCrArGrArUrUrGrCrArUrGrUrUrArGrUrCrCrUrU
	4	5'-rGrArArCrCrArGrArArGrCrUrUrUrCrGrUrCrArGrUrArGAG	5'-rCrUrCrUrArCrUrGrArCrGrArArArGrCrUrUrCrUrGrGrUrUrCrCrU
	5	5'-rCrArArGrGrArGrCrArUrGrCrArArArGrArCrArArUrCrCTG	5'-rCrArGrGrArUrUrGrUrCrUrUrUrGrCrArUrGrCrUrCrCrUrUrGrArA
	6	5'-rGrGrArCrArUrUrGrArGrCrArArGrUrGrArUrUrArCrCrCTG	5'-rCrArGrGrGrUrArArUrCrArCrUrUrGrCrUrCrArArUrGrUrCrCrArU
	7	5'-rCrArGrCrCrArArGrGrUrGrGrUrGrArGrArGrArGrGrUrGTT	5'-rArArCrArCrCrUrCrUrCrUrCrArCrCrArCrCrUrUrGrGrCrUrGrGrA
	8	5'-rGrGrGrUrCrArArGrArGrArUrGrArUrUrArUrGrUrCrUrUrUrAGG	5'-rCrCrUrArArArGrArCrArUrArArUrCrArUrCrUrUrGrArCrCrCrUrU

2.4.3 qPCR

Real-time quantitative polymerase chain reaction (qPCR) was performed to validate the efficiency of gene knockdown following transfection using PrimeTime qPCR assays (IDT). Transfected cells were grown to confluence and a sample of 10^5 cells lysed using Cell-to-CT kit (Ambion/Life Technologies) according to the manufacturer's instructions. Complementary DNA (cDNA) was generated using reverse transcription (RT) PCR of cell lysates according to the manufacturer's instructions. Briefly, cell pellets were lysed by incubating in 50µl Ambion lysis buffer containing 2U DNase I for 8 minutes at room temperature. Ten microlitres of lysate was added to 40µl of Ambion RT master mix and heated at 37°C for 1 hour followed by 95°C for 5 minutes. qPCR was then performed using the Ambion Taqman system as described by the manufacturer in conjunction with custom PrimeTime qPCR assays purchased from IDT. Per 20µl reaction 10µl ABI master mix, 2µl PrimeTime assay, 1µl housekeeping probe (mouse β-actin, 4µM), 1µl mixed housekeeping primers (at 9µM each) and 2µl nuclease free water were combined with 4µl RT reaction in a single well of an optical plate (Applied Biosystems). The specific PrimeTime primers and probes used for each target are shown in **Table 2.3**. Where possible PrimeTime assays were designed to target exon-exon boundaries and so prevent amplification of genomic DNA. However, this was not possible for murine *Prnp*. A custom, 5' VIC-tagged probe and primer set was designed for murine β-actin for use as a housekeeping gene. qPCR was run on a FAST 500 thermocycler using the manufacturer's standard protocol with 40 cycles of amplification. Relative gene expression was then calculated using the $\Delta\Delta C_T$ method where:

$$Percentage\ gene\ expression = 100 \times 2^{-\Delta\Delta CT}$$

***Table 2.3 Gene targets and the relevant PrimeTime assay qPCR primers and probes designed for each**. All probes were labelled with 6-FAM/ZEN/IBFQ 5'-3' as described by IDT, assays were designed to deliver a primer to probe ratio of 2.0.*

Target		Sequence
Prnp	*Forward primer*	CTTCCTCATCTTCCTGATCGTG
	Probe	CTTGTTCCTTCGCATTCTCGTGGTCT
	Reverse Primer	GGGACACAGAGAAGCAAGAAT
Npc1	*Forward primer*	TTTCTGATAACCCCAACCCC
	Probe	AGTGGCCCCAATGTAAGTGTCATCTC
	Reverse Primer	GTCAGCGGAGGTCTTAAGTATG
Npc2	*Forward primer*	TCAACATCACCTTTACCAGCG
	Probe	CACTCAGTCCCAGAACAGCACGG
	Reverse Primer	TGATTCCACTCTTACAACCGTC
Dhcr24	*Forward primer*	AGAACTACCTGAAGACAAACCG
	Probe	CCCTGAGACACTACTACCACCGACA
	Reverse Primer	GAAGAGGTAGCGGAAGATGG
Hmgcr	*Forward primer*	GCCCTCAGTTCAAATTCACAG
	Probe	TGCCATTCCACGAGCTATATTTTCCCTT
	Reverse Primer	TTCCACAAGAGCGTCAAGAG
β-Actin	*Forward primer*	ACCTCCTACAATGAGCTGCG
	Probe	TCTGGGTCATCTTTTCACGGTTGGC
	Reverse Primer	CTGGATGGCTACGTACATGG

2.4.4 Western blotting

Western blots were performed alongside qPCR to validate the knockdown efficiency of DsiRNA transfection and examine effects on other proteins. Transfected cells were grown to confluence in a 96-well plate and ~7×10^5 cells (10 wells) collected and pelleted. Pellets were lysed in radio immunoprecipitation assay (RIPA, 50mM Tris, 150mM NaCl, 0.5% sodium deoxycholate, 1% Triton (v/v), pH 7.4) buffer containing 0.4 µl benzonase and 1 µl protease inhibitor cocktail (Sigma) per millilitre and mixed 1:1 with 2× SDS Sample buffer (Novex) containing 4% 2-mercaptoethanol before heating for 5 minutes at 100°C. Forty microlitres of each sample were then transferred to a 16% Tris/Glycine gel and run alongside SeeBlue Plus 2 ladder (Life Technologies) for 90 minutes at 200V in SDS/TRIS/glycine running buffer (pH 8.3). The gel was blotted onto PVDF membrane in Tris/glycine blotting buffer containing 20% methanol (v/v, pH 8.5) at 35V for 180 minutes. Both running and blotting buffers were obtained as 10X solutions from Pierce. The membrane was blocked with 5% milk in PBST (PBS with 1:200 Tween-20 added) for 30 minutes and then incubated overnight at room temperature with the required primary antibody in PBST (typically at a 1:5000 dilution of manufacturer's stock unless otherwise noted). Actin was used as a loading control: the membrane was cut between the protein of interest and actin using the ladder as a guide and blocked as above. The actin section of membrane was incubated overnight with mouse anti-actin (AbCam, 1:8000) and processed in parallel with the membrane section containing the protein of interest. Following overnight incubation the membrane was washed in PBST (3x5 minutes) and incubated with the relevant chemiluminescence-conjugated secondary antibody (typically 1:6500 in PBST, 1:10000 for actin) for one hour at room temperature. The membrane was then washed in PBST again as above, drained and incubated for 5 minutes with West Pico chemiluminescence substrate (Thermo Fisher) before draining and exposing to film (Biomax MR, Kodak) under a red safelight. For targets of a similar size to actin, including PrP, it was not possible to cut the membrane and label both simultaneously. Instead membranes were stripped and re-probed for actin to confirm

equal loading. Membranes were washed 3x1 minute with PBS and then incubated for 15 minutes with 5ml Restore Western blot stripping buffer (Sigma) at room temperature. Membranes were then again washed 3x1 minute with PBS and blocked with 5% milk/PBST as above before re-probing with anti-actin. Western blotting was analysed using greyscale scanned JPEG images in ImageJ software.

2.4.5 Amplex Red assay to determine cholesterol levels

Quantification of cholesterol in cells can be assessed by filipin labelling but this did not allow for high throughput screening. The Amplex Red cholesterol assay (Invitrogen) allows for colorimetric measurement of cholesterol and cholesteryl ester levels within cells based on the oxidation of cholesterol to resurofin and quantifies cholesterol levels in 96-well plate format. Cells were transfected and grown as for Western blotting above. Confluent cells were washed once with PBS and then lysed using 200µM sucrose in TE buffer (100µl/well) before being diluted 1:10 with Amplex Red reaction buffer. Fifty microlitres of diluted sample was transferred to a black-wall 96-well plate to which 50µl of Amplex Red master mix (prepared according to manufacturer's instructions) was added. Samples were excited at 540nm with emission read at 590nm at 10 minute intervals (up to 40 minutes) whilst incubating at 37°C. Peak signal was typically observed after 30 minutes incubation.

2.4.6 Ultracentrifugation to isolate lipid rafts on Optiprep gradients

Lipid rafts were isolated in a protocol adapted from the work of Waheed and Jones (2002). Cell pellets of 3 million cells were resuspended in 1ml of TNET buffer (50mM Tris-HCl, pH 7.4, 150mM NaCl, 5mM EDTA, 0.5% (v/v) Triton X-100, pH 7.4) containing 1µl/ml protease inhibitor cocktail (Sigma), incubated on ice for 20 min, and then homogenized by vortexing for 30 seconds. The cell lysate was adjusted to 35% Optiprep (Sigma, 1.5ml Optiprep, 1ml lysate) and overlaid with 6ml of 30% Optiprep in TNET (3ml Optiprep, 3ml TNET) and then with 500µl of 5% Optiprep in TNET, in Beckman SW 41 tubes. Samples were centrifuged for 16 hours at 41000rpm (equivalent

to 207000 x *g* across samples) at 4 °C and fractionated from the top. The fractions 1-9 defined as 1ml fractions and further divided into 333µl fractions to better examine gradients. Aliquots of 333µl fractions were pooled to reconstitute a complete gradient of 1ml fractions (see **Figure 2.2**). Collecting fractions in this way allowed for examination of the complete gradient as well as a more detailed look at the fractions immediately containing PrP^C in optimisation experiments. SDS sample buffer containing 4% 2-mercaptoethanol was added to aliquots of each fraction of the gradient in equal parts and run on Western blot as described above (2.4.4). The cholesterol content of fractions was determined by Amplex Red assay as described above (2.4.5). Aliquots of each fraction were diluted 1:10 for the assay and fluorescence compared to a standard curve of cholesterol concentrations to quantify the concentration of cholesterol per sample.

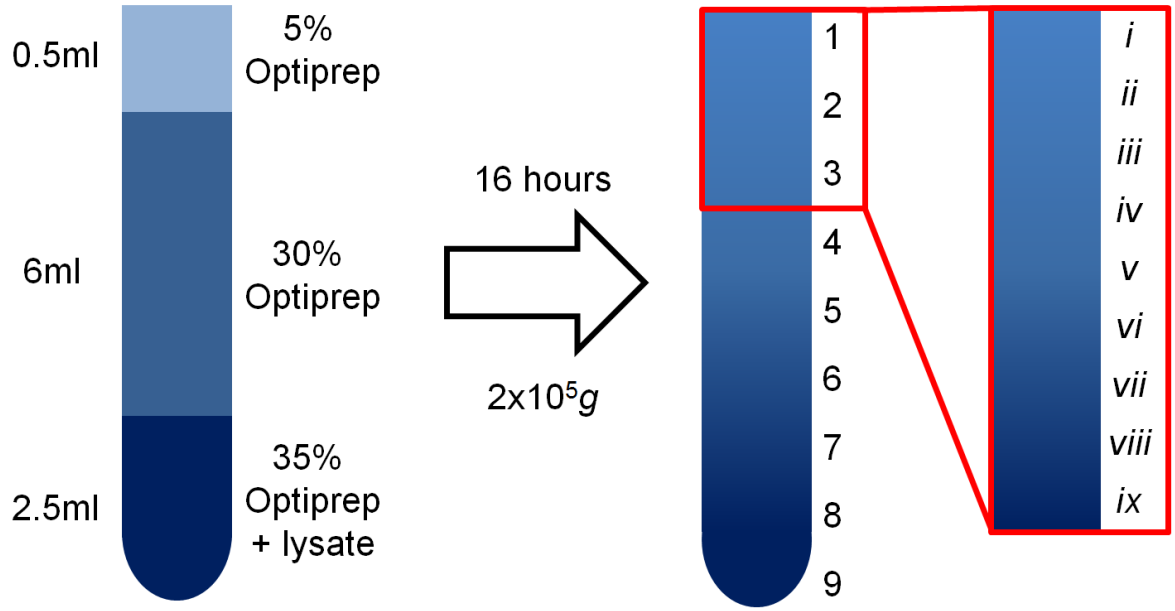

Figure 2.2 Formation of Optiprep gradients to isolate lipid rafts *Following ultracentrifugation a continuous Optiprep gradient was formed. Fractions 1-9 were defined as 1ml each subsequently collected from the top of the gradient. To better examine insoluble proteins near the top of the gradient in some experiments fractions were collected at smaller volumes and aliquots pooled to reconstitute the original fractions.*

2.4.7 Cholera Toxin labelling of fractions

Where required lysates were pre-incubated with biotinylated cholera toxin subunit B (CtxB-b) to label GM1 gangliosides and so identify raft-containing Optiprep fractions. Pellets of $3x10^6$ cells

in 1.5ml Eppendorf tubes were resuspended in 500µl 10µg/ml CtxB-b in PBS and rocked for 45 minutes at 4°C. Samples were then washed 3 times by centrifuging at 16000*g* for 5 minutes and resuspending the pellet in 500µl PBS. Washed samples were then run on Optiprep gradients as above (**2.4.6**). To visualise CtxB-b membranes were blocked overnight in 5% milk/PBST followed by 1 hour incubation with 1/10000 streptavidin-HRP (Life Technologies) in PBST. After washing with PBST 3 times for 5 minutes the membranes were incubated with West PICO and exposed to film as described (**2.4.4**).

2.5 Subcloning

Cells were plated at limiting dilutions (100-200 cells/plate) into 10cm petri dishes and allowed to grow for seven days. Monoclonal colonies were picked using a p20 pipette and transferred into single wells of a 96-well plate. To synchronise cell growth of distinct subclones, cells were split for 2-3 passages at approximately 70% confluence. Clones with very fast or very slow cell doubling rates were discarded.

2.5.1 Cryopreservation of subcloned cells

Subcloned cells were frozen in 96-well plates to preserve subcloned variations which may affect prion propagation. Clones selected for SCA were duplicated in 96-well plates and grown to confluence before cryopreservation. Confluent wells were re-suspended in 150µl of growth medium and then gently mixed with a further 100µl of growth medium, containing 30% DMSO to give a final DMSO concentration of 12%. To prevent degassing of media during freezing, 50µl sterile mineral oil (Sigma) was layered above the growth medium. Plates were sealed with Parafilm and immediately insulated by swaddling in tissue and placing in Styrofoam boxes. These boxes were then placed into a freezer overnight at -80°C. Frozen plates were removed from insulation and stored at -80°C until required. Selected clones were resurrected by rapidly thawing the entire plate in a 37°C water bath. Plates were then cleaned externally with 70% ethanol and placed into a tissue culture MSC, Parafilm was removed and discarded and the

mineral oil layer carefully removed from wells by pipetting. Fifty microlitres of fresh growth media was added to wells and the entire plate was then placed into standard tissue culture conditions for approximately 16 hours. After cells adhered the medium was removed. The wells of selected clones were suspended in 300µl of fresh growth media and transferred to fresh plates for expansion.

2.5.2 Identification of prion susceptible cell lines

To characterise the suitability of cells for inclusion in this study cells were subjected to the SCA using serial dilutions of RML and Me7 homogenates from 10^{-3} down to 10^{-5}. Uninfected cells from each line were used as negative controls. Suitable cell lines were those judged to be similarly infected by each homogenate according to Elispot spot count. In late 2012 we purchased a small stock of 22L prions from the Roslin Institute, Edinburgh, to include in the study. The CAD5 cell line was screened against RML, Me7 and 22L at 1:10 serial dilutions of each homogenate between 10^{-4} and 10^{-7}.

2.5.3 Identification of exclusively propagating clones

Subclones were infected with two different prion strains, RML and 22L. The selectivity score (SS) is defined as the proportion of spots generated by RML infection compared to the number of spots from both 22L and RML:

$$SS = \frac{RMLspots}{RMLspots+22Lspots}$$

After examining pilot data we found it was necessary to further rank hit subclones based on the degree to which the preferred strain was propagated over the non-preferred strain. We therefore calculated the fold difference (FD) as the ratio of spots from preferred strain to spots from the non-preferred strain.

$$FD = \frac{Preferred\ strain\ spots}{Non-preferred\ strain\ spots}$$

CHAPTER 3 RESULTS

3.1 Investigating the role of cellular cholesterol in prion propagation

3.1.1 Rationale

The prion protein incorporates into lipid-rich detergent resistant domains in the cell membrane ('lipid rafts') by virtue of its GPI-anchor. Lipid raft association affects the function of mature PrP^{C} (Lewis and Hooper, 2011) and influences intracellular trafficking of the prion protein (Morris et al., 2006). Lipid rafts containing PrP are cholesterol rich and are required for cell surface localisation of PrP (Gilch et al., 2005). Controversy exists as to whether lipid rafts facilitate or limit prion replication and has prompted investigations into how different raft components interact with PrP.

Early work by Albert Taraboulos and colleagues demonstrated that inhibition of cholesterol synthesis impaired prion propagation (Taraboulos et al., 1995). Similarly in several studies treatment with statins, which inhibit cholesterol synthesis, increased lifespan of prion infected mice but did so without any apparent changes in levels of cholesterol or PrP^{Sc} (Mok et al., 2006, Kempster et al., 2007, Haviv et al., 2008). In cell free models of prion conversion such as Protein Misfolding Cyclic Amplification (PMCA) lipids are required as a co-factor for prion conversion; synthetic lipids have been used for minimal component PMCA and lipids may form a compartment which increases proximity of PrP^{C} and PrP^{Sc} during prion conversion (NR et al., 2007, Wang et al., 2010). Interestingly depletion of glypican-1, which promotes association of PrP^{C} with lipid rafts, has been shown to reduce prion propagation (Hooper, 2011). Lipid rafts are disputed as a site for prion conversion, with other studies suggesting that acidic organelles such as lysosomes may be the site of prion replication (Borchelt et al., 1992, Marijanovic et al., 2009, Yim et al., 2015). A recent review (Hannaoui et al., 2014) addressed evidence for cholesterol as a co-factor for prion conversion but did little to investigate contradictory findings.

Work in the group of Chiara Zurzolo shows that lipid raft association stabilises PrP (Sarnataro et al., 2004), which may limit prion replication. Similarly in a cell free model Baron and Caughey

demonstrated that prion replication is limited by linking PrP^C to raft-like liposomes by a GPI anchor (Baron and Caughey, 2003). It is possible that lipid raft components other than cholesterol influence prion replication. Indeed Naslavsky et al have demonstrated that the rate of prion replication is inversely proportional to the sphingomyelin content of cultured prion-infected neuroblastoma cells (Naslavsky et al, 1999). In light of the work of Prinz et al, which showed that oligodendrocytes are resistant prion infection (Prinz et al, 2004), it is likely that sphingomyelin limits prion replication.

The aim of this project was to investigate the effect of depletion of *Hmgcr, Dhcr24, Npc1* and *Npc2*; and subsequent changes in cholesterol, on prion propagation. In this chapter I will present evidence that cholesterol limits prion replication in cells. We employed a gene silencing approach to inhibit both cholesterol synthesis and trafficking, and show here that reducing available cholesterol in cells increases prion replication *in vitro.*

3.1.2 Perturbing cellular cholesterol synthesis increases prion replication

Previously chronic prion infection has been shown to induce expression of cholesterogenic genes in cells (Bach et al., 2009). However, we observed no difference in total cellular cholesterol between S7 and iS7 in the Amplex Red cholesterol assay (**Figure 3.1 D**). Notably in the work of Bach et al, chronic prion infection increased expression of *Srebp2*, a transcriptional activator of *Hmgcr*. *Hmgcr* encodes 3-hydroxy-3-methyl-glutaryl-CoA reductase (HMGCR), the rate limiting step of cholesterol synthesis. We reasoned that as HMGCR acts early in the cholesterol synthesis pathway production of intermediate molecules would also be affected by increased HMGCR activity. In an attempt to avoid perturbation of intermediate molecules in cholesterol synthesis we elected to also investigate the effects of perturbing 3β-hydroxysteroid-Δ24 reductase, which catalyses the final step in cholesterol synthesis and is encoded by *Dhcr24*.

The Scrapie Cell Assay (SCA) is a method for detecting infectious prion titres in cultured cells (Klohn et al., 2003). Prion infected cells are passaged over multiple splits before quantifying the

number of cells containing PrP^{Sc} by Elispot (see **Methods 2.2.1**). Gene silencing of both *Dhcr24* and *Hmgcr* led to an increase in PrP^{Sc}-positive cells in both the SCA and in chronically prion infected cells (**Figure 3.1 A, B**). A similar increase in PrP^{Sc}-positive cells was seen regardless of which gene was silenced, suggesting reduction of cholesterol rather than an unexpected effect of either gene was responsible for increased prion replication. Silencing of both *Dhcr24* and *Hmgcr* by siRNA was recapitulated in CAD5 cells and was associated with a significant increase in PrP^{Sc}-positive cells in the SCA (**Figure 3.1 C**). Multiple siRNAs were tested for each gene; the relative change in PrP^{Sc}-positive cells for S7 and CAD5 cells are summarised in **Table 3.1**.

Despite testing multiple commercial antibodies per target it was not possible to gauge the level of Dhcr24 or Hmgcr protein due to poor antibody specificity. Similarly we discovered late in the project that our cDNA preparation and qPCR protocols, from which we had been quantifying siRNA effects on mRNA levels, were prone to contamination and so we elected to gauge siRNA effect by cholesterol phenotype. Silencing of *Dhcr24* reduced cholesterol in cells as measured by Amplex Red assay (**Figure 3.1 E**). Furthermore, silencing *Hmgcr* reduced filipin labelling in cells compared to controls (**Figure 3.1 F**). As silencing *Dhcr24* can lead to accumulation of desmosterol (Waterham et al., 2001, Zerenturk et al., 2013), and filipin is a semi-promiscuous label which can stain sterols other than cholesterol, this method was not employed to visualise cholesterol in cells where *Dhcr24* was silenced.

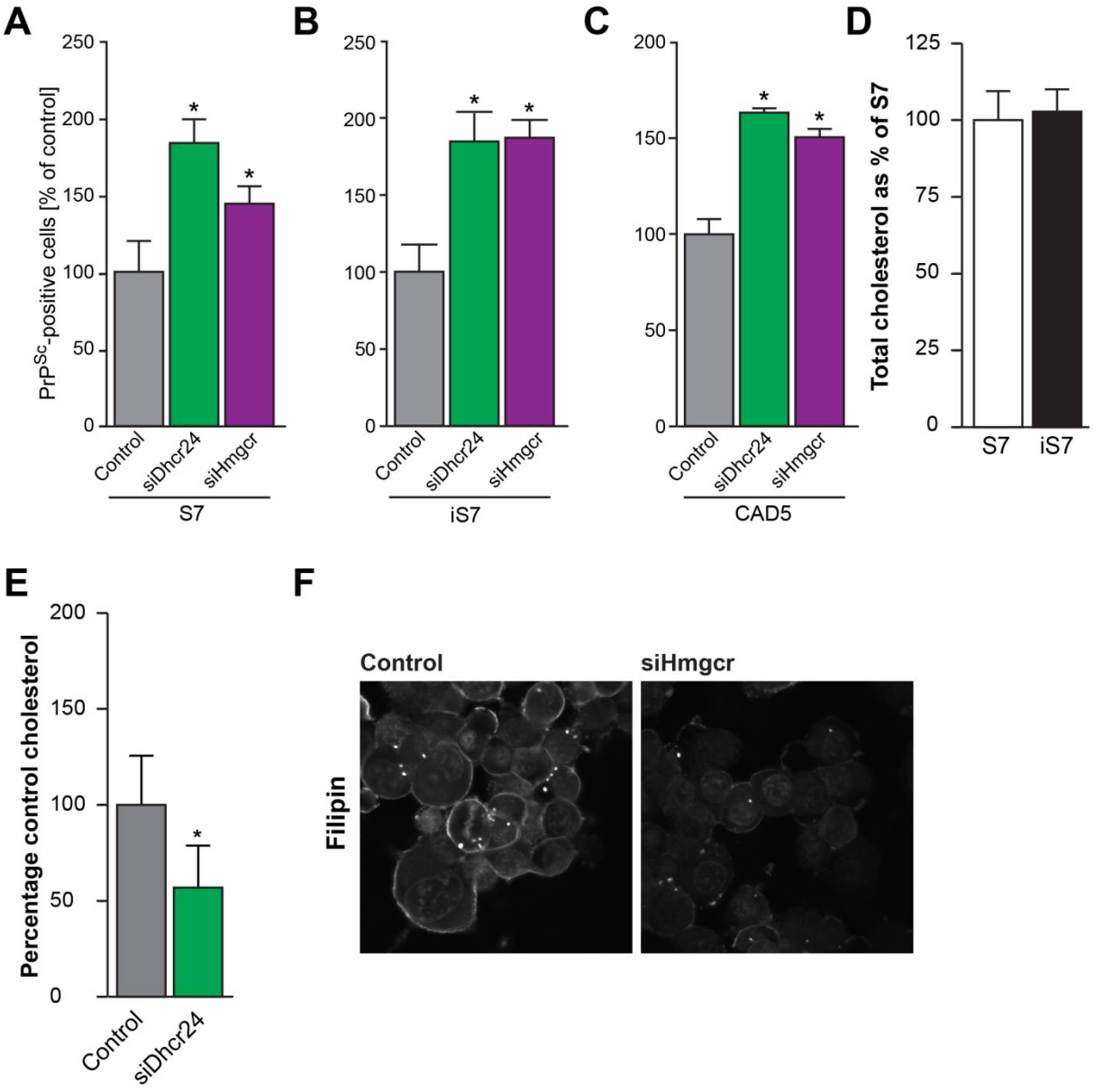

Figure 3.1 Silencing Dhcr24 and Hmgcr increases prion propagation *Dhcr24 and Hmgcr were transiently silenced in cells by transfection with siRNA. S7 (**A**) and CAD5 (**C**) cells were infected with 10^{-5} RML prion brain homogenate in cell culture media 3 days after transfection and passaged 3 times in the SCA. Chronically RML-infected iS7 cells were seeded for Elispot 3 days post-transfection (**B**). The proportion of PrP^{Sc}-positive cells on Elispot assay was normalised to percentage of control cells transfected with non-silencing siRNA. Total cholesterol in samples of S7 and iS7 cells was determined using the Amplex Red assay and normalised to total S7 cholesterol (**D**). **E** Dhcr24 was transiently knocked down in S7 cells by siRNA transfect. After 3 days growth total cholesterol levels were determined by Amplex Red assay and normalised to S7 cells transfected with non-silencing siRNA. **F** Hmgcr was transiently silenced in S7 cells by siRNA transfection. After 3 days growth cells were fixed with PFA, permeabilised with digitonin and labelled with filipin. Multiple siRNAs (outlined in **Table 3.1**) were tested against non-silencing control siRNA. Significant difference to control was calculated using Student's t-test, * p<0.01*

Lovastatin inhibits the activity of HMGCR and so inhibits cholesterol synthesis. Treating iS7 cells with lovastatin was toxic at concentrations above 300nM as measured using the CellTitre Glo ATP assay (Promega). Below this concentration there was a non-significant trend towards increased PrP^{Sc} positive cells following lovastatin treatment (**Figure 3.2 A**). This result contradicts the findings of Taraboulos et al (1995) who reported increased PrP^{Sc} in ScN2a cells following treatment with lovastatin. Crucially, Taraboulos et al treated cells with lovastatin in reduced fat medium and supplemented cells with mevalonate to provide a substrate for non-steroidal pathways in the absence of HMGCR activity. However, as mevalonate is produced by HMGCR-mediated reduction of 3-hydroxy-3-methylglutaryl-CoA this would likely not alter cholesterol levels in cells.

Incubation of S7 cells with methyl-β cyclodextrin (MβCD), a cholesterol sequestering agent, dose dependently reduced total cholesterol measured in the Amplex Red assay (**Figure 3.2 B**). Chronically prion infected iS7 cells treated with MβCD exhibited a trend towards increased PrP^{Sc} positive cells in chronically prion-infected iS7 cells. The number of PrP^{Sc} positive cells declined sharply at concentrations of MβCD of 100uM and above, although toxicity was not detected in the CellTitre Glo assay below 1mM MβCD (**Figure 3.2 C**). Treatment with sub-toxic concentrations of MβCD did not alter levels of PrP^{C} compared to vehicle-treated controls (**Figure 3.2 D**).

Our results demonstrate that perturbing cholesterol synthesis by gene silencing decreases cellular cholesterol and increases prion propagation. Treatment with small molecules to reduce cellular cholesterol did not significantly increase prion replication and proved toxic at higher doses. It is possible that significant increases prion replication were limited in our system by drug toxicity occurring before cholesterol levels had been sufficiently reduced.

Table 3.1 Silencing Dhcr24 and Hmgcr increases prion propagation in S7 and CAD5 cells. *The number of PrP^{Sc}-positive cells on Elispot assay was normalised to fold change compared to control cells for the scrapie cell assay (SCA). Significant differences to control were calculated using Student's t-test (p value). SD – standard deviation. The siRNA sequences are given in* ***Methods Table 2.2****.*

S7				
Gene Target	**siRNA**	**SCA**		
		Fold Change	**SD**	**p value**
Dhcr24	**1**	0.88	0.30	0.066
	2	1.83	0.26	1.118×10^{-27}
	3	1.42	0.28	1.407×10^{-9}
	4	1.39	0.27	2.71×10^{-4}
	5	1.38	0.30	6.72×10^{-3}
	6	0.94	0.37	0.480
	7	0.98	0.21	0.785
	8	0.88	0.21	0.120
	9	0.90	0.20	0.726
	10	0.83	0.18	0.022
	11	1.74	0.38	2.44×10^{-4}
	12	1.63	0.42	8.09×10^{-5}
Hmgcr	**1**	1.01	0.21	0.964
	2	1.44	0.18	4.429×10^{-5}
	3	1.34	0.14	0.003
	4	1.18	0.20	0.054
	5	1.45	0.19	0.003
	6	1.29	0.29	0.209
	7	1.06	0.11	0.058
	8	0.79	0.11	0.048

CAD5				
Gene Target	**siRNA**	**SCA**		
		Fold Change	**SD**	**p value**
Dhcr24	**1**	1.37	0.23	0.002
	2	0.87	0.18	0.198
	3	1.11	0.23	0.263
	4	1.63	0.08	1.263×10^{-8}
Hmgcr	**1**	1.29	0.30	0.009
	2	1.50	0.14	1.918×10^{-6}
	3	1.08	0.22	0.405
	4	1.00	0.22	0.959
	5	1.18	0.20	0.006
	6	1.05	0.16	0.349
	7	1.47	0.20	1.814×10^{-8}
	8	1.18	0.10	6.403×10^{-4}

3.1.3 Increased precursor availability does not increase cellular cholesterol

We reasoned that increased prion propagation following perturbation of cholesterol synthesis may be reversed by increasing cellular cholesterol. Due to difficulties in overexpressing genes in our cell lines we sought other methods to increase cholesterol levels in cells. Squalene is produced by combination of two Farnesyl diphosphate molecules and is a precursor to cholesterol which has been shown to have some protective effects (Gabas-Rivera et al., 2014). Crucially squalene is produced after the action of HMGCR, the rate limiting step of cholesterol biosynthesis. We considered whether supplementing cell media with squalene could drive cholesterol synthesis in cultured cells. Adding 10% squalene to cell media impaired S7 cell growth, and Amplex Red assay of cells treated with squalene at concentrations below this level did not show a significant change in cholesterol levels relative to untreated control cells (**Figure 3.2 E**).

3.1.4 Depletion of lipoproteins in growth serum disrupts S7 cell membranes

As the use of small molecules to reduce cholesterol did not cause significant changes in prion propagation at sub-toxic doses we sought out alternate methods to deplete cholesterol in cells without gene silencing. Reduction of exogenous lipids is frequently used over short incubations to reduce cellular cholesterol (Hao et al., 2001, Cheng et al., 2006, Malnar et al., 2012). As the SCA requires 3 weeks to complete we investigated how prolonged depletion of lipids in serum affected cell viability. Lipoprotein-deficient serum (LDS, Sigma) was used to completely replace the 10% fetal bovine serum (FBS) typically used in production of S7 cell culture medium. S7 cells were grown in chamber slides in medium containing either FBS or LDS for 3 days after which they were fixed, permeabilised and PrP labelled with ICSM18 antibody. Whilst cells cultured with FBS exhibited brightly labelled continuous membrane PrP the membranes of cells cultured with LDS displayed patchy and weakly labelled PrP (**Figure 3.2 F**). Incubation with LDS also reduced total cell numbers, suggesting toxicity or arrested cell growth. Due to the severity of PrP disruption and potential toxic effect LDS was not used for further experimentation.

Figure 3.2 Treatment with small molecules which alter cholesterol levels does not significantly alter prion propagation A *Chronically prion infected iS7 cells were treated with lovastatin for 3 days and seeded for Elispot. The number of PrP^{Sc}-positive cells was normalised to control cells treated with DMSO (blue line). Lovastatin toxicity was assessed as percentage viability of control cells and determined by the CellTitre Glo assay (Promega, red line).* ***B*** *Treatment of cells with methyl-ß cyclodextrin (MßCD) for 24 hours significantly reduced cholesterol in the Amplex Red assay compared to untreated control cells. * p<0.01, Student's t-test.* ***C*** *Chronically prion infected iS7 cells were treated with MßCD for 3 days and seeded for elispot. The number of PrP^{Sc}-positive cells was normalised to untreated control cells (blue line), MßCD toxicity was determined by the CellTitre Glo assay (Promega, red line).* ***D*** *Uninfected S7 cells were treated with MßCD as above and lysed in RIPA buffer. Cell lysates were run on SDS-PAGE and membranes probed for PrP (ICSM18, top blot) and Actin (bottom blot).* ***E*** *The cell culture medium of uninfected S7 cells was supplemented with squalene and cells grown for 3 days. Total cellular cholesterol was determined relative to untreated control cells using the Amplex Red cholesterol assay.* ***F*** *S7 cells were incubated for 3 days with Optimem containing either 10% fetal bovine serum (FBS) or lipoprotein-deficient serum (LDS). Cells were fixed with 4% PFA for 20 minutes, permeabilised with 0.04% Triton X-100 for 10 minutes and PrP labelled with ICSM18 (green).* ***(Figure on next page)***

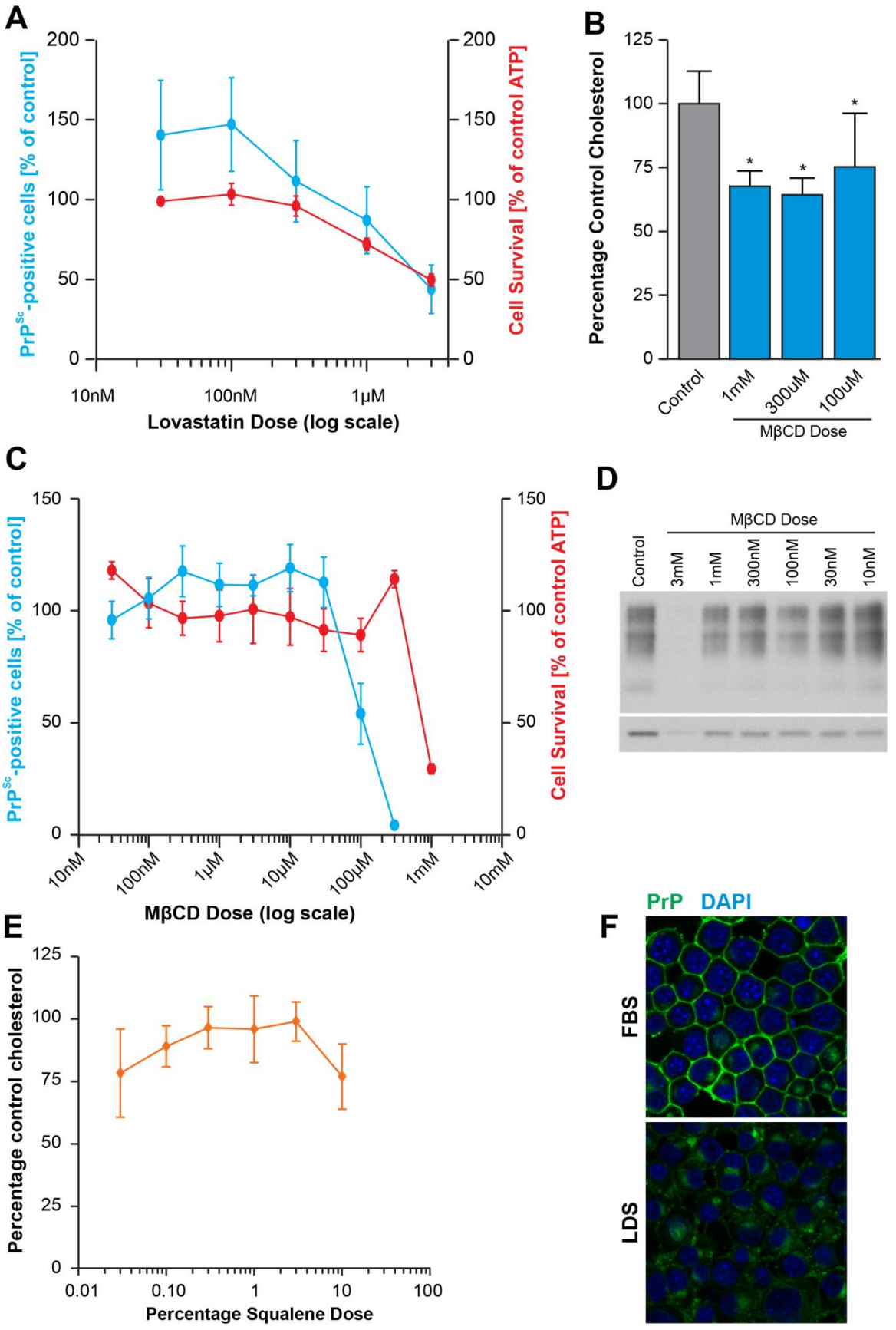
A
PrP^Sc-positive cells [% of control]
Cell Survival [% of control ATP]
200
150
100
50
0
10nM
100nM
1μM
Lovastatin Dose (log scale)
B
Percentage Control Cholesterol
125
100
75
50
25
0
Control
1mM
300uM
100uM
MβCD Dose
C
PrP^Sc-positive cells [% of control]
Cell Survival [% of control ATP]
10nM
100nM
1μM
10μM
100μM
1mM
10mM
MβCD Dose (log scale)
D
MβCD Dose
Control
3mM
1mM
300nM
100nM
30nM
10nM
E
Percentage control cholesterol
0.01
0.10
1
10
100
Percentage Squalene Dose
F
PrP
DAPI
FBS
LDS

3.1.5 Optimisation of filipin labelling

Filipin III is a sterol binding protein which is fluorescent under ultraviolet excitation. Filipin optimisation was performed in untransfected S7 cells and first required optimisation of fixation conditions. Cells were fixed with 4% PFA for either 10 or 20 minutes followed by permeabilisation with either Triton-X 100 (TX100) or digitonin and then labelled with varying concentrations of filipin. Treatment with ice cold acetone for 30 seconds was used to strip neutral lipids from fixed cells and so provide a negative control for optimisation. At 20 minutes PFA fixation filipin was found to produce auto-fluorescence regardless of the labelling concentration used. Furthermore, permeabilising cells with TX100 disrupted cell membranes and produced bright filipin artefacts. Digitonin permeabilisation left membranes relatively undisrupted and was more effective with increased concentration (**Figure 3.3 A**). As expected increasing filipin concentration increased intensity of labelling. Whilst previous studies have used 5µg/ml filipin to label cholesterol we found that a 10 minute fix with 4% PFA, followed by 5 minutes permeabilisation with 100µg/ml digitonin and labelling with 20µg/ml filipin in PBS gave the best mix of label intensity and contrast on cell membranes (**Figure 3.3 B**). Filipin labelling under these conditions was selective for neutral lipids as demonstrated by loss of signal following 30 seconds acetone treatment (**Figure 3.3 C**). To better reveal intracellular cholesterol fixed cells were instead permeabilised for 10 minutes with 50µg/ml digitonin prior to labelling with 20µg/ml filipin in PBS. These conditions were considered optimal and taken forward for the remaining images shown in this study. Notably we did not observe a phenotypic difference between S7 and chronically prion infected iS7 cells by filipin labelling (**Figure 3.3 D**).

Figure 3.3 Optimisation of filipin labelling A *10ug/ml filipin labelling of S7 cells fixed with 10' 4% PFA and permeabilised with increasing digitonin concentrations for 5' or 10'.* ***B*** *Comparison of 10ug/ml and 20ug/ml filipin labelling of S7 cells following digitonin permeabilisation.* ***C*** *Fixed and permeabilised S7 cells were labelled with filipin following 30s treatment with PBS or ice cold acetone to strip neutral lipids.* ***D*** *Filipin labelling of S7 cells and chronically prion infected iS7 cells in the presence or absence of acetone treatment.* ***(Figure on next page)***

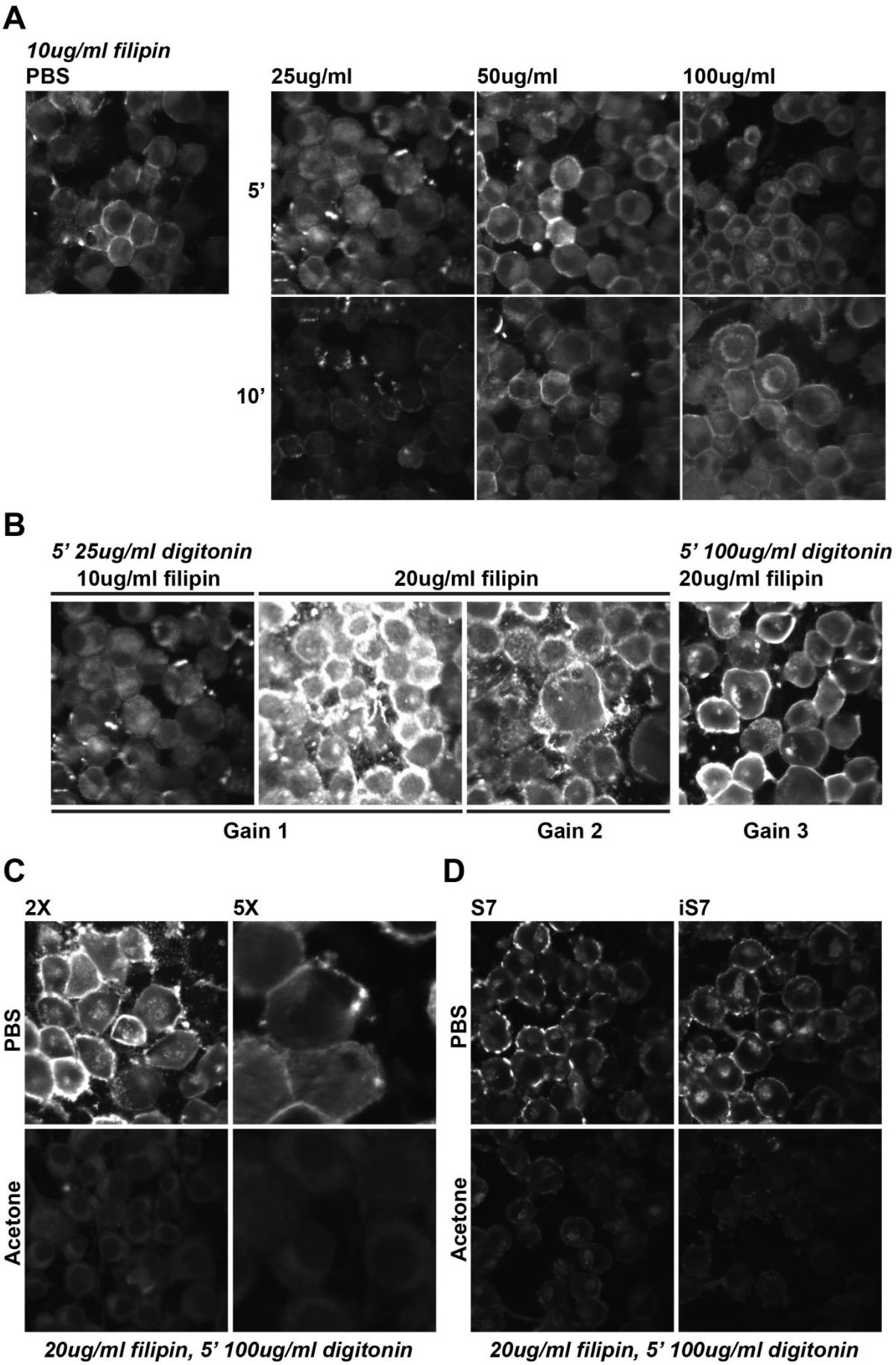
A
10ug/ml filipin
PBS
25ug/ml
50ug/ml
100ug/ml
5'
10'
B
5' 25ug/ml digitonin
10ug/ml filipin
20ug/ml filipin
5' 100ug/ml digitonin
20ug/ml filipin
Gain 1
Gain 2
Gain 3
C
2X
5X
PBS
Acetone
20ug/ml filipin, 5' 100ug/ml digitonin
D
S7
iS7
PBS
Acetone
20ug/ml filipin, 5' 100ug/ml digitonin

3.1.6 Silencing Niemann-Pick type C genes impairs cholesterol trafficking

Niemann-Pick type C is a fatal neurodegenerative lipid storage disorder associated with mutations in both *Npc1* and *Npc2* genes (Blom et al., 2003, Sturley et al., 2004). Loss of function of either *Npc1* or *Npc2* has been widely reported to lead to accumulation of cholesterol in lysosomes (Verot et al., 2007, Karten et al., 2009, Vance, 2010, Deffieu and Pfeffer, 2011). Here gene silencing was used to recapitulate loss of Npc1 and Npc2 function in our cell models to examine the effects of impaired cholesterol trafficking on prion replication.

3.1.6 (a) Gene silencing of Npc1 and Npc2 exerts unexpected opposing effects on prion replication

Given Npc1 and Npc2 act sequentially to export cholesterol from lysosomes, and cholesterol is thought to be involved in prion replication, it was expected that gene silencing of *Npc1* and *Npc2* would exert similar effects on prion replication. As previously reported silencing of *Npc1* in S7 cells decreased the number of PrP^{Sc}-positive cells in the SCA (Gilch et al., 2009). Unexpectedly silencing *Npc2* increased the number of PrP^{Sc}-positive cells almost two-fold (**Figure 3.4 A**). Both phenotypes were confirmed across 3 independent experiments containing 12 technical repeats each ($p<0.01$). Similarly silencing *Npc1* in chronically infected iS7 cells decreased PrP^{Sc}-positive cells, but silencing *Npc2* did not produce a significant effect compared to non-silencing control (**Figure 3.4 B**). Gene silencing with siRNA was also performed in CAD5 cells. Silencing *Npc2* increased the number of PrP^{Sc} positive cells; however an increase in PrP^{Sc} positive cells was also seen following *Npc1* silencing (**Figure 3.4 C**). As with *Hmgcr* and *Dhcr24* Multiple siRNAs were tested for *Npc1* and *Npc2*; the relative change in PrP^{Sc}-positive cells for S7 and CAD5 are summarised in **Table 3.2**.

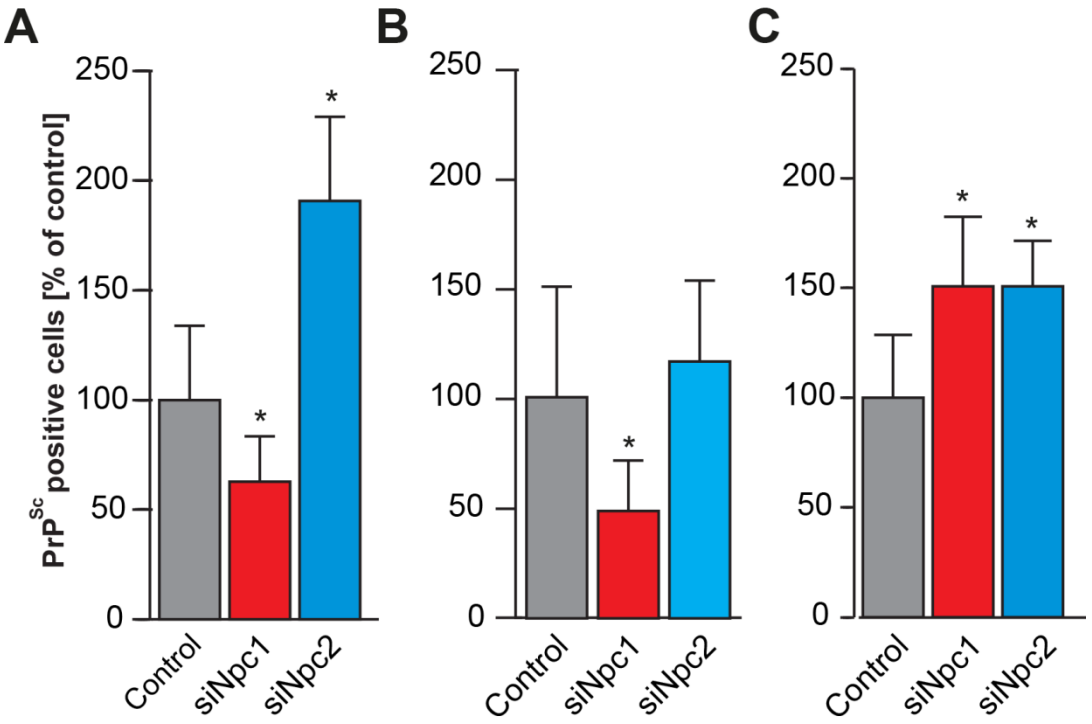

Figure 3.4 Silencing Npc1 and Npc2 alters prion propagation *Npc1 and Npc2 were transiently silenced in cells by transfection with siRNA. S7 (**A**) and CAD5 (**B**) cells were infected with 10^{-5} RML prion brain homogenate in cell culture media 3 days after transfection and passaged 3 times in the SCA. Chronically RML-infected iS7 cells were seeded for Elispot 3 days post-transfection (**C**). The proportion of PrP^{Sc}-positive cells on Elispot assay was normalised to percentage of control cells transfected with non-silencing siRNA. Significant difference to control was calculated using Student's t-test, * p<0.01*

Table 3.2 Silencing Npc1 and Npc2 exert opposing effects on prion propagation in S7 and CAD5 cells. *Gene expression was calculated as percentage expression in control cells transfected with non-silencing siRNA. PrP^{Sc}-positive cells on Elispot assay was normalised to fold change compared to control cells for the scrapie cell assay (SCA). Significant differences to control were calculated using Student's t-test (p value). The siRNA sequences are given in* ***Methods Table 2.2****.*

S7				
Gene Target	**siRNA**	**SCA**		
		Fold Change	**SD**	**p value**
Npc1	**1**	0.98	0.25	0.510
	2	0.63	0.21	6.023×10^{-7}
	3	0.73	0.21	1.466×10^{-4}
Npc2	**1**	1.91	0.38	5.356×10^{-29}
	2	1.29	0.43	6.938×10^{-5}
	3	1.12	0.35	0.087
CAD5				
Gene Target	**siRNA**	**SCA**		
		Fold Change	**SD**	**p value**
Npc1	**1**	1.51	0.32	1.256×10^{-4}
	2	0.95	0.35	0.651
	3	1.01	0.30	0.940
	4	1.22	0.20	0.038
	5	1.53	0.39	2.216×10^{-4}
	6	1.06	0.24	0.553
Npc2	**1**	1.45	0.13	6.970×10^{-5}
	2	1.49	0.30	1.886×10^{-4}
	3	1.51	0.21	3.716×10^{-5}
	4	1.40	0.27	0.001

3.1.6 (b) Gene silencing of Npc1 and Npc2 causes accumulation of cholesterol in lysosomes

*Npc*1 and *Npc2* were silenced by transient transfection of siRNA into cells. Multiple siRNAs were tested per gene target, with the siRNA giving best gene silencing taken forward for further phenotype testing. As with *Dhcr24* and *Hmgcr* despite testing multiple commercial antibodies per target it was not possible to gauge the level of Npc1 or Npc2 protein due to poor antibody specificity. As with our experiments on cholesterol synthesis we elected to qualify siRNA effect by cholesterol phenotype.

To confirm that cholesterol accumulated in lysosomes of *Npc1*- and *Npc2*-silenced cells confocal imaging was used. Initially BODIPY-cholesterol was used to mark cholesterol. Although analysis using Volocity software did show a slight increase in co-localisation of BODIPY-cholesterol with Lamp1-positive vesicles in gene silenced cells (**Figure 3.5 A**) the probe was found to be sensitive to the fixation conditions used and as such an alternate marker of cholesterol was sought. Filipin labelling showed clear accumulation of cholesterol in cells where *Npc1* and *Npc2* were silenced (**Figure 3.5 B**). This suggests that the opposing effects of *Npc1* and *Npc2* silencing on prion propagation in our models are independent of cholesterol as the same cholesterol phenotype is observed with loss of function of both genes.

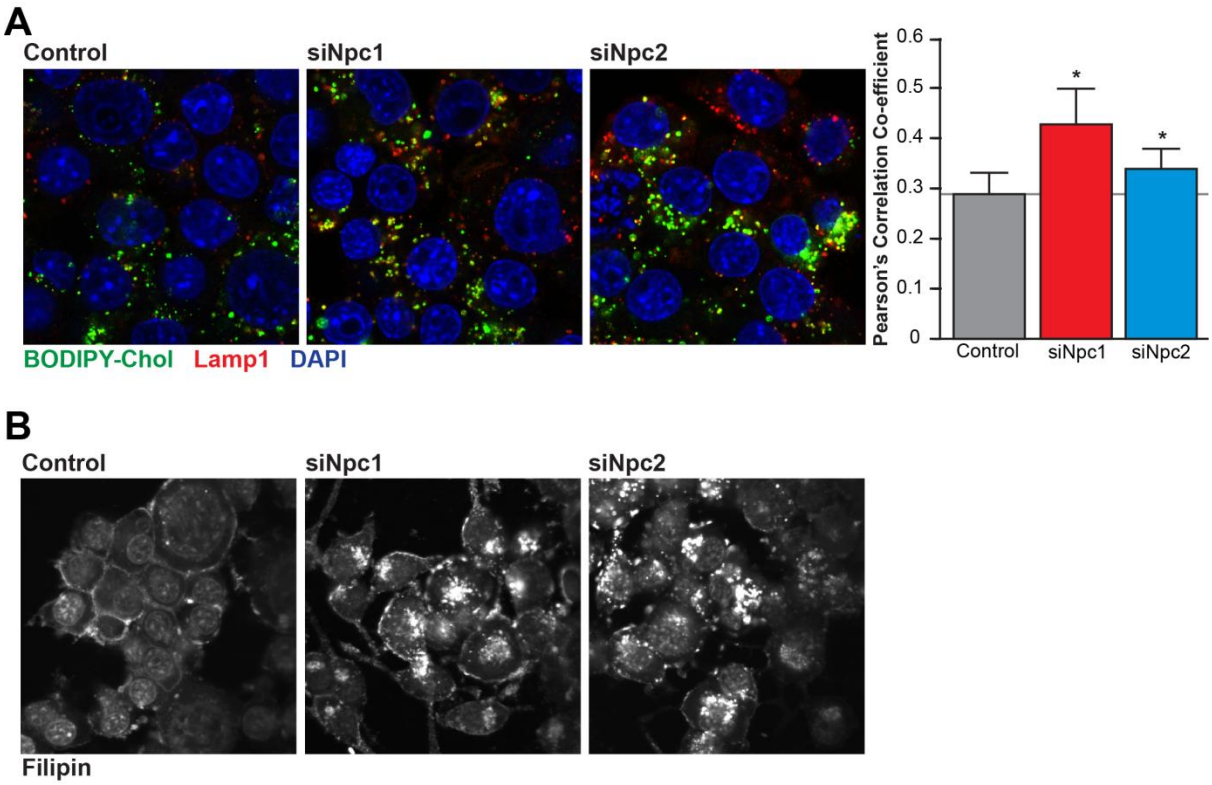

Figure 3.5 Silencing Npc1 and Npc2 causes accumulation of cholesterol in lysosomes A *Co-localisation of BODIPY-cholesterol (green) with Lamp1-positive lysosomes (red) in S7 cells silenced with siRNA targeting Npc1 and Npc2. Chart shows co-localisation of BODIPY-cholesterol and Lamp1 assessed by Pearson's Correlation Coefficient using Volocity software. * p<0.05, mean ± standard deviation of 10 images.* ***B*** *Filipin labelling of S7 cells silenced with siRNA targeting Npc1 and Npc2, fixed by 10' 4% PFA and permeabilised by 10' 50ug/ml digitonin. Representative images shown.*

3.1.7 Gene silencing of Npc1 but not Npc2 reduces PrP^C protein levels

Following the widely accepted Protein-only hypothesis prion replication cannot occur without the availability of PrP^C to act as substrate for conversion to PrP^{Sc}. Altered trafficking of cholesterol may in turn alter trafficking of PrP. Recently work in our lab has uncovered extracellular matrix deposits of disease-associated PrP termed PrP^d (Marbiah et al., 2014), with levels of PrP^d being found to correlate with changes in prion infection. Confocal imaging of chronically prion infected iS7 cells in which *Npc1* had been silenced showed a reduction in both membrane PrP and deposited PrP^d (**Figure 3.6 A**). Gene silencing of *Npc2* led to a marked increase of PrP^d in chronically prion infected cells in line with increased PrP^{Sc}-positive cells in the SCA. Similar imaging of uninfected S7 cells following silencing of *Npc1*, but not *Npc2*, revealed a decrease in membrane PrP^C (**Figure 3.6 B**). This effect was not seen in CAD5 cells (**Figure 3.6 C**). To confirm this reduction in PrP^C was not due to an off-target effect of the siRNA used (siNpc1.2) Western blotting was performed with cell lysates following gene silencing with a further five siRNAs targeting *Npc1*. All siRNAs targeting *Npc1* tested reduced PrP^C compared to control cells treated with non-silencing siRNA; however no siRNA targeting *Npc2* significantly altered PrP^C levels (**Figure 3.6 D**). Silencing of *Npc1* and *Npc2* did not decrease PrP^C levels in CAD5 cells (**Figure 3.6 E**).

Figure 3.6 Silencing Npc1 reduces expression of PrP^C *Npc1 and Npc2 were transiently silenced in iS7 (**A**), S7 (**B**) and CAD5 (**C**) cells in chamber slides by siRNA transfection; after 3 days growth cells were fixed with PFA and permeabilised by 30s treatment with ice-cold acetone and 10 minutes treatment with 3M GTC before antibody labelling PrP (ICSM18, green) and Lamp1 (red). In all cases nuclei were labelled with DAPI (blue). Reduced PrP^C following silencing of Npc1 but not Npc2 was confirmed by Western blotting in S7 cells (**D**) but notCAD5 cells (**E**). The relative density of ICSM18 signal was calculated using ImageJ software and normalised to actin signal. Representative blots shown.* ***(Figure on next page)***

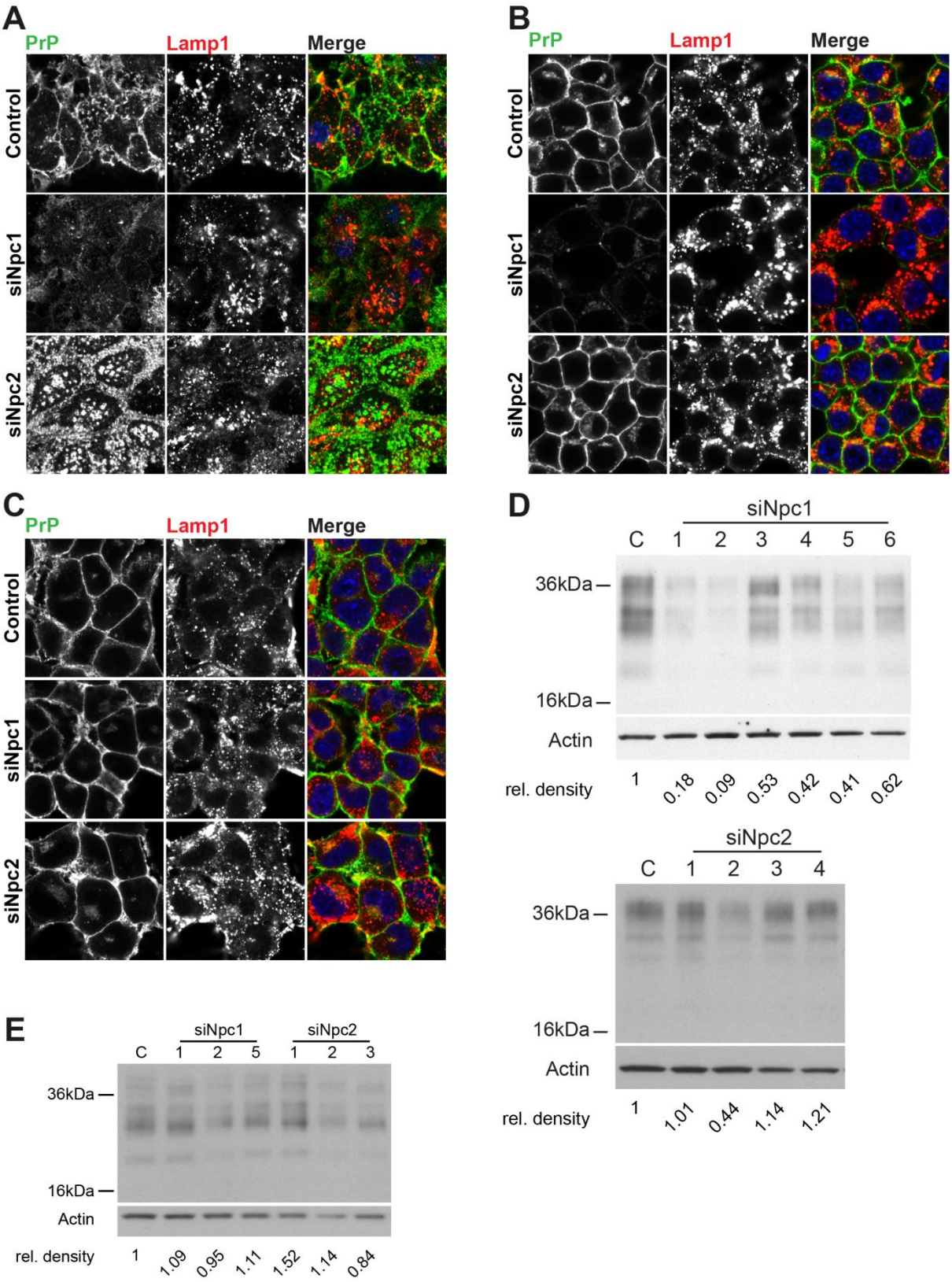
A
PrP
Lamp1
Merge
Control
siNpc1
siNpc2
B
PrP
Lamp1
Merge
Control
siNpc1
siNpc2
C
PrP
Lamp1
Merge
Control
siNpc1
siNpc2
D
siNpc1
C 1 2 3 4 5 6
36kDa
16kDa
Actin
rel. density 1 0.18 0.09 0.53 0.42 0.41 0.62
siNpc2
C 1 2 3 4
36kDa
16kDa
Actin
rel. density 1 1.01 0.44 1.14 1.21
E
siNpc1
siNpc2
C 1 2 5 1 2 3
36kDa
16kDa
Actin
rel. density 1 1.09 0.95 1.11 1.52 1.14 0.84

3.1.8 Gene silencing of Npc1 decreases lysosomal pH

The activity of some lysosomal enzymes is dependent on pH, and many such enzymes are more active in more acidic environments (Pillay et al., 2002). Lysosomal pH is maintained by the flux of ions across the lysosome membrane, particularly the import of H^+ ions via an ATP-dependent pump (Vandyke, 1993, DiCiccio and Steinberg, 2011). The accumulation of cholesterol or other cargo in lysosomes may disrupt ionic flux and so alter lysosomal pH. Intracellular pH changes were monitored by live-imaging of cells pre-incubated with Lysosensor Green DND-189 ('Lysosensor', Life Technologies) which accumulates and exhibits increased fluorescence intensity in acidic compartments. Silencing *Npc1* but not *Npc2* increased Lysosensor fluorescence compared to control cells indicating decreased pH (**Figure 3.7 A**). Increased Lysosensor fluorescence co-localised with Dextran Texas Red in live cells indicating the acidic compartments were lysosomes (**Figure 3.7 B**). Increased lysosomal acidity may in part account for the reduction in PrP^C observed following *Npc1* gene silencing in S7 cells. That we did not see this effect in CAD5 cells suggests reduced PrP^C is due to an unknown factor in N2a-S7 cells and not a direct result of *Npc1* silencing.

We reasoned that the reduction of PrP^C observed following silencing of Npc1 could be due to increased degradation of PrP^C and so may be reversed by directing PrP trafficking away from lysosomes. Rab9 has been shown to function in the transport of mannose-6-phosphate receptors and epidermal growth factor receptors (EGFR) from late endosomes to the trans-Golgi network (Ng et al., 2012) and reversed the effect of U18666A (which can cause phenotypes similar to *Npc1* silencing) in decreasing PrP^{Sc} (Gilch et al., 2009). S7 cells overexpressing Rab9 were kindly provided by Lucy Sheytanova. Overexpression of Rab9 in S7 cells did not rescue PrP^C reduction following *Npc1* silencing (**Figure 3.7 C**).

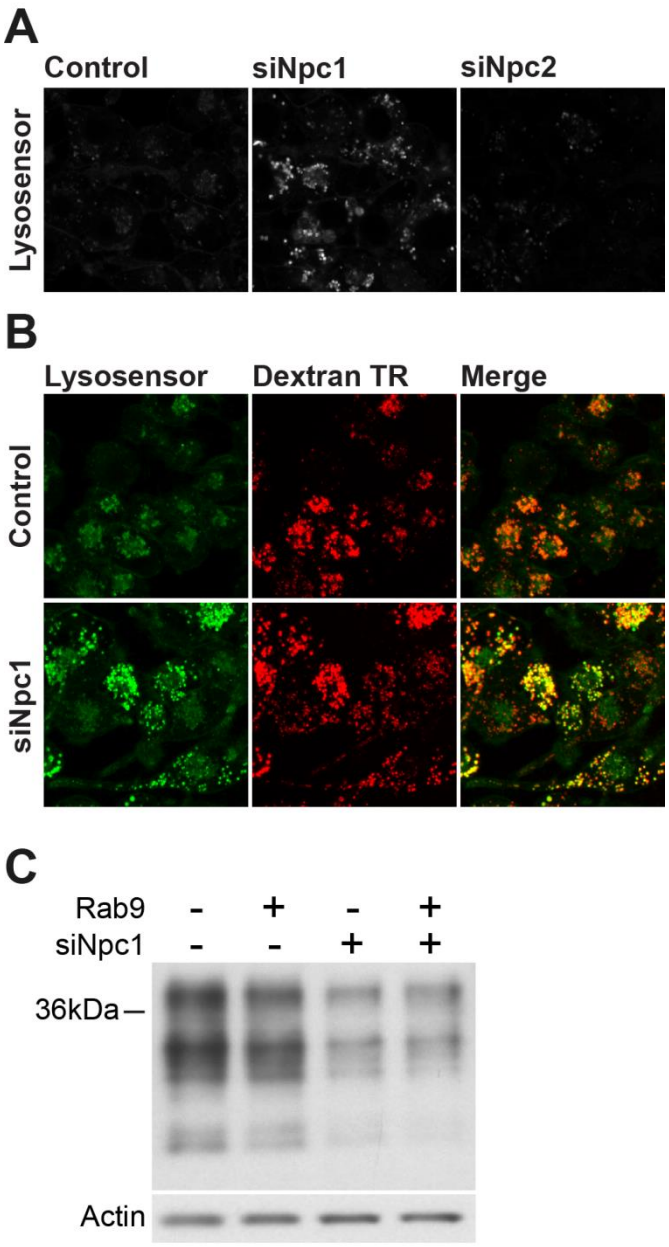

Figure 3.7 Silencing Npc1, but not Npc2, alters lysosomal activity in uninfected cells A *Live cell imaging with lysosensor green DND-189 in cells silenced with siRNA targeting Npc1 and Npc2. Fluorescence indicates acidic compartments.* ***B*** *Co-localisation of lysosensor (green) fluorescence with Dextran Texas Red (red) in S7 cells silenced with siRNA targeting Npc1. Cells were incubated overnight with 100µg/ml Dextran Texas Red followed by 30 minutes incubation with 100nM Lysosensor immediately prior to imaging.* ***C*** *S7 cells stably overexpressing Rab9 or empty pLNCX.2 vector were transfected with siRNA targeting Npc1 and grown for 3 days. Cell lysates were run on SDS-PAGE and membranes probed for PrP (ICSM18, top blot) and Actin (bottom blot).*

3.1.9 Detection of lipid microdomains in the cell membrane

Recent work by Chiara Zurzolo and colleagues (Sarnataro et al., 2004) suggests that PrP^{C} is stabilised in lipid rafts. Theoretically PrP^{C} could become less stable, and so be more readily converted to PrP^{Sc}, if lipid rafts are disrupted. We initially sought to observe changes in lipid rafts by confocal microscopy using GM1 to mark lipid rafts. Cholera toxin subunit B (CtxB) is a well characterised label for GM1 (Vanheyningen, 1976, Jobling et al., 2012) and we employed a pulse-chase protocol to detect changes in both surface presentation and intracellular trafficking of GM1. In chronically infected iS7 cells CtxB co-localised with deposits of disease associated PrP^{d} in the extracellular matrix (**Figure 3.8 A**). S7 cells exhibited very low expression of GM1, with occasional cells showing high CtxB labelling, whilst CAD5 cells displayed an intense membrane signal when labelled with AlexaFluor-555 conjugated CtxB (**Figure 3.8 B**). Colocalisation of CtxB and PrP^{d} in the extracellular matrix of iS7 cells suggested that prion infection caused sequestration of GM1/CtxB into prion deposits, but the scarcity of CtxB-positive iS7 and S7 cells prevented further investigation. The intensity of labelling in CAD5 cells precluded further investigation as it was not possible to view individual lipid raft domains under the conditions tested.

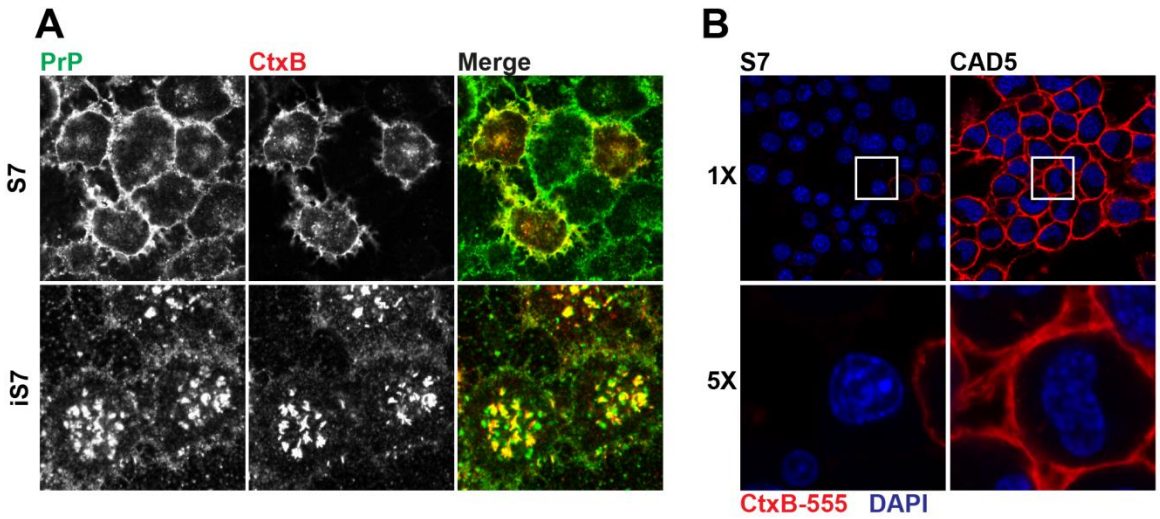

Figure 3.8 Basement membrane deposits of PrP^d contain GM1 A *S7 and iS7 cells were grown in chamber slides, pulsed with 5µg/ml CtxB-555 (red) at 12°C for 30 minutes to label GM1 then immediately fixed with PFA and permeabilised by 30s treatment with ice-cold acetone and 10 minutes treatment with 3M GTC to uncover PrP^d deposits in the basement membrane of infected cells. PrP was labelled with ICSM18 antibody (green) following permeabilisation.* ***B*** *CAD5 cells exhibit higher and more uniform GM1 expression than S7. S7 and CAD5 cells were labelled with CtxB-555 as above, fixed with PFA and permeabilised with 0.04% Triton X-100. All slides were counterstained with DAPI (blue) to label nuclei. Representative images shown.*

3.1.9 (a) Optimisation of gradient centrifugation to isolate lipid rafts

As an alternative to confocal microscopy we instead elected to isolate lipid rafts by gradient centrifugation in order to investigate alterations in rafts following cholesterol perturbation. We adapted the protocol of Waheed and Jones (2002) to isolate lipid rafts by ultracentrifugation on a continuous Optiprep gradient. As our rotor required the use of larger ultracentrifuge tubes than those used by Waheed and Jones the final volume of the gradient was doubled to 9ml as described in Methods (**Section 2.4.6**). In all tests the spin speed was kept consistent at 41000rpm, the maximum available for the SW 41Ti rotor used. At full speed this exerted an average acceleration of 207000*g* down the gradient. As we would be using cultured cells rather than tissue we needed to optimise the number of cells prepared per lysate and so compared pellets of 1 million, 3 million and 10 million S7 cells. No signal was observed following fractioning of 1 million cells but both 3 million and 10 million cells showed good signal in fractions towards the top of the gradient on Western blot (**Figure 3.9 A**). Due to reduced reagent requirements and lower background signal pellets of 3 million cells were taken forward for further experimentation. As PrP was only observed in a single 1ml fraction using 3 million cells the sensitivity of the assay was increased by further dividing fractions 1-4 as described in Methods which allowed for observation of smaller movements of PrP through the gradient.

We reasoned that a 16 hour centrifugation step at over 200000*g* may compress our gradient and lead to PrP only being located in a single fraction. To address this we compared the 16 hour spin to shorter 4 and 8 hour spins at the same speed using 5 million cells per pellet. On short (1 minute) exposure of membrane to film only the 16 hour spin showed detectable PrP in more than one fraction, which was mainly found in the first and second fraction of the gradient (**Figure 3.9 B**). Longer (10 minutes) exposure of film showed detectable levels of PrP across the gradient for both 16 and 8 hour spins, whilst the 4 hour spin showed separate pools of PrP in the upper and lower fractions of the gradient (**Figure 3.9 C**). The 16 hour spin time was selected for further investigation of PrP and lipid rafts. In order to increase resolution down the gradient fractions

were collected in smaller volumes which could be pooled to reproduce the initial 9 fractions as described in Methods (**Section 2.4.6**). Gradient centrifugation of CAD5 cells revealed that PrP^C was primarily located in fractions also containing CtxB-labelled GM1, indicating lipid rafts. Conversely Lamp1, which is found in lysosomal membranes (Carlsson and Fukuda, 1989), was spread across the upper end of the gradient including PrP^C and CtxB-containing fractions (**Figure 3.9 D**).

Figure 3.9 Optimisation of lipid raft isolation using Optiprep gradients A *Pellets of 10^6, $3x10^6$ and 10^7 S7 cells were lysed on ice in 1ml TNET buffer and run on Optiprep gradients for 16 hours as described. 1ml fractions were collected from the top of the gradient and run on SDS-PAGE to probe for PrP (ICSM18). Pellets of $3x10^6$ S7 cells were run on Optiprep gradients at 207000g for 4, 8 and 16 hours. 1ml fractions were collected from the top of the gradient and run on SDS-PAGE to probe for PrP (ICSM18); membranes were exposed for 1 minute (**B**) and 10 minutes (**C**) to determine location of PrP^C. **D** $3x10^6$ CAD5 cells were incubated with 10µg/ml biotinylated CtxB in PBS for 45 minutes at 4°C and washed 3 times by pelleting and resuspending in PBS. Labelled cells were run on Optiprep gradients as above for 16 hours. 1ml fractions were collected from the top of the gradient and run on SDS-PAGE to probe for PrP (ICSM18, top blot) and Lamp1 (bottom blot marked 98kDa). CtxB was detected by blocking membrane overnight in 5% milk/PBST and incubating with Streptavidin-HRP (Sigma, 1:20000 in PBST). Labelling CtxB in this way produced a single band at approximately 11kDa per containing fraction.* ***(Figure on next page)***

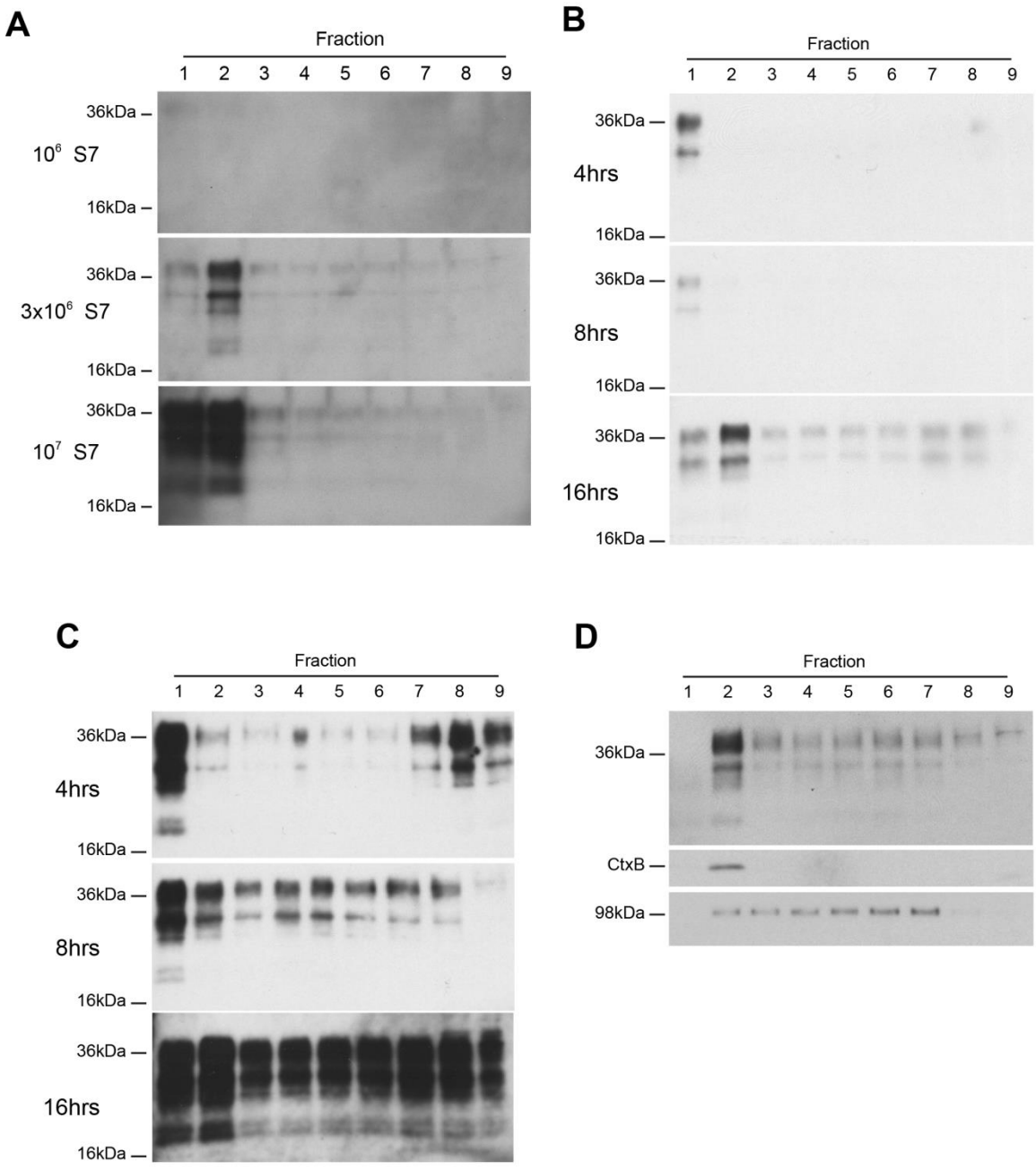
A
Fraction
1 2 3 4 5 6 7 8 9
36kDa
10^6 S7
16kDa
36kDa
3x10^6 S7
16kDa
36kDa
10^7 S7
16kDa
B
Fraction
1 2 3 4 5 6 7 8 9
36kDa
4hrs
16kDa
36kDa
8hrs
16kDa
36kDa
16hrs
16kDa
C
Fraction
1 2 3 4 5 6 7 8 9
36kDa
4hrs
16kDa
36kDa
8hrs
16kDa
36kDa
16hrs
16kDa
D
Fraction
1 2 3 4 5 6 7 8 9
36kDa
CtxB
98kDa

3.1.9 (b) Impaired cholesterol synthesis and trafficking shifts PrP^C from raft fractions to lower buoyant densities

We observed a shift of PrP across the gradients in chronically infected iS7 cells compared to S7 cells (**Figure 3.10 A**) which was also seen in comparison of CAD5 and RML prion infected iCAD5 cells. Labelling CtxB in CAD5 and iCAD5 cells revealed that PrP shifted out of GM1-containing fractions in iCAD5 cells (**Figure 3.10 B**).

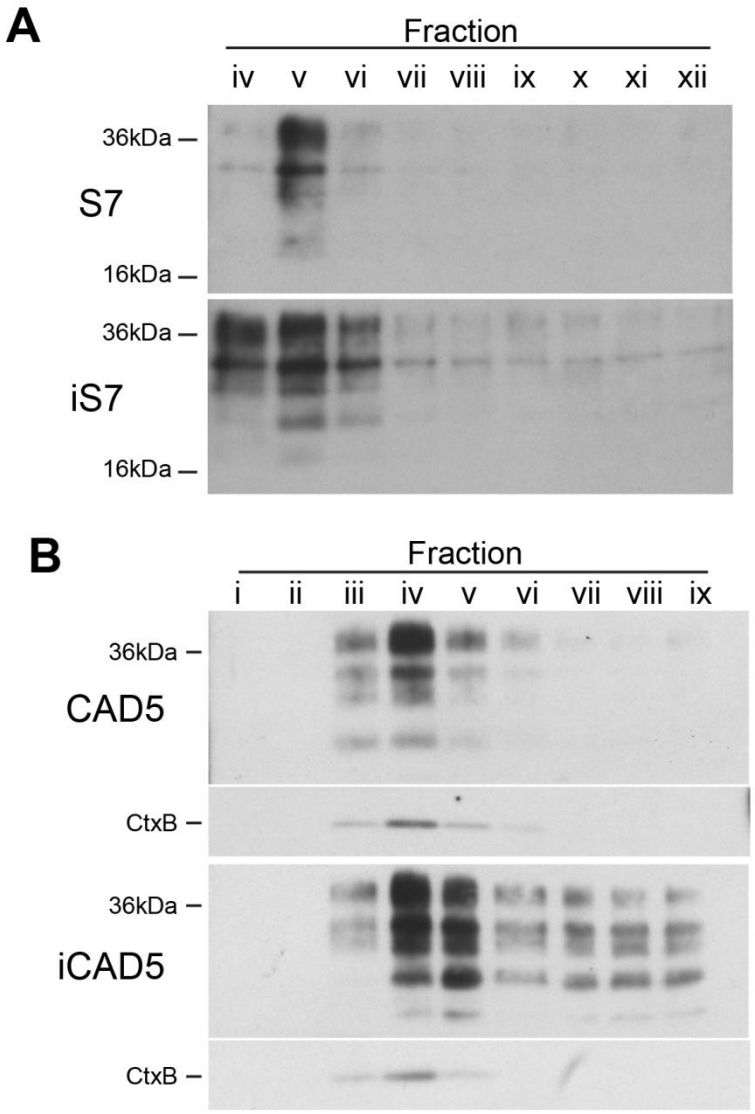

Figure 3.10 Prion infection shifts PrP out of lipid raft fractions on Optiprep gradients *Pellets of $3x10^6$ S7/iS7 (**A**) and CAD5/RML-infected iCAD5 (**B**) were run on Optiprep gradients as described above. Twelve 333µl fractions (i-xii) were collected from the top of the gradients and run on SDS-PAGE to probe for PrP (ICSM18). As above CtxB labelling of CAD5 fractions was achieved by pre-incubation of cell pellets with biotinylated CtxB and probing blotted membranes with Streptavidin-HRP.*

Knockdown of *Dhcr24* has previously been reported to reduce PrP flotation in low-density fractions of sucrose gradients (Crameri et al., 2006). Silencing of both *Dhcr24* and *Npc2* shifted PrP^C down Optiprep gradients compared to control cells (**Figure 3.11 A**). Remarkably this phenotype could be reproduced by siRNA knockdown of *Dhcr24* and *Npc2* in primary neuronal cultures (**Figure 3.11 B**). As with comparison of chronically infected and uninfected cells labelling of CtxB in gradients was limited to CAD5 cells. Silencing *Dhcr24* shifted PrP^C out of CtxB-labelled fractions however silencing *Npc2* also produced a shift of CtxB down the gradient (**Figure 3.11 C**). Gradients were performed a minimum of three times in cultured cells. In primary neurons only two repeats were performed due to time constraints and the availability of acceptable and viable cell cultures. With one exception, as with silencing *Npc2* (see **Figure 3.6**) we did not observe a difference in PrP levels following *Dhcr24* silencing (**Figure 3.12**). In an attempt to better characterise gradients samples were subject to a BCA assay, however protein levels were found to be so low as to not produce any signal above background using BSA standards increasing from 25pg/ml.

Figure 3.11 Impaired cholesterol trafficking and synthesis shifts PrP out of raft fractions *Pellets of $3x10^6$ S7 (**A**) and CAD5 (**C**), and 10^6 primary cortical neurons (**B**), were prepared from cells transiently transfected with siRNA targeting Dhcr24 and Npc2. Lysates were run on Optiprep gradients as above for 16 hours and twelve 333µl fractions collected from the top of the gradient. Selected fractions were run on SDS-PAGE to probe for PrP (ICSM18). CAD5 cells were pre-incubated with biotinylated CtxB as described in Methods (**2.4.7**) to label GM1-containing fractions.* ***(Figure on next page)***

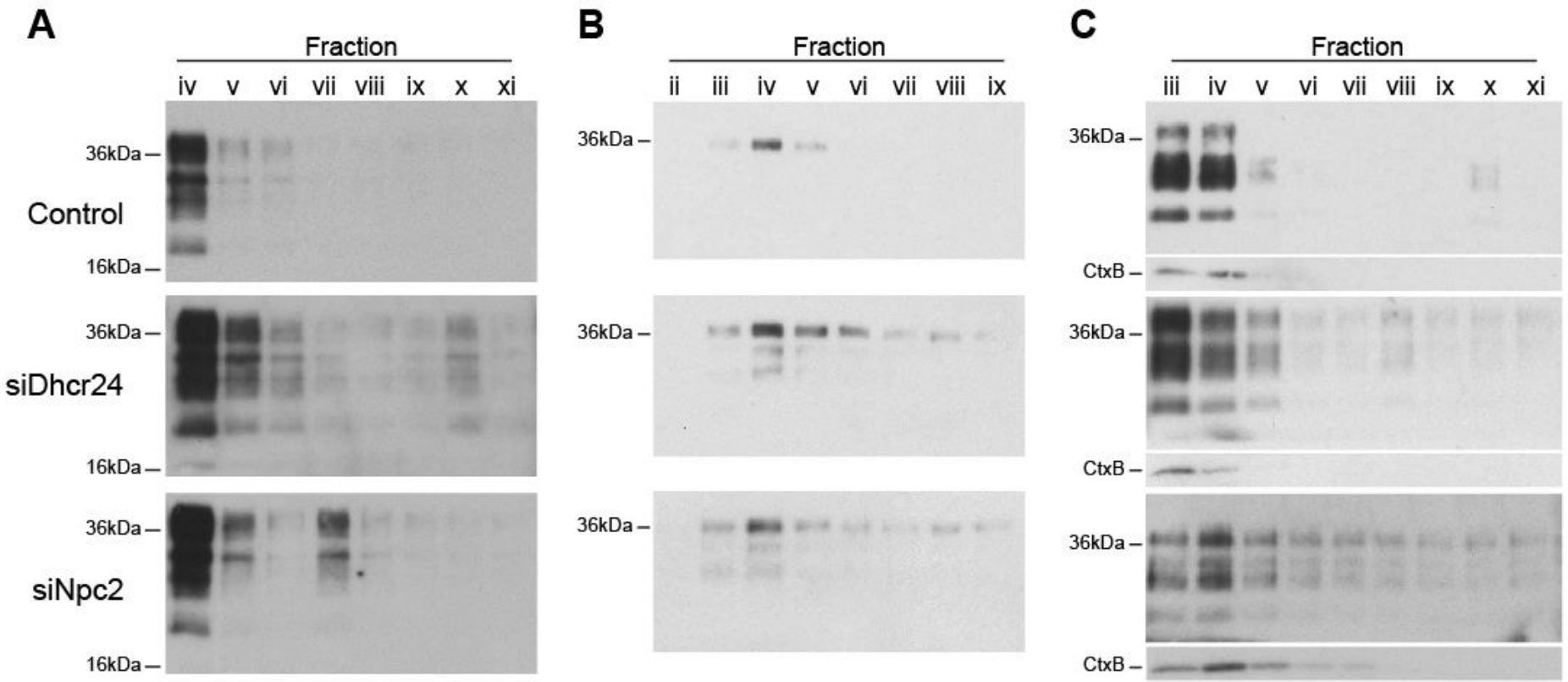
A
Fraction
iv v vi vii viii ix x xi
36kDa
Control
16kDa
36kDa
siDhcr24
16kDa
36kDa
siNpc2
16kDa
B
Fraction
ii iii iv v vi vii viii ix
36kDa
36kDa
36kDa
C
Fraction
iii iv v vi vii viii ix x xi
36kDa
CtxB
36kDa
CtxB
36kDa
CtxB

Figure 3.12 Silencing Dhcr24 does not alter PrP^C levels in S7 cells *Pellets of 1x10^6 S7 were prepared from cells transiently transfected with siRNA targeting Dhcr24, lysed in RIPA buffer and run on SDS-PAGE to probe for PrP (ICSM18). Following the first probe membranes were stripped and re-probed with anti-actin antibody to control for protein loading. Blots were analysed using ImageJ software, relative protein levels are shown in below each lane (RD). Only siRNA Dhcr24.1 increased PrP levels. This siRNA was earlier removed from other experiments due to a lack of effect in the SCA.*

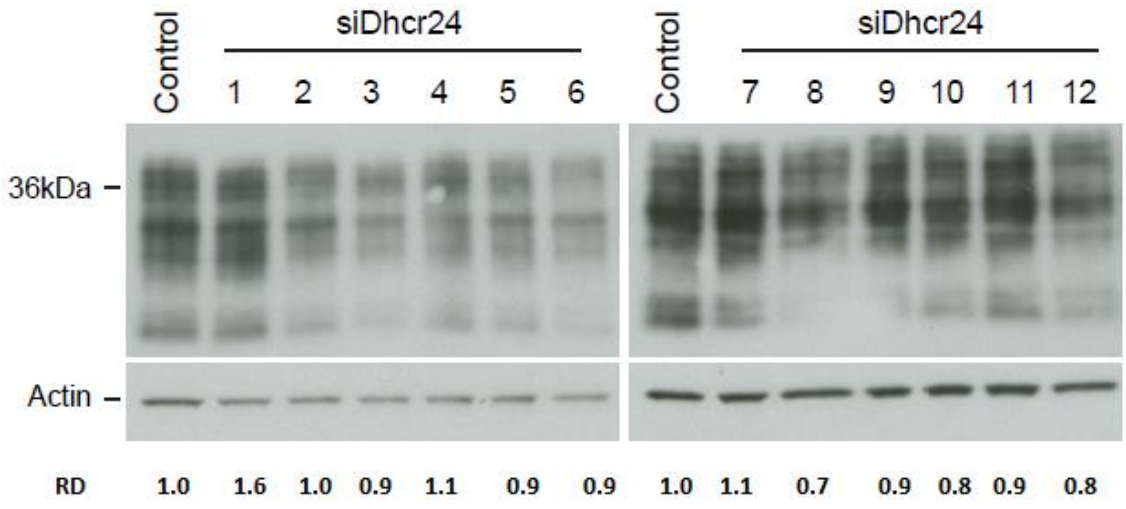

3.2 Rare variant subclones of CAD5 cells selectively propagate different prion strains

3.2.1 Rationale

Prion strains are characterised by the proportional 'pattern' of glycosylation they exhibit, their *in vivo* incubation time and the lesion profiles and pattern of PrP^{Sc} deposition they produce in infected tissue (Collinge, 2005). A growing body of evidence suggests that the species barrier that limits cross-species transmission of prion disease may in part be due to susceptibility to different prion strains (Hagiwara et al., 2013). Prion strains may contain pools of different PrP^{Sc} conformers (Collinge, 2010). There is growing evidence that prion strains can adapt to different host cells (Li et al., 2010) with the implied possibility that only a few conformers are able to replicate in a given host and so outgrow their competition. Strains are highly robust and can be passaged *in vivo* multiple times without altering their characteristics.

Cell culture models have revealed that different cell lines are susceptible to infection by different prion strains (Mahal et al., 2007) although all strains are thought to be infectious *in vivo*. This suggests that prion strain susceptibility is a cellular factor and as such may be genetically encoded. Furthermore, it stands to reason that if a given set of cellular factors encodes susceptibility to a given prion strain and the cell line itself is susceptible to multiple prion strains then it may be possible to alter susceptibility to one prion strain but not the other. It is possible that differences in cellular susceptibility to different prion strains could help account for the different patterns of PrP^{Sc} deposition observed in brain tissue. We asked whether it was possible to isolate cells which are restricted in susceptibility to a single strain from a less restricted parent line. As with the recent work of Marbiah et al (2014) deriving multiple cell lines from the same parent line should reduce differences in gene expression unrelated to the phenotypes being selected for. I show here that subcloning of the CAD5 cell line, which is susceptible to multiple prion strains, will yield rare variant subclones which exclusively propagate a single strain. These

rare variants may exhibit a different pattern of gene expression than their cousins, providing a 'gene signature' for strain selection.

The work of Mahal et al (2007) compared the cell lines PK1, R33, LD9 and CAD5, and the prion strains RML, 22L, Me7 and 301C. At the outset of this project we had access to all 4 cell lines (as well as the PK1 subclone PK1-11) and prion strains RML and Me7. PK1, R33 and CAD5 are derived from mouse neuroblastoma whilst LD9 are derived from mouse fibroblast. The PK1 subclone S7 used elsewhere in this thesis was judged unsuitable for this project as it had previously been subcloned and selected for high RML susceptibility (Marbiah et al., 2014).

The aim of this project was to isolate rare variant subclones which exclusively propagate a single prion strain, and to then investigate cellular factors underlying this strain selection.

3.2.2 LD9, R33 and PK1-11 cells are unsuitable for identifying rare variant cell subclones

To isolate rare cognate cell clones which exclusively propagate a single prion strain we checked whether any of the parent cell lines were susceptible to multiple prion strains. Serial dilutions of RML and Me7 infected brain homogenate were used to perform an SCA for LD9, PK1-11 and R33 cells. PK1-11 cells were found to be highly susceptible to RML but not Me7 rendering them unsuitable for the project (**Figure 3.13 A**). Both LD9 and R33 were found to propagate RML and Me7 prions similarly; however the low susceptibility to either homogenate rendered R33 unsuitable for use (**Figure 3.13 B**). Whilst LD9 cells were a strong candidate based on this data (**Figure 3.13 C**), they were highly adherent and not suitable for high-throughput screening of subclones using automated equipment.

Figure 3.13 The responses of PK1-11, R33 and LD9 cells to prion infection are unsuitable for rare variant subclone isolation *PK1-11, R33 and LD9 cells were infected with RML (blue) and Me7 (red) homogenate in concentrations increasing from 10^{-5} to 10^{-3} dilutions of homogenate in growth media. Control cells were uninfected. After reaching confluence post-3rd passage cells were seeded for elispot at a density of 20000 cells per well and PrP^{Sc} levels were assessed.* ***A*** *PK1-11 cells are highly susceptible to RML prion infection and respond proportionally to changing homogenate concentration, but are resistant to the Me7 prion strain.* ***B*** *R33 cells are not susceptible to both RML and Me7 prion strains.* ***C*** *LD9 cells respond similarly to both RML and Me7 prion strains. However, the highly adherent nature of these cells made them unsuitable for high throughput screening. In all cases 12 wells of a 96 well plate were challenged with each dilution of homogenate. Bars show mean spot count ± standard deviation for each dilution, control = growth media with no homogenate.* **(*Figure on next page)***

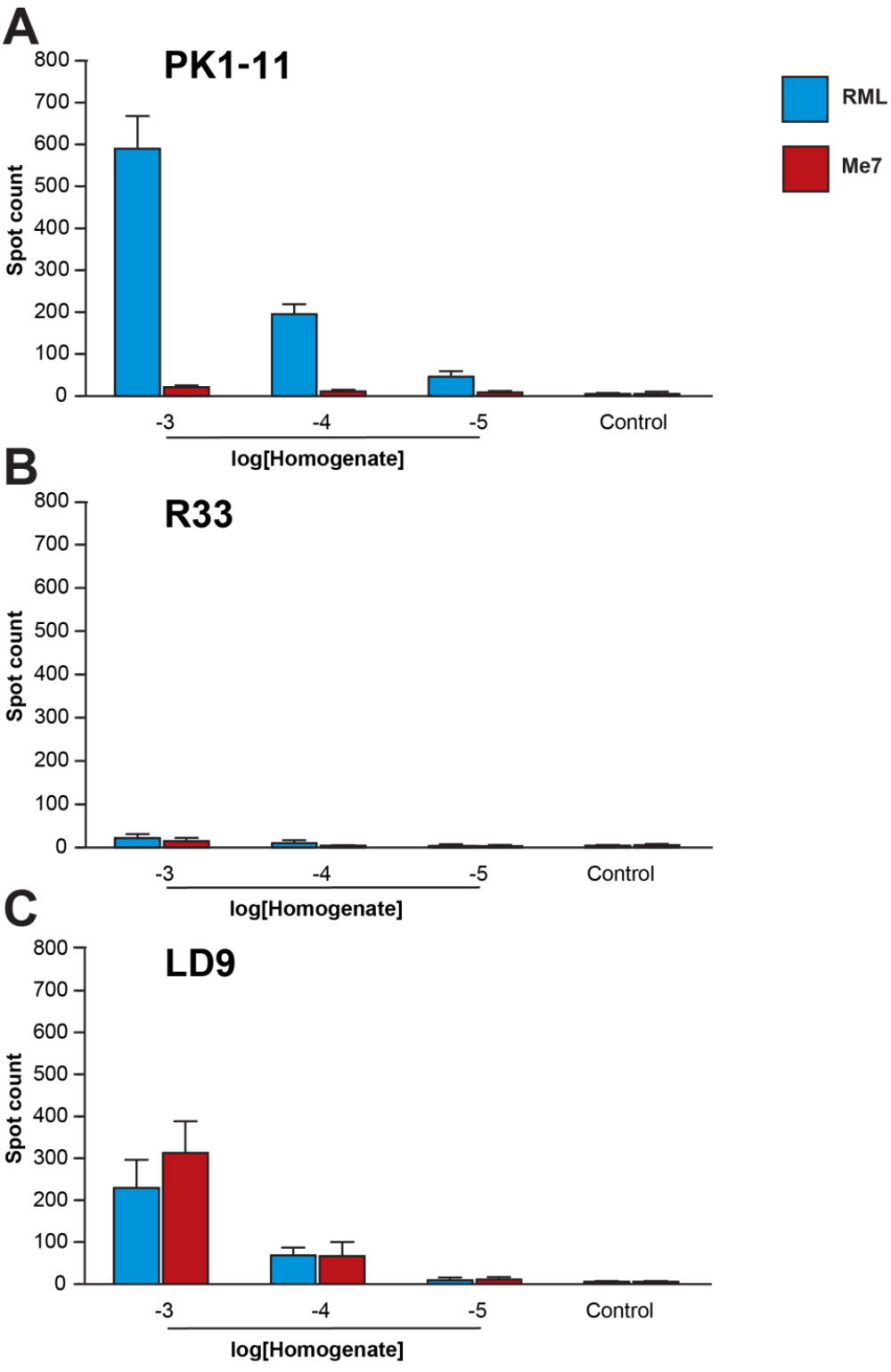
A
PK1-11
RML
Me7
Spot count
800
700
600
500
400
300
200
100
0
-3
-4
-5
Control
log[Homogenate]
B
R33
Spot count
800
700
600
500
400
300
200
100
0
-3
-4
-5
Control
log[Homogenate]
C
LD9
Spot count
800
700
600
500
400
300
200
100
0
-3
-4
-5
Control
log[Homogenate]

3.2.3 CAD5 cells are highly susceptible to RML and 22L prion strains

To test whether the catecholaminergic cell line CAD5 was suitable for use in our search for exclusively propagating cognate cell clones a trial SCA was performed with serial dilutions of each homogenate. Three prion strains, RML, 22L and Me7, were tested at concentrations between 10^{-4} and 10^{-7} dilutions of brain homogenate. Cells were found to be highly susceptible to two strains, RML and 22L, consistent with previous reports (Mahal et al., 2007). The cells were less susceptible to the third strain, Me7, and yielded spot numbers higher than background only at the highest concentration of homogenate used (**Figure 3.14**). Due to their high susceptibility to RML and 22L we selected CAD5 cells for a proof of concept experiment.

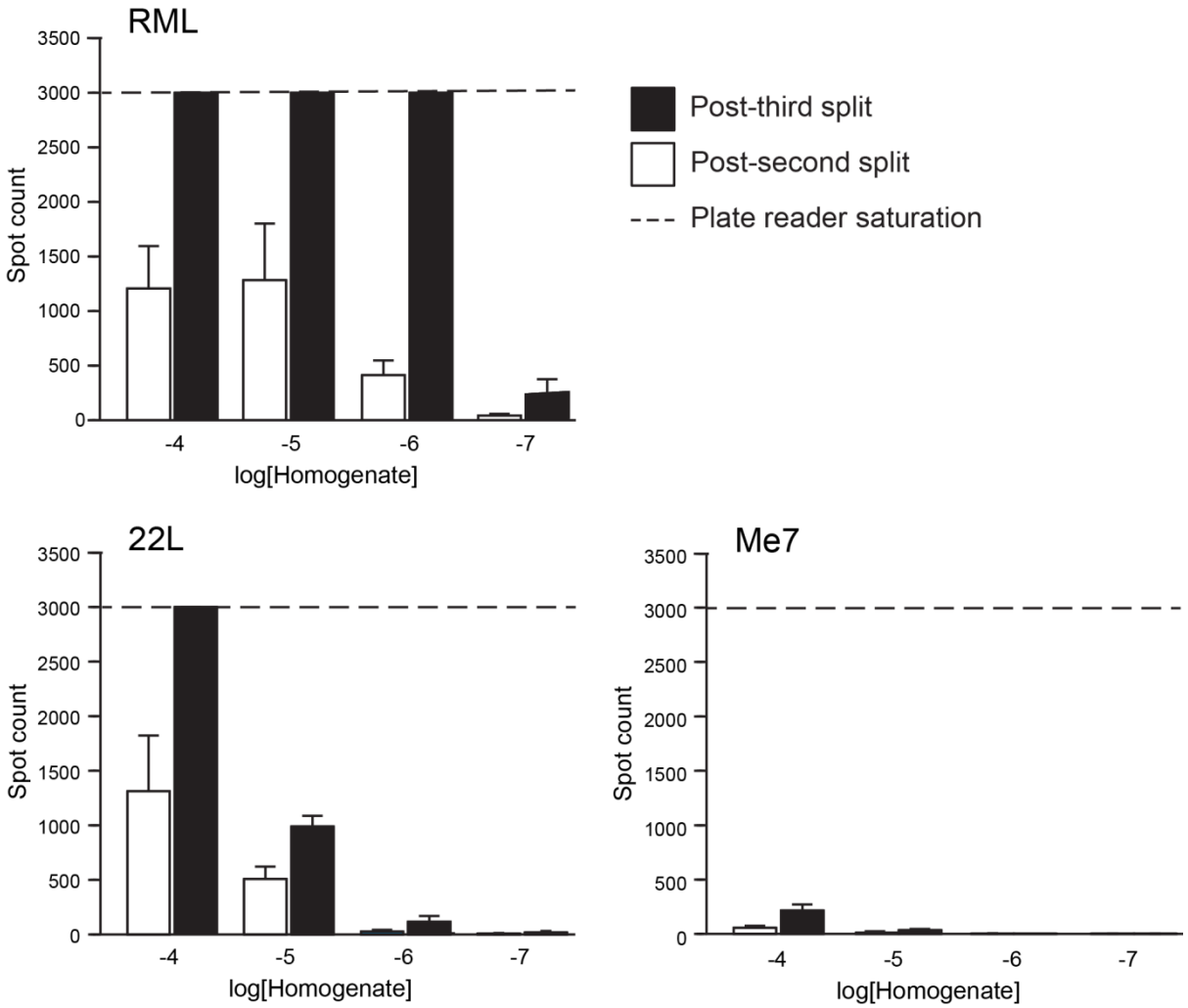

Figure 3.14 CAD5 cells are highly susceptible to multiple prion strains and are suitable for rare variant subclone isolation *Elispots of 20000 cells per well were collected at post-2nd (white bars) and post-3rd (black bars) splits of the SCA for CAD5 cells infected with serial dilutions of RML, 22L and Me7. At higher concentrations of homogenate both RML and 22L led to saturation of the plate reader used above 3000 spots (dotted line) so no absolute spot count was recorded. CAD5 cells were relatively unsusceptible to Me7, returning a mean of only 216 spots at post-3rd elispot for the highest homogenate concentration tested. Bars show mean spot count ± standard deviation for each dilution.*

3.2.4 CAD5 subcloning yields rare variant cells which are exclusively susceptible to distinct prion strains

Following the identification of CAD5 as a viable cell line, 288 subclones were infected with a 10^{-5} dilution of RML and 22L. Across the subclone population the mean response to both RML and 22L infection was similar (**Figure 3.15 A**). A selectivity score (SS) was calculated as described in methods, with the mean SS being 0.485 ± 0.186 (3sf ± standard deviation, **Figure 3.15 B**). In this initial experiment we identified 13 rare variants, a 'hit rate' of ~4.5%. Of the 13 clones identified, 9 selectively propagated RML whilst 4 preferred 22L (outlined in **Table 3.3**). Rare variants such as these may eventually be used to identify potential gene signatures for strain selectivity once sufficient subclones have been isolated. Whilst validating our pilot data it became clear that cell susceptibility to prion infection would be lost over multiple passages consistent with previous findings. We therefore elected to optimise a high throughput cryopreservation method in order to retain the early characteristics of our subclones with restricted susceptibility to prion strains.

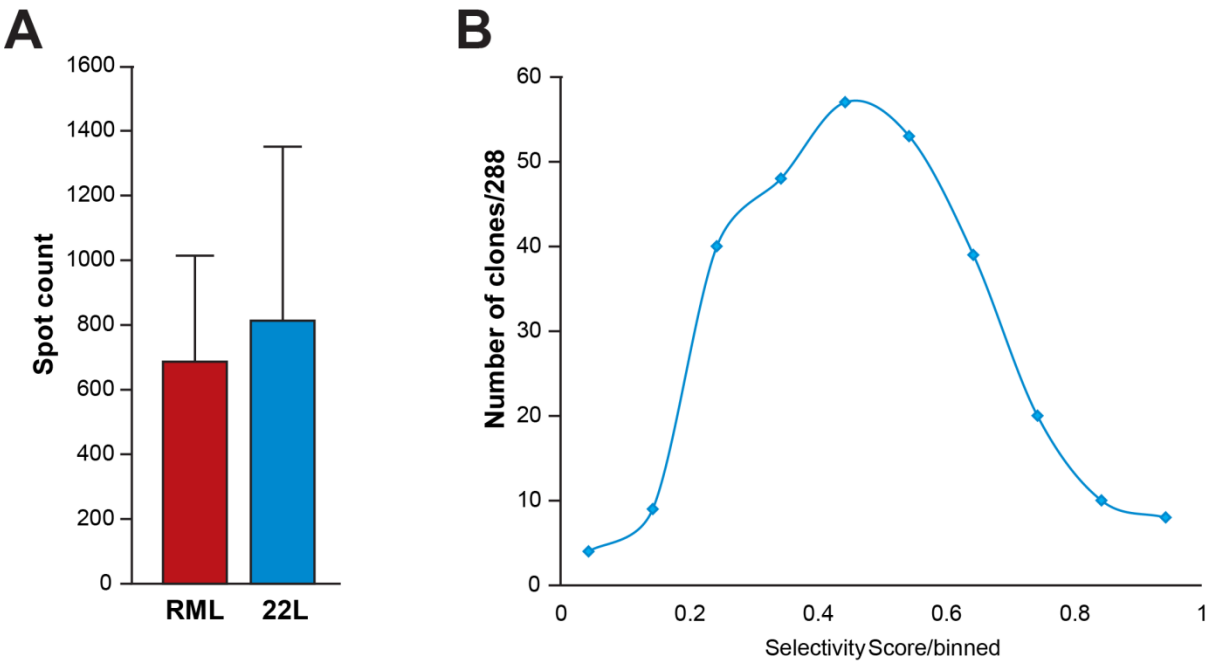

Figure 3.15 CAD5 subcloning yields rare variant subclones which exclusively propagate a single prion strain A *The mean and standard deviation of RML (687±327) and 22L (812±538) elispot spot count for a pilot run of 288 subclones infected with 10^{-5} RML or 22L homogenate in the SCA. Each subclone was tested twice against each prion strain.* ***B*** *The selectivity score was calculated as the ratio of RML spots to total spots for each subclone and assumed a Gaussian distribution, giving a mean of 0.485 across the experiment with a standard deviation of 0.186. 13/288 subclones gave scores more than 2 standard deviations from the mean and were classed as variants. Of these rare variants 9 displayed a preference for RML and 4 a preference for 22L.*

Table 3.3 Rare variant CAD5 subclones exclusively propagate distinct prion strains. *RML- and 22L-preferring subclones were selected in addition to non-preferring subclones, listed according to experimental plate layout. RML, 22L = number of spots on elispot for each prion strain. SS = selectivity score, the ratio of RML spots to total spots for each subclone. FD = fold preference for the preferred prion strain (preferred/non-preferred).*

RML Preferring				
Subclone	***RML***	***22L***	**SS**	**RML FD**
1B8	*131*	*11*	0.923	11.9
1E9	*1018*	*70*	0.936	14.5
1F11	*992*	*89*	0.918	11.1
2A4	*1080*	*99*	0.916	10.9
2D12	*460*	*50*	0.902	9.2
2F6	*493*	*75*	0.868	6.6
3A6	*694*	*65*	0.914	10.7
3C11	*477*	*45*	0.914	10.6
3G8	425	31	0.932	13.7
22L Preferring				
Subclone	***RML***	***22L***	**SS**	**22L FD**
1A2	*30*	*763*	0.038	25.4
1G1	*9*	*165*	0.052	25.4
2A9	*13*	*283*	0.044	18.3
2G4	*20*	*305*	0.062	21.8

3.2.5 Expansion of CAD5 subcloning assay for increased throughput

Whilst validating our pilot data it became clear that cell susceptibility to prion infection would be lost over time consistent with previous findings. We therefore elected to optimise a high throughput cryopreservation method in order to retain the early characteristics of our subclones with restricted susceptibility to prion strains.

Although 96-well plate freezing allowed increased throughput we were still limited by the number of Elispot assays which could be performed simultaneously. A further 480 subclones were screened against both RML and 22L prion strains, testing 2 biological repeats per homogenate and freezing an additional copy of each subclone to preserve the lowest passage cell iteration possible. Elispot data was again collected at post-3rd passage giving spots counts of 1431±850 for RML and 1091±923 for 22L (mean ± standard deviation). Selectivity scores were calculated with mean 0.565 and standard deviation 0.169 across the population (**Figure 3.16**); subclones were selected if the selectivity score lay more than 2 standard deviations from the mean. To increase stringency of selection a threshold of at least 500 spots for the preferred homogenate was required to class a subclone as responsive. This yielded 3 RML-responsive and 2 22L-responsive subclones, an additional 4 neutral subclones were selected to serve as controls (**Table 3.4**).

Upon resurrection only 5 of the selected subclones were viable (3 RML preferring, 1 22L preferring, 1 neutral). These subclones were expanded and again challenged with 10^{-5} RML and 22L, testing 8 repeat wells per subclone. Selectivity scores were again calculated for each subclone and compared to selectivity scores obtained in the initial test (**Figure 3.16 C**). Non-selective preference and preference for RML were maintained, whilst the 22L-preferring subclone lost selectivity and became non-preferring. Our findings here demonstrate that whilst improved cryopreservation increases the chances of procuring rare variant subclones further work is required to ensure these clones remain viable as candidates for our investigation.

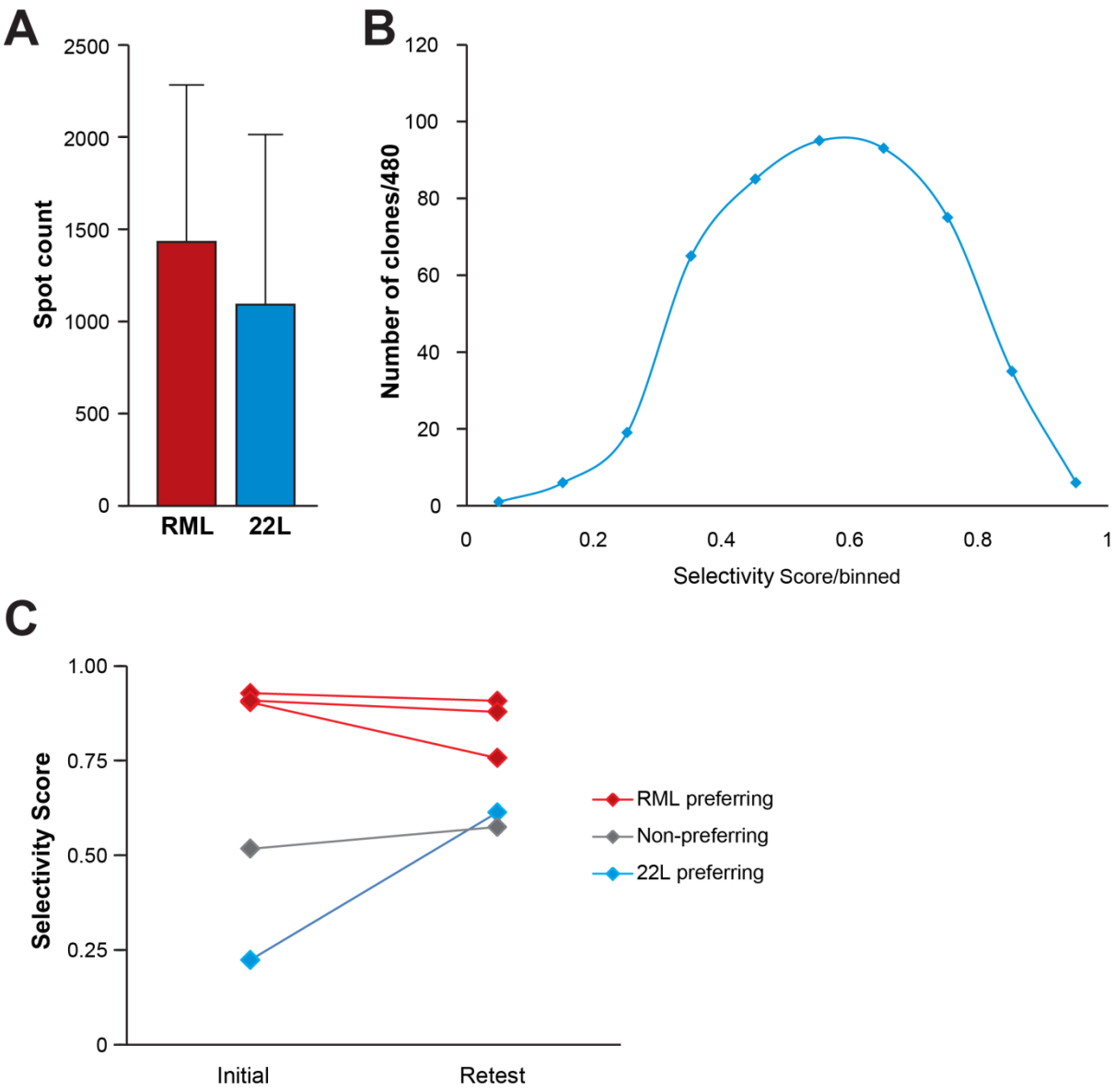

Figure 3.16 Selective susceptibility to RML is preserved in subclones A *An increased cohort of 480 subclones was infected with 10^{-5} RML or 22L in the SCA. The new cohort maintained the high mean spot count and standard deviation observed in the pilot run. RML spot count (1431±850) trended to be higher than 22L spot count (1091±923).* ***B*** *Selectivity scores across the cohort assumed a Gaussian distribution with mean 0.565 and standard deviation 0.169. 3 RML preferring, 2 22L preferring and 4 non-preferring subclones were selected for further work.* ***C*** *Upon resurrection selected subclones were expanded (8 wells/test). 3 RML preferring, 1 22L preferring and 1 non-preferring subclone survived resurrection and were retested with 10^{-5} RML and 22L in the SCA (8 wells/test). RML preference (red points/lines) and neutral preference (grey points/line) was maintained whilst 22L preference (blue points/line) was lost as selectivity score moved above 0.5.*

Table 3.4 Subclones selected for further analysis following increased throughput subcloning. *RML- and 22L-preferring subclones were selected in addition to non-preferring subclones, listed according to experimental plate layout. RML1, RML2, 22L1, 22L1 = number of spots on elispot for each technical repeat, means and standard deviations given as RML/22L Mean and SD. SS = selectivity score, the ratio of RML spots to total spots for each subclone. FD = fold preference for the preferred prion strain (preferred/non-preferred), FD for 22L used for non-preferring subclones*.

RML Preferring										
Subclone	***RML 1***	***RML 2***	**RML Mean**	**RML SD**	***22L 1***	***22L 2***	**22L Mean**	**22L SD**	**SS**	**RML FD**
A1G	*3152*	*2514*	2833	451	*127*	*475*	301	246	0.904	9.4
C10F	*2186*	*2653*	2420	330	*239*	*137*	188	72	0.928	12.9
C11F	*1858*	*975*	1417	624	*161*	*124*	143	26	0.909	9.9
22L Preferring										
Subclone	***RML 1***	***RML 2***	**RML Mean**	**RML SD**	***22L 1***	***22L 2***	**22L Mean**	**22L SD**	**SS**	**22L FD**
A5G	*819*	*938*	879	84	*3237*	*2856*	3047	269	0.224	3.5
D4F	*235*	*327*	281	65	*706*	*1937*	1322	870	0.175	4.7
Non Preferring										
Subclone	***RML 1***	***RML 2***	**RML Mean**	**RML SD**	***22L 1***	***22L 2***	**22L Mean**	**22L SD**	**SS**	**22L FD**
A4F	*1725*	*1956*	1841	163	*1792*	*1800*	1796	6	0.506	1.0
C4C	*2397*	*2137*	2267	184	*2220*	*2195*	2208	18	0.507	1.0
C2E	*2159*	*1820*	1990	240	*1807*	*1905*	1856	69	0.517	1.1
D8A	*1846*	*1701*	1774	103	*1860*	*1898*	1879	27	0.486	0.9

CHAPTER 4 DISCUSSION

4.1 Impairment of the cholesterol metabolism facilitates prion propagation

This work provides evidence that perturbation of cholesterol facilitates prion propagation in cells. Inhibition of cholesterol synthesis by transient knockdown of *Dhcr24* and *Hmgcr* both reduced cellular cholesterol levels and increased prion propagation. Similarly, the sequestration of cholesterol in lysosomes by silencing of *Npc2* increased prion replication. A thorough study of cell- and gene-dependent effects following transcriptional silencing of *Npc1* and *Npc2*, two genes with a role in cholesterol trafficking, provides a rational to understand conflicting data of this work with previous studies. Previous work by Gilch et al (2009) demonstrated that silencing of *Npc1* decreased the level of PrP^{Sc} in N2a cells, a result that could be replicated in this work, but is in conflict to the increase in prion replication following *Npc2* knockdown. As *Npc1* and *Npc2* work in tandem to export cholesterol from lysosomes, and silencing of either gene causes accumulation of cholesterol, effects on the corresponding rates of prion replication were expected to follow the same trend. Further characterisation of *Npc1*-silencing in S7 cells, a subclone of N2a, revealed that PrP^{C} levels were depleted alongside an increase in lysosome acidity in *Npc1*-, but not in *Npc2*-silenced cells. Reasoning that decreased PrP^{C} would limit prion replication (S et al., 1996, Daude et al., 2003), we tested silencing of *Npc1* in CAD5 cells. Whilst PrP^{C} levels were indistinguishable from control levels, knockdown of *Npc1* and *Npc2* cells in CAD5 cells significantly increased the rates of prion replication in both cases. This suggests that the decrease in prion propagation following loss-of-*Npc1* function is cholesterol-independent and caused by an unidentified cellular factor. In summary, lysosomal sequestration of cholesterol by transcriptional silencing of *Npc1* and *Npc2* is associated with increased prion replication when PrP^{C} expression levels remain unaltered, a conclusion that is in agreement with an increase of prion replication rates at limiting cholesterol levels following perturbation of cholesterol biosynthesis.

To better understand how both the reduction and sequestration of cholesterol may explain an increase in prion propagation, the distribution of PrP^C between raft and non-raft membrane domains was investigated. Gradient ultracentrifugation revealed a shift of PrP^C from raft to lower buoyant density membrane fractions following silencing of *Dhcr24* and *Npc2*. In agreement with this result, sucrose gradient density centrifugation of lysates from $Dhcr24^{+/-}$ mouse brain homogenates showed a shift of PrP^C from raft to lower buoyant density fractions when compared to wild-type mice (Abad-Rodriguez et al., 2004, Crameri et al., 2006). Lipid raft association is known to stabilise PrP^C (Sarnataro et al., 2004) and we asked whether lipid raft disruption by cholesterol depletion predisposed PrP^C to conversion into PrP^{Sc}.

Altered cholesterol metabolism has implications for other neurodegenerative diseases such as Alzheimer's disease. By studying the role of cholesterol in PrP processing and prion replication it may be possible to better understand pathology in other diseases. Notably, PrP levels have been shown to regulate beta secretase cleavage of APP (Parkin et al., 2007), an effect which may in part be mediated by PrP binding to lipid rafts. Similarly, work by Bart de Strooper and colleagues have shown differential activity of gamma secretase dependent on lipid raft association (Nesic et al., 2012) suggesting that further study of cholesterol in neurodegenerative disease could help us understand how APP processing is affected by lipids. Indeed, *Dhcr24* expression is known to correlate with protection against Alzheimer's disease (Crameri et al., 2006). Our data here suggests that expression of *Dhcr24* (and so production of cholesterol) may limit prion replication which could have implications for the formation of amyloid plaques in other disease. Interestingly the interaction of PrP with lipids has been suggested as a potential mechanism for neurotoxicity in Alzheimer's disease. In a recent paper Watt et al suggested that PrP-dependent uptake of zinc is disrupted by binding of Aβ oligomers to PrP (Watt et al, 2014). Disruption of lipid rafts and PrP by Aβ binding may contribute to toxic effects in Alzheimer's disease.

4.1.1 Reduction in the availability of cholesterol promotes prion replication

Our findings directly contradict reports that cholesterol depletion impairs prion propagation and indicates that cholesterol is not a co-factor for prion replication. Instead our data suggests that reduced cellular cholesterol facilitates prion propagation. We perturbed cholesterol synthesis by silencing of *Hmgcr* and *Dhcr24* which are key genes in the Mevalonate pathway. Silencing *Hmgcr* almost completely depleted membrane cholesterol and increased prion replication. Similarly silencing *Dhcr24* reduced total cellular cholesterol by ~40% and increased prion replication. We elected to silence *Dhcr24* as it acts late in the synthesis of cholesterol and so would not be expected to disrupt production of other intermediate molecules. Indeed silencing of *Dhcr24* in cells has previously been shown decrease cholesterol alongside accumulation of desmosterol, whilst complete knockout of *Dhcr24* in mice was lethal (Wechsler et al., 2003, Mirza et al., 2006). Contrary to our reasons for targeting *Dhcr24 Hmgcr* acts early in the Mevalonate pathway and is required for production of many intermediate and bioactive molecules. *Hmgcr* is however the rate limiting enzyme in cholesterol synthesis and is also the target of the statin family of cholesterol lowering drugs. We did not observe toxic or growth effects when silencing either *Hmgcr* or *Dhcr24*, possibly due to cells retaining sufficient cholesterol to maintain normal functions over the 3 day silencing period. We did not attempt to overexpress *Dhcr24* or *Hmgcr* in order to increase cholesterol production. As *Hmgcr* is rate limiting we did not expect to see a significant increase in cholesterol production with *Dhcr24* overexpression. Similarly, cholesterol synthesis is tightly regulated (Pfrieger, 2003, Yeganeh et al., 2014) and it is possible that negative feedback would prevent increased cholesterol production when overexpressing *Hmgcr*. Finally work in our group and others have shown difficulty in stably overexpressing genes in S7 and CAD5 cell models. We were concerned that the rigorous infection and selection protocols required for gene expression in our cell lines would impair prion propagation and so sought other methods to increase cholesterol in cells.

Subsequent experiments performed after completion of my research indicate that knockdown of *Dhcr24* with certain siRNAs, particularly Dhcr24.2, may increase cell proliferation in chronically infected iS7 cells. Throughout my experimentation phase we were careful to monitor cell proliferation, reasoning that altered proliferation could impact prion propagation, and did not observe changes in cell growth when silencing *Dhcr24*. In repetition experiments an increase in the rate of prion propagation after transcriptional silencing of Dhcr24 as described in the results section could not be confirmed by an independent researcher. In these experiments the rate of prion replication was normalised to the cell number. As a decrease in cholesterol levels resulted in an increase of cell proliferation, an effect that had previously not been noticed, no significant changes in prion replication were observed under these conditions. Further experiments will be undertaken to clarify these findings. Critically cholesterol depletion by MβCD has been shown to enhance myoblast proliferation, putatively by increased expression of the cell cycle regulator p53 (Portilho et al., 2012). Conversely increased cholesterol has been shown to rescue cell proliferation defects in the CNS (Cunningham et al., 2015) and it is possible that cholesterol exerts different effects on cell proliferation in different tissues.

We also investigated impaired cholesterol trafficking alongside cholesterol synthesis. As referenced throughout this thesis, in 2009 Gilch et al demonstrated that inducing cholesterol accumulation in lysosomes of prion infected N2a cells by silencing *Npc1* or with the small inhibitor U18666A impaired prion replication. In line with the work of Taraboulos et al (Taraboulos et al, 1995) this was interpreted as limiting the availability of cholesterol as a co-factor for prion replication. Whilst U18666A does cause cholesterol accumulation in lysosomes it is not fully characterised and may cause other off target effects (Cenedella, 2009, Browman and Zurzolo, 2013). Our data confirms that silencing Npc1 in the N2a subclone S7 causes accumulation of cholesterol in lysosomes and reduces the number of PrP^{Sc}-positive cells in our assays. However when silencing *Npc1* in CAD5 cells, which are from a distinct lineage to N2a cells, we observed increased prion replication. Furthermore silencing *Npc2*, which produced an

identical phenotype of lysosomal cholesterol accumulation as silencing of *Npc1*, increased prion replication in both S7 and CAD5 cells. We found a decrease in PrP^{C} levels in S7 cells following *Npc1* silencing and reasoned this may explain reduced PrP^{Sc} in these cells (see **section 4.1.3** below). When interpreted in the context of our findings that impaired cholesterol synthesis promotes prion replication our work on *Npc1* and *Npc2* suggests that accumulation of cholesterol may facilitate prion replication through a similar mechanism. With both reduced synthesis and impaired trafficking of cholesterol there would be expected to be a net reduction in available cholesterol in cells which may disrupt lipid rafts. If lipid rafts stabilise PrP^{C} as reported in the work of Sarnataro et al (2004) then a loss of lipid rafts may destabilise PrP^{C} allowing for more ready conversion to PrP^{Sc}.

Over the course of our study we utilised several methods of tracking and quantifying cholesterol in cells. We initially experimented with tracking cholesterol by confocal imaging with the aim of eventually tracking cholesterol in live cells. In 2008 work in Elina Ikonen's lab characterised boron dipyrromethene difluoride cholesterol (BODIPY-cholesterol) as a marker of cholesterol trafficking in live cells (Holtta-Vuori et al., 2008). Using BODIPY-cholesterol we were able to track cholesterol intracellularly but did not observe membrane labelling in fixed or live cells. Furthermore, as BODIPY-cholesterol is an analogue of cholesterol we were unable to use it to quantify cholesterol levels in cells. Filipin III is a cholesterol binding toxin which is isolated from bacteria and fluoresces when excited with ultraviolet (UV) light (Schroeder et al., 1971). Michael Duchen (UCL Department of Physiology) kindly allowed us access to his UV capable confocal microscope but due to the logistics of preparing samples for imaging we were unable to examine filipin labelling in live cells. Additionally, due to the wide emission spectrum of filipin (Norman et al., 1972) we were unable to label samples with antibodies alongside filipin to determine the location of different organelles relative to cholesterol. We were able to determine relative cholesterol levels both intracellularly and in cell membranes using filipin labelling in fixed cells. Using a combination of BODIPY-cholesterol and filipin staining experiments we were able to

determine that our silencing of *Npc1* and *Npc2* produced the expected phenotype of cholesterol accumulation in S7 cells. To quantify cholesterol levels in cells we used the commercial Amplex Red cholesterol assay (Life Technologies). This assay allowed us to determine total cholesterol in cells and with optimisation may allow for differentiation between esterified and free cholesterol. Modifying the assay in this way would be useful in investigating the effects such as *Acat1* and *Lipa* which produce enzymes to esterify cholesterol and hydrolyse cholesterol esters respectively.

Although the role of cholesterol in prion propagation remains controversial in published literature it is possible that more recent studies interpret data in light of early work by Albert Taraboulos and colleagues which showed that lovastatin inhibits prion replication (Taraboulos et al., 1995). In our hands lovastatin proved toxic to cells above 300nM and concordantly reduced PrP^{Sc} levels in chronically prion infected iS7 cells. However at sub-toxic concentrations there was a trend for lovastatin treatment to increase prion replication, an effect which was mimicked by treatment with the cholesterol sequestering agent methyl β-cyclodextrin. A key experimental difference between our work and that of Taraboulos et al is that mevalonate was used to supplement treated cells in the latter study in order to provide for non-steroidal pathways downstream of HMGCR activity. We opted not to supplement cells with mevalonate as this still feeds into cholesterol synthesis (Goldstein and Brown, 1990) and would be expected to nullify the action of lovastatin.

Furthermore the reduction in PrP^{Sc} observed by Taraboulos et al was primarily seen when lovastatin treatment was combined with use of reduced-fat serum in cell media, an effect reversed by supplementing media with cholesterol (Taraboulos et al., 1995). Depletion of exogenous cholesterol and other lipids by 'starving' cells with depleted media is a common research technique and has previously been shown to reduce cell membrane integrity (Grundner and Jokhadar, 2014) and increase membrane protein shedding (Murai et al., 2011). In our hands

complete replacement of fetal bovine serum with lipoprotein-deficient serum proved toxic, severely disrupted cell membranes and altered distribution of PrP^C. Indeed, work by Gilch et al (2005) has shown that cholesterol is required for cell surface localisation of PrP^C and so depletion of lipids including cholesterol would be expected to replicate this effect. Whilst Taraboulos and colleagues successfully demonstrated reduction in PrP^{Sc} by depletion of exogenous lipids our data suggests that this may be due to impaired cell cycling and availability of PrP^C.

Methyl β-cyclodextrin (MβCD) sequesters cholesterol from cell membranes and has previously been shown to cure prion infection in cells (Prior et al., 2007). Prior et al demonstrated that 500µM MβCD reduced PrP^{Sc} levels by almost 60% in N2a cells chronically infected with 22L prions. Whilst we did not test a 500µM dose of MβCD we observed reduced PrP^{Sc} at doses of 100µM and 300µM which was associated with approximately 25% reduction in cellular cholesterol. Treatment with 1mM MβCD was toxic as measured by the CellGlo Titre assay but did not reduce levels of PrP^C or actin on Western blot. We elected to treat cells for 3 days after allowing cells to adhere whilst Prior et al passaged cells in the presence of MβCD for 1 week. Cholesterol can also be increased in cells by incubating MβCD with cholesterol prior to treating cells (Christian et al., 1997). In this system MβCD-cholesterol acts as a cholesterol donor however Prior et al observed that this further reduced PrP^{Sc} when used in combination with MβCD. This suggests that the effect of MβCD in reducing PrP^{Sc} may occur independently of cholesterol, and furthermore the fact that addition of cholesterol further reduced PrP^{Sc} levels may help support our hypothesis that cholesterol limits prion replication. As MβCD has an antiprion effect we did not attempt to increase cellular cholesterol using MβCD-cholesterol in our study.

In an attempt to increase cholesterol production in cells I supplemented culture medium with squalene. Squalene is a cholesterol precursor which is generated after Farnesyl diphosphate in the Mevalonate pathway (Nurenberg and Volmer, 2012), and so does not feed into non-

cholesterogenic pathways. Despite increasing squalene dose to 10% (v/v) in medium, a concentration which was toxic for cells, no sub-toxic squalene dose increased cellular cholesterol as measured by the Amplex Red cholesterol assay (Life Technologies). It is possible that squalene was not taken up into cells and so was not used as a substrate for cholesterol synthesis. Due to difficulties in overexpressing gene candidate coding sequences in N2a subclones and CAD5 cells we were unable to test the effect of overexpression of *Dhcr24* or *Hmgcr* on prion propagation. Expression of cholesterogenic genes is tightly regulated (Yeganeh et al., 2014) and it is possible that had gene overexpression been successful effects may have been limited by negative feedback from transcription factors.

4.1.2 Altered cholesterol metabolism reduces association of PrP^C with lipid rafts

As cholesterol is a key component of lipid rafts in the cell membrane we reasoned that disrupted cholesterol metabolism could impair association of PrP with lipid rafts. As lipid rafts have been shown to stabilise PrP^C (Sarnataro et al., 2004) we hypothesised that perturbed cholesterol synthesis and trafficking would shift PrP^C out of rafts leading to reduced stability and increased availability for conversion to PrP^{Sc}. We initially attempted to visualise lipid rafts by confocal microscopy. Whilst we tested several antibodies against known lipid raft components including flotillin-1, flotilin-2 and CD81 few worked at the high level of specificity required for fluorescence imaging. Subsequently we used Cholera toxin subunit B (CtxB) conjugated to the red Alexa Fluor 555 fluorophore (Sigma) which binds tightly to the sphingolipid GM1 (Sugimoto et al., 2001). Imaging of CtxB in S7 cells was not possible due to low numbers of cells which could be labelled. Conversely, CAD5 cells were intensely labelled by CtxB to the point where we were unable to discriminate between different membrane regions by microscopy. The discrepancy in CtxB labelling between S7 and CAD5 cells suggests that only a few S7 cells present GM1 ganglioside on the cell membrane. Whilst this does not rule out lipid raft formation in S7 cells it suggests that these may be formed from different sphingolipid components. Research by other groups indicates that lipid rafts in N2a cells also contain sphingomyelin and that the rate of prion

replication is inversely proportional to the level of sphingomyelin present in rafts (Naslavsky et al., 1999).

As an alternative to microscopy we opted to isolate rafts by gradient centrifugation. A key biological determinant of lipid rafts is their resistance to detergents at low temperatures and several protocols exist for raft isolation on gradients (Naslavsky et al., 1997, Crameri et al., 2006, Persaud-Sawin et al., 2009). We opted to adapt a protocol using Optiprep which had previously been used to isolate lipid rafts in COS-7 cells and demonstrated raft sensitivity to methyl-β cyclodextrin treatment (Waheed and Jones, 2002). The protocol was found to be sensitive to both the amount of lysate loaded onto gradients and the length of time for which the samples were centrifuged. Our optimised protocol used lysate from 5 million cells, which gave good signal on Western blot without accumulating insoluble material in the top of the gradient, and a 16 hour spin which showed good definition of raft and non-raft fractions on the gradient. By pre-incubating CAD5 cells with biotinylated CtxB prior to lysis we were able to determine the location of GM1, and by extension lipid rafts, on gradients. Discussion of the data has since indicated that the concentration of TX-100 used may have been too high and partially solubilised rafts. This may account for spreading of PrP across fractions, and would require further optimisation in subsequent experiments if this study were to be continued.

As previously reported PrP^C was found in lipid raft fractions in gradients of uninfected cells whilst PrP from lysates of prion infected cells migrated across the gradient and was found in more soluble fractions as well as rafts (Lewis et al., 2012). We observed a shift in PrP in gradients run using lysates of both RML infected S7 and CAD5 cells. Remarkably this shift of PrP out of raft fractions could be partially replicated by silencing of *Dhcr24* and *Npc2* in both S7 and CAD5 cell lines as well as primary neuronal cultures. In 2006 Crameri et al showed a loss of PrP^C buoyancy in raft fractions in lysates of mice heterozygous for expression of *Dhcr24* whilst overexpression of *Dhcr24* in SH-SY5Y cells increased PrP^C buoyancy in these fractions. Similarly Naslavsky et al

demonstrated that PrP^C buoyancy in low density fractions could by blocked by treating samples with Saponin suggesting cholesterol is required for this phenotype (1997). We did not attempt gradient centrifugation of cells treated with MβCD or lovastatin as our data from chronically infected cells suggested that these treatments were not as clean a model of cholesterol reduction as gene silencing. In their comparison of the different effects of cyclodextrins on prion infection Prior et al showed that PrP^{Sc} but not PrP^C is shifted to soluble fractions of sucrose gradients of lysates of β-cyclodextrin treated cells (2007). β-cyclodextrin reduced cholesterol by a similar amount to MβCD in this study and also caused a slight shift in GM1 towards soluble fractions, indicating that cholesterol may be partly responsible for detergent resistance in lipid rafts. Our data supports evidence that PrP-containing lipid rafts are cholesterol-rich and can be disrupted by silencing key genes involved in cholesterol metabolism. As silencing *Dhcr24* and *Npc2* led to increased prion propagation in cells we reasoned that a change in cellular environment could make PrP^C more available for conversion to PrP^{Sc}, potentially as a result of reduced stability after exiting lipid rafts.

Taken together our findings indicate that cholesterol limits prion replication and that this may be due to the requirement of cholesterol in targeting PrP^C to lipid rafts. Our data directly contradicts previous reports from the Prusiner lab that inhibition of cholesterol synthesis impairs prion replication (Taraboulos et al., 1995). Recently the role of cholesterol in prion disease was reviewed by Hannaoui et al, approaching the subject from a viewpoint that cholesterol facilitates prion replication (2014). Several key findings are discussed including disruption of PrP-containing lipid rafts following cholesterol depletion and links between cholesterol and Aβ formation in Alzheimer's disease; however it becomes apparent that in several cases the role of cholesterol may have been overlooked in favour of accepting the findings in the early work of Taraboulos et al. Indeed in cases cholesterol remained unchanged by treatment (Mok et al., 2006, Kempster et al., 2007, Haviv et al., 2008), and in some cases links to disruption of cholesterol metabolism were speculative (Mange et al., 2000). Whilst for the

main part these were elegant, expertly performed experiments it seems possible that results may have been misinterpreted in light of early data presented by the Nobel Prize winning Stan Prusiner.

4.1.3 Npc1 knockdown in S7 cells reduced PrP^C levels

Niemann-Pick type C disease is characterised by lysosomal accumulation of cholesterol (Sturley et al., 2004) and can be caused by loss of function in *Npc1* or *Npc2* (Vance, 2006). Because of the similarities in the loss of function phenotype for *Npc1* and *Npc2* we initially assumed silencing either gene would produce a similar effect on prion replication. Silencing Npc1 has previously been reported to impair prion propagation in N2a (Gilch et al., 2009) an effect thought to be mediated by enhanced degradation of PrP^{Sc}. In agreement with Gilch et al we observed a reduction in PrP^{Sc}-positive cells when silencing *Npc1* in SCA of uninfected and chronically prion infected S7 cells which are an N2a subclone (Klohn et al., 2003). Our data shows that silencing of *Npc1* also reduced PrP^C in S7 cells. In line with the protein-only hypothesis the availability of PrP^C limits prion replication. Silencing *Npc1* did not reduce PrP^C in CAD5 cells and silencing *Npc2* did not alter PrP^C levels in either S7 or CAD5 cells. As silencing of Npc1 and *Npc2* produces an identical phenotype, and silencing *Npc1* in CAD5 increased the number of PrP^{Sc}-positive cells, our data indicates that the previously reported effects of *Npc1* silencing on prion replication may be independent of cholesterol. Furthermore, as reduced PrP^C was limited to silencing *Npc1* in S7 but not CAD5 cells it appears likely that this is the result of an S7-specific intermediate factor and not necessarily a result of *Npc1* loss of function.

We considered whether silencing of *Npc1* altered lysosomal function and so increased degradation of PrP^C. Experiments using Lysosensor green DMD-189 revealed that lysosomes in *Npc1*-silenced cells were more acidic than lysosomes in control cells transfected with non-silencing siRNA. As lysosomal enzymes are more active in more acidic environments (Pillay et al., 2002) we hypothesised that PrP^C and other proteins were degraded more efficiently in

lysosomes of *Npc1*-silenced cells. Since evidence suggests PrP^C is normally recycled through sorting endosomes rather than being trafficked to lysosomes we also considered whether PrP^C was being increasingly diverted to lysosomes in *Npc1*-silenced cells. Although we did not investigate PrP turnover further in these cells it may be possible to confirm whether reduced PrP^C is a result of increased degradation or impaired protein synthesis using a cycloheximide assay to block protein synthesis (Obrig et al., 1971). If silencing *Npc1* impairs synthesis alone then PrP^C levels would be expected to decrease evenly between silenced and control cells. Conversely, increased degradation would become apparent by a more rapid decrease in *Npc1*-silenced cells compared to controls. Given we observed changes in lysosomes in line with increased lysosomal activity increased degradation rather than perturbed synthesis seems the more likely candidate for the reduction in PrP^C seen when silencing *Npc1*.

In an attempt to reverse PrP^C depletion following *Npc1* ablation in S7 cells we overexpressed Rab9. Rab9 is a GTPase which functions in the transport of cargo away from the endosomal/lysosomal system (Ng et al., 2012). In the work of Gilch et al expression of Rab9 partially reversed the observed reduction in PrP^{Sc} following treatment with U18666A (Gilch et al, 2009). We reasoned that *Npc1* knockdown may alter intracellular trafficking, and perhaps increase the likelihood of lysosomal degradation of, PrP^C. As such overexpression of Rab9 was an attempt to remove PrP^C from the lysosomal compartment prior to degradation. Although Rab9 overexpression did not alter PrP^C levels this does not mean that other regulators of endocytosis would be similarly unable to prevent reduction of PrP^C. Given that Arf6 has been shown to restore cholesterol trafficking in $Npc1^{-/-}$ cells it may be interesting to examine whether Arf6 expression similarly rescues PrP^C levels following *Npc1* knockdown. Indeed, expression of constitutively active Arf6 (with the point mutation Q67L) altered PrP^C trafficking and suggested a role for Arf6 in clathrin-independent endocytosis of PrP (Kang et al., 2009).

4.1.4 Future work

Due to time restraints work not covered here will investigate the ability of PrP^{C} from different gradient fractions to covert to PrP^{Sc}. Protein Misfolding Cyclic Amplification (PMCA) is an in vitro model of prion replication whereby sequential rounds of sonication and incubation are used to amplify a prion seed in samples containing PrP^{C} (Saborio et al., 2001). Recently it has been demonstrated that PrP^{C} isolated from high buoyancy fractions in sucrose gradients is not a substrate for PMCA (Mays et al., 2014) suggesting that raft association protects against prion conversion. Initial experiments indicate that PrP^{C} obtained from gradient fractions is a substrate for PMCA conversion, albeit with a very low yield in part due to low levels of protein in each fraction. We attempted to increase protein concentration by loading higher cell numbers onto gradients; however this resulted in a large pool of insoluble material which occupied the top 1ml of the gradient and did not shift following gene knockdown. To overcome low fraction protein levels we are attempting a two-round PMCA protocol whereby fractions are first used to amplify an RML seed with limited sonication followed by a seeding the product of this round into mouse brain homogenate for an increased sonication step.

Alongside PMCA it may be possible to determine the stability of PrP in gradients biochemically. In work not shown here we attempted to clone a tetracysteine binding motif into PrP^{C} to allow for biarsenical labelling similar to the work of Taguchi et al (2008). Although theoretical we reasoned that a cryptic motif would become available for binding during denaturation, allowing us to determine PrP stability as a function of denaturation time or concentration of denaturing agent. Existing protocols have employed denaturation with urea (Kim et al., 2009) and guanidine (Peretz et al., 2001) to determine the stability of various proteins. We generated multiple tetracysteine-containing PrP clones but were unable to stably express our constructs, halting work on this experiment in favour of more promising leads. As an alternative we are now considering antibody labelling of PrP. As our antibody of choice, ICSM18, recognises a linear epitope (Klohn et al., 2012) it may prove difficult to determine the level of protein unfolding due to denaturation. The ability of misfolded PrP to resist degradation by PK is a key biochemical

characteristic of PrP^{Sc} (Oesch et al., 1985). It may be possible to determine the stability of PrP^{C} in different gradient fractions by testing resistance to a low concentration of PK over increasing digestion times.

Following the early work of Taraboulos et al there have been multiple attempts to thwart prion disease using cholesterol-lowering drugs. Notably Simvastatin, an analogue of lovastatin already used in patients to protect against hyperlipidaemia (Thanh et al., 2012), has been shown to increase the lifespan of prion infected mice (Mok et al., 2006, Kempster et al., 2007, Haviv et al., 2008). However these studies do not show differences in levels of PrP^{Sc} and in some cases do not show a reduction in CNS cholesterol (Mok et al., 2006, Kempster et al., 2007). Interestingly in one study demonstrating a neuroprotective effect of Simvastatin a parallel increase in PrP^{Sc} was observed (Haviv et al., 2008) although cholesterol levels were not changed. This suggests that antagonism of the mevalonate pathway reduces prion toxicity independent of cholesterol. As our data shows reduced cholesterol following *Dhcr24* knockdown increasing prion replication in cell culture it will be important to see how this translates to effects *in vivo*. Work by Mirza et al (2006) has shown that *Dhcr24*-null mice are not viable and so we intend to knockdown *Dhcr24* by RNAi in wild type mice. We have outsourced production of AAV constructs to Vector Core (Penn State University) containing novel short hairpin RNA targeting *Dhcr24*. While the final experimental planning is ongoing the overall intention is to silence *Dhcr24* in the brains of young prion infected mice and to observe differences in lifespan and prion deposition.

Prion infection is known to stimulate cholesterol biosynthesis (Bach et al., 2009) although we did not observe a difference in cholesterol levels between uninfected and infected S7 cells. Having recently discussed these findings with Ina Vorberg, who directed the studies of Bach and Gilch, we considered how prion infection may disrupt cholesterol metabolism to account for these changes. Prion infection may partially disrupt lipid raft structure and cholesterol metabolism (Kumar et al., 2008, Cui et al., 2014) which could feedback to the cholesterol

synthesis pathway. Controversially, if cholesterol limits prion replication as suggested by our data, then increased cholesterol production following prion infection may be seen as an adaptive response aimed at preventing the spread of PrP^{Sc}. Although there is no strict evidence for either theory it seems more likely that cells respond to perturbed cholesterol homeostasis rather than initiate an innate protective mechanism against prion disease.

4.1.5 Implications for prion disease

The site of conversion of PrP^{C} to PrP^{Sc} remains elusive. Both endosomes/lysosomes (Borchelt et al., 1992, Marijanovic et al., 2009) and membrane domains (Kaneko et al., 1997, Sunyach et al., 2003) have been suggested as potential conversion sites. In a 2002 review of the role of lipid rafts in disease Jacques Fantini proposed that raft association increased PrP^{C} and PrP^{Sc} proximity and so facilitates prion propagation (Fantini et al., 2002). Conversely, Roger Morris has suggested that conversion to PK-resistant PrP occurs after PrP^{C} leaves lipid rafts to be internalised and trafficked intracellularly (Morris et al., 2006). There is growing evidence for this theory: GPI-linked PrP^{C} in model rafts resists conversion to PrP^{Sc} in cell free models (Baron et al., 2002), depletion of sphingomyelin from rafts increases prion replication (Naslavsky et al., 1999) and PrP^{Sc} formation is reduced when formation of the multivesicular body is impaired (Yim et al., 2015). Our data suggests that cholesterol depletion shifts PrP^{C} out of rafts and that this is associated with increased prion replication.

Given that cholesterol lowering drugs prolong survival time in prion infected mice, and early research suggested that inhibition of cholesterol synthesis prevents accumulation of PrP^{Sc}, reducing cellular cholesterol presents an attractive target for treatment of prion disease. However our data contradicts these findings and demonstrates that impaired cholesterol synthesis and trafficking increases prion replication. If PrP^{Sc} is the toxic agent in prion disease then its increased replication would be expected to hasten patient mortality. So as not to diddle future patients out of a potentially effective treatment further research is required to assess the

role of cholesterol in prion replication. Our data suggests that cholesterol reduction disrupts binding of PrP^C to lipid rafts which promotes prion replication by an unknown mechanism. Naslavsky et al have previously demonstrated that sphingomyelin reduction by treatment with fumonisin B1 (FB1) increased levels of PrP^{Sc} in chronically infected cells (Naslavsky et al., 1999). The theory that sphingomyelin impairs prion replication is supported by evidence that oligodendrocytes, which express high levels of sphingomyelin for myelin sheath production, are resistant to prion infection (Prinz et al., 2004). In a more recent study FB1 treatment reduced PrP^{Sc} in RML-infected GT1 cells, with the authors suggesting differences in the models used between the studies accounted for this contrast (Agostini et al., 2013). Notably Naslavsky et al reported that PrP^C association with raft fractions was not affected by FB1 treatment, and as previously reported by Gilch et al it is the cholesterol component of lipid rafts required for binding of PrP^C (2005). Given that PrP has a sphingolipid binding domain analogous to the V3 loop of HIV envelope protein (Mahfoud et al., 2002) and lipid raft association is involved in stabilising PrP^C (Sarnataro et al., 2004) a potential protective role for both cholesterol and sphingolipid components of lipid rafts emerges. Theoretically sequestration of PrP^C into rafts by cholesterol-GPI anchor interaction allows for sphingomyelin binding to the V3-like loop stabilising PrP^C and limiting prion replication. Depletion of cholesterol prevents sequestration of PrP^C into rafts, preventing sphingomyelin binding and so rendering PrP^C unstable enough for prion replication. Similarly when sphingomyelin is depleted PrP^C still binds to cholesterol in rafts but is not stabilised by binding at the V3-like loop allowing for prion replication. This model is represented in **Figure 4.1**. In this model prion replication would occur in non-cholesterol or sphingolipid depleted systems when PrP^C is trafficked out of rafts for endosomal recycling. The site of prion conversion remains controversial and this model would not discriminate between conversion in non-raft membrane areas or along the endocytotic pathway.

There are several experiments which could be performed to test this model. Previously Naslavsky et al have shown that treatment of prion infected cells with PDMP, a glycosphingolipid

inhibitor which increased sphingomyelin levels, reduced PrP^{Sc} in cells (Naslavsky et al, 1999). It may be possible to block sphingolipid binding to PrP^{C}, either using a small inhibitor or by expressing a truncated PrP mutant which lacks the V3-like loop region. It may be interesting to see whether the V3-like loop is required for conversion or is exclusively involved in sphingolipid binding and protein stability. We would be able to rapidly screen truncation mutants of PrP expressed in cells using the SCA, and indeed this technique has recently been used in the MRC Prion Unit to perform an alanine mutagenesis screen of critical regions in PrP for prion replication (Savroop Bhamra & Parmjit Jat, unpublished observations). We could also investigate PrP stability using a denaturing assay such as those suggested above to investigate the stability of PrP^{C} in different gradient fractions. It is possible that alterations in the V3-like loop could decrease protein stability by preventing sphingomyelin binding, however if an introduced mutation sufficiently alters folding of PrP then stability may be increased. As such other assays to determine protein structure, perhaps x-ray crystallography, may be required downstream to investigate this model.

Potentially the effects of sphingomyelin and cholesterol in limiting prion replication may be synergistic. As such treatments which reduce levels of both cholesterol and sphingomyelin should further increase prion replication compared to treatment which only reduces one of the two lipids. As both cholesterol and sphingomyelin are key components of the cell membrane a reduction in both may be toxic to cells. Early in this project we considered whether stable knockdown of genes such as *Dhcr24* would be counterproductive, with the most efficiently silenced cells effectively selecting themselves out of experiments due to impaired viability. It may therefore be necessary to titrate treatments to balance lipid reduction and cell viability, and a combination of gene silencing and treatment with small inhibitors may prove useful.

4.2 Cellular factors influence susceptibility to prion strains

Cultured cell lines display different patterns of susceptibility to different prion strains. Similarly, different prion strains elicit different patterns of neuronal lesions and PrP^{Sc} deposition *in vivo*. It stands to reason that differences between different cell types affect permissiveness to different prion strains leading to these effects. Given the suggestion that prion strains exist as a pool of conformer quasispecies and the discovery that prion strains can adapt to differences in brain and cultured cells (Li et al., 2010) we considered whether cellular factors affected the ability of prion strains to propagate. We reasoned that isolation of closely related cells which propagate different prion strains would allow for examination of these cellular factors with minimal masking from other cell phenotypes.

Whilst this project's primary aim of isolating subclones which exclusively propagate a single prion strain was met we did not attempt the second objective of determining which cellular factors regulate susceptibility to different prion strains. This was primarily due to the time required to build a substantial cohort of rare variant subclones which was limited by the time required to passage subclones through the SCA. Even with high throughput screening on the MRC Prion Unit robots, which allow for up to 20 96-well plates to be processed in a single run, the number of tests required for each subclone limited us to a maximum of 480 subclones per run.

4.2.1 CAD5 subcloning yields rare variant cells which exclusively propagate a single prion strain

The catecholaminergic neuronal cell line CAD5 is susceptible to both RML and 22L prion strains and gives similar levels of propagation of each strain as assessed by Elispot following the SCA. By subcloning CAD5 cells we were able to isolate rare variant cells which exclusively propagate either RML or 22L. Whilst only a small cohort of these rare variants was isolated our data suggest that exclusive propagation of RML was maintained over several passages.

In agreement with previous reports we found CAD5 cells to be slightly more susceptible to RML than 22L or Me7 (Mahal et al., 2007). This was especially apparent at higher concentrations of homogenate where RML infection led to the number of PrP^{Sc}-positive CAD5 cells saturating the detector used in our assays. We excluded Me7 from further experimentation as the number of PrP^{Sc}-positive cells obtained in our assays was far less than the spot counts recorded for 22L or RML. At the 10^{-5} dilution of homogenate used for our cohorts there was a notable increase in PrP^{Sc}-positive cells following RML infection compared to infection with 22L in our initial experiments, however this difference was not seen in our screening assays. Data from both subclone runs showed similar responses across the entire population to RML and 22L, with high standard deviations for both homogenates indicating wide variation in the number of PrP^{Sc}-positive cells recorded. By transforming spot count data into the ratio of RML spots compared to total spots (selectivity score, SS) we were able to account for preferences in cells whilst also accounting for the expectation that different subclones would be more or less susceptible to prion infection by any strain. When the number of subclones was plotted as a function of SS the data assumed a normal distribution with a mean close to 0.5 suggesting our subclone populations were not biased in susceptibility towards either RML or 22L.

Despite the distribution of SS being seemingly without skew we isolated greater numbers of RML-exclusive than 22L-exclusive subclones. Additionally our pilot data suggests that exclusive susceptibility to RML is more stable than exclusive susceptibility to 22L. We attempted to reduce bias in this study by infecting cells with the same dilution of each homogenate but in light of the work of Mahal et al a more tailored approach may be more appropriate for future work. Mahal et al characterised response indexes (RI) for the prion strains tested, equivalent to the reciprocal of the homogenate concentration required to produce 300 spots on an elispot of 20000 cells (Mahal et al., 2007). It may be better to titre our infections to the RI obtained for our homogenates in our cells. We did produce a crude attempt at this comparing infection of CAD5 cells with RML and 22L over 4 log dilutions of homogenate but only considered this as evidence

of susceptibility to each strain in our experimental plan. Mahal et al showed similar RIs for both RML and 22L in CAD5 cells. By comparing concentrations of homogenates which should produce equal numbers of PrP^{Sc}-positive cells per strain we may be able to reduce bias towards one strain. Of course changing the volume of homogenate added to cells may in itself skew results as there is the potential for toxic (non-prion) agents such as reactive oxygen species to be conferred by brain tissue (Driver et al., 2000). As such samples may need to be buffered to a fixed concentration using uninfected mouse brain homogenate as a negative control for prion infection studies.

Both RML and 22L are mouse adapted strains of Scrapie PrP^{Sc} and as such may display similar adaptations to cell lines. Indeed the work of Mahal et al reveals that four cell lines which propagate 22L also propagate RML (2007). Whilst this did not prevent us from isolating exclusively propagating rare variant subclones in this study it is possible that a more notable difference could be seen in a cell line which demonstrates highly competent replication of one strain but a more limited (but still detectable) replication of another. To continue using the work of Mahal as an example CAD5 cells recorded a RI ~30-fold greater for 22L than the 301C prion strain (2007). For reference Mahal et al recorded only a 2-fold difference in RI between RML and 22L in favour of RML. Building on further work from this lab it may be possible to isolate extremely rare variant subclones which propagate 301C preferably to 22L which may display more pronounced differences than those seen between RML- and 22L-preferring subclones.

4.2.2 Cell lines other than CAD5 were not suitable for subcloning

Prior to selecting CAD5 as our cell line of choice for this project we tested several other lines. For various reasons these cell lines were unsuitable for our experimental design but our work with them supports the hypothesis that cellular factors influence susceptibility to different prion strains. PK1-11 and R33 cells are both derived from the N2a cell line (Klohn et al., 2003) but display different susceptibility to RML prions. Similarly whilst both PK1-11 and LD9 cells are

susceptible to RML only LD9 cells were susceptible to Me7 in our initial experiments. We sourced 22L prions fairly late in the project after ruling out these cell lines and so did not test propagation of 22L in R33, LD9 or PK1-11 cells. Previously R33, LD9 and PK1 (of which PK1-11 are a subclone) cell lines have been shown to be susceptible to 22L prions although to different extents (Mahal et al., 2007).

We excluded R33 cells on the basis that they are resistant to prion infection by RML and Me7. This is unsurprising given that R33 were originally isolated as an RML-resistant subclone of N2a cells (Klohn et al., 2003). Subcloning of R33 may prove interesting in the future to identify subclones which regain susceptibility to RML. We recently published work similar to this whereby prion-resistant PK1 subclones were isolated alongside highly susceptible cells (Marbiah et al., 2014). In this study we identified a network of gene expression associated with remodelling of the extracellular matrix which also regulated susceptibility to prion infection. In this study the gene expression of R33 and other N2a subclones were mapped to 3D transcript profiles which revealed that R33 cells were distinct from other subclones used in the study. As such it is possible that cellular factors other than those which regulate extracellular matrix remodelling are responsible for resistance to prion infection in R33 cells.

PK1-11 cells were excluded from further experimentation as they were susceptible to RML but not Me7. It is possible that PK1-11 may also be susceptible to 22L prions but this was not tested here. We reasoned that a cell line which already exclusively propagated one prion strain, but not another, provided evidence that strain susceptibility is encoded by cellular factors but was not a good model for our intended study. If PK1-11 cells are susceptible to 22L, which is likely given that the parent PK1 cell line is susceptible (Mahal et al., 2007), then these cells may be a potential model in the future to confirm our CAD5 findings. Not only might we be able to confirm if a given set of genes or processes are required for susceptibility to a given strain but the PK1-11 model may prove more stable than CAD5. Noticeably in out pilot study exclusive susceptibility

to 22L was lost over a few passages. If exclusive susceptibility is not stable then we may be unable to confirm cellular factors underlying this phenotype. If PK1-11 cells provide a more stable model of exclusive susceptibility to 22L than CAD5 they may be a more useful model in future work.

Whilst LD9 cells were susceptible to both RML and Me7 prion strains we did not take them forward in this study as they were unsuitable for high throughput screening. We found LD9 cells were far more adherent than N2a subclones and so unsuitable for resuspension on our in house robot. Automated processing was of particular importance to our experimental design as we thought exclusively susceptible subclones would be very rare and so require screening of large subclone cohorts. Prior to obtaining 22L prions LD9 presented the best option for our subcloning project. LD9 cells could be passaged in the SCA by hand and as such we attempted to optimise automated passaging of LD9 cells on our robot. We considered whether the bore of the pipette tips used on the robot combined with the pressure applied was insufficient to aspirate cells from the plate surface. We tested several different types and sizes of pipette tips, along with different resuspension volumes, but were unable to easily resuspend LD9 in growth media. Our standard culture conditions to maintain LD9 in petri dishes requires trypsinisation to passage cells. We attempted to optimise trypsinisation for the 96 well plate format and were able to successfully passage LD9 cells on the robot in this way. However we reasoned that as trypsin can cause the internalisation of surface proteins such as PrP (Caughey et al., 1988) doing so may interfere with prion propagation as the site of conversion of PrP^{C} to PrP^{Sc} is currently unknown. By this point in the study we had characterised the response of CAD5 cells to RML and 22L and so LD9 cells were dropped in favour of this model.

4.2.3 Future work

Future investigation into cellular factors determining susceptibility to prion strains would ideally begin by determining differences in gene expression between subclones susceptible to different

prion strains. As demonstrated by our recent publication (Marbiah et al., 2014) there is a gene signature associated with prion susceptibility which could mask differences between rare variant subclones. As such non-preferring subclones would serve as a baseline of gene expression from which to detect alterations. During isolation of subclones we observed a high variation in susceptibility to both prion strains across the population of subclones. Similar to the revertant subclones isolated by Marbiah et al (2014) some subclones displayed low to negligible susceptibility to both RML and 22L. These cells were largely ignored for the purposes of this study but in future work it may be interesting to test whether the regulatory genes identified by Marbiah et al also limit prion susceptibility in revertant CAD5 subclones. A key observation in our recent study was that prion susceptibility could be induced in prion resistant cells either by differentiation with retinoic acid or knockdown of any one of a subset of identified genes. Similarly we would be able to validate which expressed genes, if any, regulate susceptibility to RML or 22L by silencing identified genes in the SCA. It is also possible that increased gene expression would aid propagation of a distinct prion strain and as such it may be necessary to overexpress certain genes to induce susceptibility to a non-preferred prion strain. Structural differences in PrP which alter susceptibility to prion conversion have previously been investigated by Atarashi et al (2006). Here substitutions in the amino acid sequence of PrP which altered protein conformation changed susceptibility of the resulting protein to conversion by 22L and Chandler prion strains. Importantly the effects of these amino acid substitutions were strain dependent, suggesting that conformational differences in a prion strain influence the strain's ability to replicate using PrP^C. These conformational differences may help to explain the species barrier which limits zoonotic transmission of prion disease.

In our second cohort we tested whether strain preference was stably retained over multiple passages. Whilst all RML-preferring and non-preferring subclones gave a similar susceptibility score over both assays the sole 22L-preferring subclone in this cohort lost preference and gave a neutral score in the repeat assay. Retesting included a higher number of technical repeats per

clone, and whilst these varied returned similar numbers of PrP^{Sc}-positive cells ('spot count') as in the initial screening run. We were careful to exclude clones in this run which yielded a spot count lower than 200 for the preferred strain as lower values would decrease differences between RML and 22L and so decrease the sensitivity of the susceptibility score. In the case of the 22L-preferring clone similar spot counts were recorded for 22L in both first and second tests, suggesting a renewed susceptibility to RML rather than a complete loss of susceptibility. Furthermore the preference for 22L was weaker across the board compared to RML. In the case of our 480 subclone cohort preference for RML was accompanied by almost 10-fold great response to RML than 22L, whilst 22L preferring subclones returned only 3- to 4-fold more spots for 22L than RML. Mahal et al recorded CAD5 response indexes of 19 and 10 for RML and 22L respectively (2007), indicating CAD5 propagate RML roughly twice as well as 22L. Although our subcloning runs did not record a significant difference in PrP^{Sc}-positive cells following infection with RML and 22L across the entire population of subclones it is possible that the CAD5 line has some bias towards propagation of RML.

Given that prion strains are known to demonstrate Darwinian adaptation (Li et al., 2010) it is possible that passaging prion strains through differentially susceptible subclones may alter the strain characteristics. Indeed, it is possible that passaged strains may become 'CAD5-adapted', and may produce a homogenous novel strain regardless of infection with RML or 22L. There are several ways this hypothesis could be tested. Firstly, if a strain adapts to propagate in a permissive CAD5 subclone the strain's characteristics may be sufficiently altered to propagate in all (or many) CAD5 subclones. As such it may be possible to propagate CAD5-adapted RML prions in a 22L-selective CAD5 subclone. Prion strains can be separated by 2 way electrophoresis (Provansal et al., 2010) and it is likely that different PrP quasispecies could exhibit different charge and mass due to differences in conformation and glycosylation respectively. If so two-directional gel electrophoresis could be employed to characterise RML and 22L before and after passage through CAD5 cells, with the aim of identifying changes in signal which could represent

adaptation to CAD5 cells. Furthermore we could also attempt to infect RML-preferring subclones with cell lysates of 22L infected 22L-preferring subclones, and vice versa. The aim of this experiment would be to test whether passaging in CAD5 cells sufficiently adapts a prion strain to allow for infection of other closely related cells.

4.2.4 Implications for prion disease

Although only a pilot study our work here has several implications for future study of prion disease. Studies into strain selection where both strains are produced from the same species, such as the mouse strains RML, 22L and Me7 used here, can provide insight as to how conformational differences in PrP^{Sc} alter its properties. Furthermore this work, and its place in understanding the quasispecies selection model of prion strain adaptation, could help us to better understand the species barrier which limits zoonotic transmission of prion disease.

The quasispecies selection model hypothesises that prion strains contain a pool of PrP^{Sc} conformers of which one is dominant and gives the strain its characteristics (Collinge, 2010). Prion strains are known to adapt to different host species and cell lines (Li et al., 2010, Mahal et al., 2010) and show faster disease progression over multiple passages (Hamir et al., 2009, Baron et al., 2011). Theoretically these adaptions could be due to selection of different prion conformers which are better able to replicate in the new host environment. Our work here was based on the assumption that cellular factors limited the ability of prion strains to propagate in different cell lines, and we have demonstrated that different subclones isolated from the same parental cell pool display differential susceptibility to different prion strains. The conformation of PrP^{C} in a host system may influence which prion strains are able to propagate. Studies into the synthesis of PrP suggest key folding events may occur as PrP^{C} is post-translationally processed in the ER (Harris, 2003). As such if different processing occurs in different cell lines there may be different conformers of PrP^{C} expressed. Different PrP^{C} conformers may provide selection pressure for PrP^{Sc} quasispecies and so may alter strain characteristics over several

passages by selecting for a different dominant quasispecies. Indeed in 2010 Li et al were able to demonstrate reversible adaptation of prion strains using swainsonine. Similar to the work suggested above our CAD5 subclones may be able to select out CAD5-competent quasispecies from RML and 22L, which could be further investigated to provide evidence for pools of different PrP^{Sc} conformers in strains in the quasispecies model.

A defining characteristic of prion strains is the different patterns of PrP^{Sc} deposition and brain lesions produced *in vivo* (Bruce, 1993). These lesion patterns seem to occur following trafficking of PrP^{Sc} from the initial site of prion infection via white matter tracts (Kordek et al., 1999) and suggest differential susceptibility to different prion strains across the brain. As we have shown here, along with other studies, prion propagation can be limited by cellular factors. As such it is possible that different brain areas are more susceptible to some prion strains than others, which may explain differences in PrP^{Sc} deposition as prions are propagated more rapidly in some types of neuron than others. If the toxic effect of prion disease is mediated by PrP^{Sc} then lesion patterns would be expected to follow brain regions where a given prion strain is more able to replicate. It is possible that differences in lipid composition and availability may influence the pattern of PrP^{Sc} deposition seen with different prion strains (Castilla and Goni, 2011). In light of our other data this may represent the ability of different conformers to overcome changes in stability in PrP^{C} in different raft environments. In our previous work we demonstrated that the gene regulatory network we identified regulated susceptibility to both RML and 22L prion strains (Marbiah et al., 2014). We did not test our lipid targets against prion strains other than RML and it is possible that we would see different effects with other strains.

4.3 Contribution to Marbiah et al

Throughout this thesis I make reference to earlier work of which I am a co-first author investigating the role of the extracellular matrix in prion replication. The abstract and citation for this publication (Marbiah et al, 2014) are provided in **Appendix 1**. I worked on this study in a parallel stream to my PhD project and have not included results (other than images of PrP^{d}) in this thesis. In preparing the study for publication I performed multiple experiments and analysed SCA and confocal imaging data. Notably I assessed the effects of gene targets in CAD5 and LD9 cells and helped characterise the PrP basement membrane density. Furthermore, I analysed data from my experiments and helped interpret these findings in the context of the study and field as a whole.

4.4 Concluding Remarks

I have shown here that prion replication is influenced by multiple cellular factors. Lipid rafts, composed of cholesterol and sphingolipids, are required for cell surface presentation of PrP^{C}, stabilise the mature prion protein and may limit prion conversion. By silencing key genes required for cholesterol homeostasis I was able to show a shift of PrP^{C} out of lipid raft fractions of cell membranes which was associated with an increase in prion replication. Our data goes against early suggestions that cholesterol is a co-factor for prion replication and instead suggests that cholesterol limits prion propagation. Further work is required to determine the molecular mechanism by which cholesterol reduction increases production of PrP^{Sc}. In light of work by our and other groups it seems likely that lipid raft association stabilises PrP^{C} and so limits prion propagation.

I have also shown that cellular factors can lead to selective propagation of different prion strains. By subcloning CAD5 cells, which propagate multiple prion strains, I was able to isolate cells which exclusively propagated a single prion strain. In the context of existing knowledge of prion strains and factors which limit prion propagation our experiments could be interpreted as

a model for differences in cellular factors required to propagate different prion strains. To determine if an underlying pattern of gene expression determines which strains a cell can propagate an increased cohort for further study would be required.

5 References

Abad-Rodriguez J, Ledesma MD, Craessaerts K, Perga S, Medina M, Delacourte A, Dingwall C, De Strooper B, Dotti CG (2004) Neuronal membrane cholesterol loss enhances amyloid pepticle generation. Journal of Cell Biology 167:953-960.

Agostini F, Dotti CG, Perez-Canamas A, Ledesma MD, Benetti F, Legname G (2013) Prion protein accumulation in lipid rafts of mouse aging brain. PLoS ONE 8:e74244.

Allen JA, Halverson-Tamboli RA, Rasenick MM (2007) Lipid raft microdomains and neurotransmitter signalling. Nature Reviews Neuroscience ;8(2):128-40.

Alonso DOV, DeArmond SJ, Cohen FE, Daggett V (2001) Mapping the early steps in the pH-induced conformational conversion of the prion protein. Proceedings of the National Academy of Sciences of the United States of America 98:2985-2989.

Andersson M, Elmberger PG, Edlund C, Kristensson K, Dallner G (1990) Rates of Cholesterol, Ubiquinone, Dolichol and Dolichyl-P Biosynthesis in Rat-Brain Slices. FEBS Letters 269:15-18.

Annaba F, Sarwar Z, Kumar P, Saksena S, Turner JR, Dudeja PK, Gill RK, Alrefai WA (2008) Modulation of ileal bile acid transporter (ASBT) activity by depletion of plasma membrane cholesterol: association with lipid rafts. American Journal of Physiology-Gastrointestinal and Liver Physiology 294:G489-G497.

Ashe KH, Aguzzi A (2013) Prions, prionoids and pathogenic proteins in Alzheimer disease. Prion 7:55-59.

Atarashi R, Sim VL, Nishida N, Caughey B, Katamine S (2006) Prion strain-dependent differences in conversion of mutant prion proteins in cell culture. J Virol 80:7854-7862.

Atkinson PH (2004) Glycosylation of prion strains in transmissible spongiform encephalopathies. Australian Veterinary Journal 82:292-299.

Bach C, Gilch S, Rost R, Greenwood AD, Horsch M, Hajj GN, Brodesser S, Facius A, Schadler S, Sandhoff K, Beckers J, Leib-Mosch C, Schatzl HM, Vorberg I (2009) Prion-induced activation of cholesterogenic gene expression by a sterol regulatory element binding protein (SREBP2) in neuronal cells. Journal of Biological Chemistry 284(45):31260-9.

Bao J, Zheng JJ, Wu DQ (2012) The Structural Basis of DKK-Mediated Inhibition of Wnt/LRP Signaling. Science 3: 2969.

Barbero-Camps E, Fernandez A, Baulies A, Martinez L, Fernandez-Checa JC, Colell A (2014) Endoplasmic Reticulum Stress Mediates Amyloid beta Neurotoxicity via Mitochondrial Cholesterol Trafficking. American Journal of Pathology 184:2066-2081.

Baron GS, Caughey B (2003) Effect of GPI-anchor-dependent and-independent prion protein association with model raft membranes on conversion to the protease-resistant isoform. Journal of Biological Chemistry 278(17):14883-92.

Baron GS, Wehrly K, Dorward DW, Chesebro B, Caughey B (2002) Conversion of raft associated prion protein to the protease-resistant state requires insertion of PrP-res (PrP(Sc)) into contiguous membranes EMBO Journal 21:1031-1040.

Baron T, Vulin J, Biacabe AG, Lakhdar L, Verchere J, Torres JM, Bencsik A (2011) Emergence of Classical BSE Strain Properties during Serial Passages of H-BSE in Wild-Type Mice. PLoS ONE 6:e15839.

Basler K, Oesch B, Scott M, Westaway D, Walchli M, Groth DF, McKinley MP, Prusiner SB, Weissmann C (1986) Scrapie and cellular PrP isoforms are encoded by the same chromosomal gene. Cell 46:417-428.

Bate C, Tayebi M, Williams A (2008) Cholesterol esterification reduces the neurotoxicity of prions. Neuropharmacology 54(8):1247-53.

Baumgartner W, Weth A, Gutberlet J, Harms G, Groschner K (2014) Localization of VE-cadherin in plasmalemmal cholesterol rich microdomains and the effects of cholesterol depletion on VE-cadherin mediated cell-cell adhesion. Biochimica et Biophysica Acta-Molecular and Cell Biology of Lipids 1841:1725-1732.

Bazar E, Sheynis T, Dorosz J, Jelinek R (2011) Heparin Inhibits Membrane Interactions and Lipid-Induced Fibrillation of a Prion Amyloidogenic Determinant. Chembiochem 12(5):761-7.

Bentinger M, Tekle M, Dallner G (2010) Coenzyme Q - Biosynthesis and functions. Biochemical and Biophysical Research Communications 396:74-79.

Berwick DC, Harvey K (2012) LRRK2 functions as a Wnt signaling scaffold, bridging cytosolic proteins and membrane-localized LRP6. Human Molecular Genetics 21:4966-4979.

Bi XY, Han XP, Zhang F, He M, Zhang Y, Zhi XY, Zhao H (2012) Triparanol suppresses human tumor growth in vitro and in vivo. Biochemical and Biophysical Research Communications 425:613-618.

Blom TS, Linder MD, Snow K, Pihko H, Hess MW, Jokitalo E, Veckman V, Syvanen AC, Ikonen E (2003) Defective endocytic trafficking of NPC1 and NPC2 underlying infantile Niemann-Pick type C disease. Human Molecular Genetics 12:257-272.

Boadu E, Nelson RC, Francis GA (2012) ABCA1-dependent mobilization of lysosomal cholesterol requires functional Niemann-Pick C2 but not Niemann-Pick C1 protein. Biochimica et Biophysica Acta-Molecular and Cell Biology of Lipids 1821:396-404.

Borchelt DR, Scott M, Taraboulos A, Stahl N, Prusiner SB (1990) Scrapie and cellular prion proteins differ in their kinetics of synthesis and topology in cultured cells. Joirnal of Cellular Biology 110:743-752.

Borchelt DR, Taraboulos A, Prusiner SB (1992) Evidence for synthesis of scrapie prion proteins in the endocytic pathway. Journal of Biological Chemistry 267:16188-16199.

Brandner S, Raeber A, Sailer A, Blattler T, Fischer M, Weissmann C, Aguzzi A (1996) Normal host prion protein (PrP^C) is required for scrapie spread within the central nervous system. Proceedings of the National Academy of Sciences USA 93:13148-13151.

Browman D, Zurzolo C (2013) Not on the menu: autophagy-independent clearance of prions. Prion 7(4):286-90.

Brown DA, London E(1998) Structure and origin of ordered lipid domains in biological membranes. Journal of Membrane Biology 164:103–114

Brown DA, Rose JK (1992) Sorting of Gpi-Anchored Proteins to Glycolipid-Enriched Membrane Subdomains During Transport to the Apical Cell-Surface. Cell 68:533-544.

Brown P, Goldfarb LG, Gibbs CJJ, Gajdusek DC (1991) The phenotypic expression of different mutations in transmissible familial Creutzfeldt-Jakob disease. European Journal of Epidemiol 7:469-476.

Bruce E (1993) Scrapie strain variation and mutation. British Medical Bulletin 49:822-838.

Bueler H, Aguzzi A, Sailer A, Greiner RA, Autenried P, Aguet M, Weissmann C (1993) Mice devoid of PrP are resistant to scrapie. Cell 73:1339-1347.

Calero O, Bullido MJ, Clarimon J, Frank-Garcia A, Martinez-Martin P, Lleo A, Rey MJ, Rabano A, Blesa R, Gomez-Isla T, Valdivieso F, Pedro-Cuesta J, Ferrer I, Calero M (2011) Genetic Cross-Interaction between APOE and PRNP in Sporadic Alzheimer's and Creutzfeldt-Jakob Diseases. PLoS ONE 6(7):e22090.

Caputo A, Sarnataro D, Campana V, Costanzo M, Negro A, Sorgato CM, Zurzolo C (2009) Doppel and PrPC co-immunoprecipitate in detergent-resistant membrane domains of epithelial FRT cells. Biochemical Journal 425(2):341-51.

Carlsson SR, Fukuda M (1989) Structure of human lysosomal membrane glycoprotein 1. Assignment of disulfide bonds and visualization of its domain arrangement. Journal of Biological Chemistry 264(34):20526-31

Carstea ED, Morris JA, Coleman KG, Loftus SK, Zhang D, Cummings C, Gu J, Rosenfeld MA, Pavan WJ, Krizman DB, Nagle J, Polymeropoulos MH, Sturley SL, Ioannou YA, Higgins ME, Comly M, Cooney A, Brown A, Kaneski CR, BlanchetteMackie EJ, Dwyer NK, Neufeld EB, Chang TY, Liscum L, Strauss JF, Ohno K, Zeigler M, Carmi R, Sokol J, Markie D, Oneill RR, vanDiggelen OP, Elleder M, Patterson MC, Brady RO, Vanier MT, Pentchev PG, Tagle DA (1997) Niemann-Pick C1 disease gene: Homology to mediators of cholesterol homeostasis. Science 277:228-231.

Carter CJ (2007) Convergence of genes implicated in Alzheimer's disease on the cerebral cholesterol shuttle: APP, cholesterol, lipoproteins, and atherosclerosis. Neurochemistry International 50:12-38.

Castilla J, Goni FM (2011) Lipids, a missing link in prion propagation. Chemical Biology 18:1345-1346.

Caughey B, Race RE, Ernst D, Buchmeier MJ, Chesebro B (1989) Prion protein biosynthesis in scrapie-infected and uninfected neuroblastoma cells. Journal of Virology 63:175-181.

Caughey B, Race RE, Vogel M, Buchmeier MJ, Chesebro B (1988) In vitro expression in eukaryotic cells of a prion protein gene cloned from scrapie-infected mouse brain. Proceedings of the National Academy of Science USA 85:4657-4661.

Caughey B, Raymond GJ (1991) The scrapie-associated form of PrP is made from a cell surface precursor that is both protease- and phospholipase-sensitive. Journal of Biological Chemistry 266 No 27:18217-18223.

Cenedella RJ (2009) Cholesterol Synthesis Inhibitor U18666A and the Role of Sterol Metabolism and Trafficking in Numerous Pathophysiological Processes. Lipids 44(6):477-87.

Chamberlain LH (2004) Detergents as tools for the purification and classification of lipid rafts. FEBS Letters 559:1-5.

Chang TY, Chang CCY, Cheng D (1997) Acyl-coenzyme A: Cholesterol acyltransferase. Annual Review of Biochemistry 66:613-638.

Chang WC, Song H, Liu HW, Lu PH (2013) Current development in isoprenoid precursor biosynthesis and regulation. Current Opinion in Chemical Biology 17:571-579.

Cheng JL, Ohsaki Y, Tauchi-Sato K, Fujita A, Fujimoto T (2006) Cholesterol depletion induces autophagy. Biochemical and Biophysical Research Communications 351:246-252.

Christian AE, Haynes MP, Phillips MC, Rothblat GH (1997) Use of cyclodextrins for manipulating cellular cholesterol content. Journal of Lipid Research 38:2264-2272.

Chu CL, Buczek-Thomas JA, Nugent MA (2004) Heparan sulphate proteoglycans modulate fibroblast growth factor-2 binding through a lipid raft-mediated mechanism. Biochemical Journal 379:331-341.

Collinge J (2005) Molecular neurology of prion disease. Journal of Neurological and Neurosurgical Psychiatry 76:906-919.

Collinge J (2010) Medicine. Prion strain mutation and selection. Science 328:1111-1112.

Collinge J, Clarke A (2007) A general model of prion strains and their pathogenicity. Science 318:930-936.

Collinge J, Sidle KC, Meads J, Ironside J, Hill AF (1996) Molecular analysis of prion strain variation and the aetiology of 'new variant' CJD. Nature 383:685-690.

Collinge J, Palmer MS, Campbell TA, Sidle KCL, Carroll D, Harding AE (1993) Inherited prion disease (PrP lysine 200) in Britain: two case reports. British Medical Journal 306:301-302.

Corder EH, Saunders AM, Strittmatter WJ, Schmechel DE, Gaskell PC, Small GW, Roses AD, Haines JL, Pericak-Vance MA (1993) Gene dose of Apolipoprotein E type 4 Allele and the risk of Alzheimer's disease in late onset families. Science 261:921-923.

Coxey RA, Pentchev PG, Campbell G, BlanchetteMackie EJ (1993) Differential Accumulation of Cholesterol in Golgi Compartments of Normal and Niemann-Pick Type-C Fibroblasts Incubated with Ldl - A Cytochemical Freeze-Fracture Study. Journal of Lipid Research 34:1165-1176.

Crameri A, Biondi E, Kuehnle K, Lutjohann D, Thelen KM, Perga S, Dotti CG, Nitsch RM, Ledesma MD, Mohajeri MH (2006) The role of seladin-1/DHCR24 in cholesterol biosynthesis, APP processing and A beta generation in vivo. EMBO Journal 25:432-443.

Cui HHL, Guo B, Scicluna B, Coleman BM, Lawson VA, Ellett L, Meikle PJ, Bukrinsky M, Mukhamedova N, Sviridov D, Hill AF (2014) Prion Infection Impairs Cholesterol Metabolism in Neuronal Cells. Journal of Biological Chemistry 289:789-802.

Cunningham D, DeBarber AE, Bir N, Binkley L, Merkens LS, Steiner RD, Herman GE (2015) Analysis of hedgehog signaling in cerebellar granule cell precursors in a conditional Nsdhl allele

demonstrates an essential role for cholesterol in postnatal CNS development. Human Molecular Genetics 24:2808-2825.
Daude N, Marella M, Chabry J (2003) Specific inhibition of pathological prion protein accumulation by small interfering RNAs. Journal of Cell Science 116:2775-2779.
Davenport KA, Henderson DM, Bian J, Telling GC, Mathiason CK, Hoover EA (2015) Insights into Chronic Wasting Disease and Bovine Spongiform Encephalopathy Species Barriers by Use of Real-Time Conversion. Journal of Virology 89(18):9524-31.
Deffieu MS, Pfeffer SR (2011) Niemann-Pick type C 1 function requires lumenal domain residues that mediate cholesterol-dependent NPC2 binding. Proceedings of the National Academy of Sciences of the United States of America 108:18932-18936.
Deleault NR, Harris BT, Rees JR, Supattapone S (2007) Formation of native prions from minimal components in vitro. Proceedings of the National Acadedy of Sciences USA 104:9741-9746.
Deleault NR, Piro JR, Walsh DJ, Wang F, Ma J, Geoghegan JC, Supattapone S (2012) Isolation of phosphatidylethanolamine as a solitary cofactor for prion formation in the absence of nucleic acids. Proceedings of the National Academy of Sciences of the United States of America 109(22):8546-51.
DiCiccio JE, Steinberg BE (2011) Lysosomal pH and analysis of the counter ion pathways that support acidification. Journal of General Physiology 137:385-390.
Dietrich C, Bagatolli LA, Volovyk ZN, Thompson NL, Levi M, Jacobson K, Gratton E (2001) Lipid rafts reconstituted in model membranes. Biophysical Journal 80:1417-1428.
Dietschy JM (2009) Central nervous system: cholesterol turnover, brain development and neurodegeneration. Biological Chemistry 390:287-293.
Driver AS, Kodavanti PRS, Mundy WR (2000) Age-related changes in reactive oxygen species production in rat brain homogenates. Neurotoxicology and Teratology 22:175-181.
Eberl H, Tittmann P, Glockshuber R (2004) Characterization of recombinant, membrane-attached full-length prion protein. Journal of Biological Chemistry 279(24):25058-65.
Ermonval M, Mouillet-Richard S, Codogno P, Kellermann O, Botti J (2003) Evolving views in prion glycosylation: functional and pathological implications. Biochimie 85:33-45.
Fantini J, Garmy N, Mahfoud R, Yahi N (2002) Lipid rafts: structure, function and role in HIV, Alzheimers and prion diseases. Expert Reviews in Molecular Medicine 2002:1-22.
Farmer JA (1998) Aggressive lipid therapy in the statin era. Progress in Cardiovascular Diseases 41:71-94.
Fassbender K, Simons M, Bergmann C, Stroick M, Lutjohann D, Keller P, Runz H, Kuhl S, Bertsch T, von Bergmannn K, Hennerici M, Beyreuther K, Hartmann T (2001) Simvastatin strongly reduces levels of Alzheimer's disease beta-amyloid peptides A beta 42 and A beta 40 in vitro and in vivo. Proceedings of the National Academy of Sciences of the United States of America 98:5856-5861.
Fraser H, Dickinson AG (1973) Scrapie in mice. Agent-strain differences in the distribution and intensity of grey matter vacuolation. Journal of Computational Pathology 83:29-40.
G M, Dickinson A, J L, P K, S B, J C (2003) Depleting neuronal PrP in prion infection prevents disease and reverses spongiosis. Science 302:871-874.
Gabas-Rivera C, Barranquero C, Martinez-Beamonte R, Navarro MA, Surra JC, Osada J (2014) Dietary Squalene Increases High Density Lipoprotein-Cholesterol and Paraoxonase 1 and Decreases Oxidative Stress in Mice. PLoS ONE 9(8):e104224.
Gabbi C, Warner M, Gustafsson JA (2014) Action mechanisms of Liver X Receptors. Biochemical and Biophysical Research Communications 446:647-650.
Gambetti P, Parchi P, Chen SG (2003) Hereditary Creutzfeldt-Jakob disease and fatal familial insomnia. Clinical Laboratory Medicine 23(1):43-64.
Gan XD, Kaplan R, Menke JG, MacNaul K, Chen YL, Sparrow CP, Zhou GH, Wright SD, Cai TQ (2001) Dual mechanisms of ABCA1 regulation by geranylgeranyl pyrophosphate. Journal of Biological Chemistry 276:48702-48708.

Ghetti B, Dlouhy SR, Giaccone G, Bugiani O, Frangione B, Farlow MR, Tagliavini F (1995) Gerstmann-Straussler-Scheinker Disease and the Indiana Kindred Brain Pathology 5: 61-75

Gidwani B, Vyas A (2014) Synthesis, characterization and application of Epichlorohydrin-beta-cyclodextrin polymer. Colloids and Surfaces B-Biointerfaces 114:130-137.

Gilch S, Bach C, Lutzny G, Vorberg I, Schatzl HM (2009) Inhibition of cholesterol recycling impairs cellular PrP(Sc) propagation. Cellular and Molecular Life Science 66(24):3979-91.

Gilch S, Kehler C, Schatzl HM (2005) The prion protein requires cholesterol for cell surface localization. Molecular and Cellular Neuroscience 31(2):346-5.

Gill ON, Spencer Y, Richard-Loendt A, Kelly C, Dabaghian R, Boyes L, Linehan J, Simmons M, Webb P, Bellerby P, Andrews N, Hilton DA, Ironside J, Beck JA, Poulter M, Mead S, Brandner S (2013) Prevalent abnormal prion protein in human appendices after cattle BSE epizootic. British Medical Journal 15;347:f5675.

Goldstein JL, Brown MS (1990) Regulation of the Mevalonate Pathway. Nature 343:425-430.

Goldstein JL, Dana SE, Faust JR, Beaudet AL, Brown MS (1975) Role of Lysosomal Acid Lipase in Metabolism of Plasma Low-Density Lipoprotein - Observations in Cultured Fibroblasts from A Patient with Cholesteryl Ester Storage Disease. Journal of Biological Chemistry 250:8487-8495.

Goold R, McKinnon C, Rabbanian S, Collinge J, Schiavo G, Tabrizi S (2013) Alternative fates of newly formed PrPSc upon prion conversion on the plasma membrane. Journal of Cell Science 126(Pt 16):3552-62.

Greeve I, Hermans-Borgmeyer I, Brellinger C, Kasper D, Gomez-Isla T, Behl C, Levkau B, Nitsch RM (2000) The human DIMINUTO/DWARF1 homolog seladin-1 confers resistance to Alzheimer's disease-associated neurodegeneration and oxidative stress. Journal of Neuroscience 20:7345-7352.

Griffith JS (1967) Self Replication and scrapie. Nature 215:1043-1044.

Grundner M, Jokhadar SZ (2014) Cytoskeleton Modification and Cholesterol Depletion Affect Membrane Properties and Caveolae Positioning of CHO Cells. Journal of Membrane Biology 247:201-210.

Guan ZZ, Söderberg M, Sindelar P, Prusiner SB, Kristensson K, Dallner G (1996) Lipid composition in scrapie-infected mouse brain: Prion infection increases the levels of dolichyl phosphate and ubiquinone. Journal of Neurochemistry 66:277-285.

Haag MDM, Hofman A, Koudstaal PJ, Stricker BHC, Breteler MMB (2009) Statins are associated with a reduced risk of Alzheimer disease regardless of lipophilicity. The Rotterdam Study. Journal of Neurology Neurosurgery and Psychiatry 80:13-17.

Hagiwara K, Hara H, Hanada K (2013) Species-barrier phenomenon in prion transmissibility from a viewpoint of protein science. Journal of Biochemistry 53(2):139-45.

Haigh CL, Edwards K, Brown DR (2005) Copper binding is the governing determinant of prion protein turnover. Molecular and Cellular Neuroscience 30(2):186-96..

Hamir AN, Kunkle RA, Richt JA, Greenlee JJ, Miller JM (2009) Serial Passage of Sheep Scrapie Inoculum in Suffolk Sheep. Veterinary Pathology 46:39-44.

Hannaoui S, Shim SY, Cheng YC, Corda E, Gilch S (2014) Cholesterol Balance in Prion Diseases and Alzheimer's Disease. Viruses-Basel 6:4505-4535.

Hao MM, Mukherjee S, Maxfield FR (2001) Cholesterol depletion induces large scale domain segregation in living cell membranes. Proceedings of the National Academy of Sciences of the United States of America 98:13072-13077.

Harris DA (2003) Trafficking, turnover and membrane topology of PrP. British Medical Bulletin 66:71-85.

Hauser PS, Ryan RO (2013) Impact of Apolipoprotein E on Alzheimer's Disease. Current Alzheimer Research 10:809-817.

Haviv Y, Avrahami D, Ovadia H, Ben Hur T, Gabizon R, Sharon R (2008) Induced neuroprotection independently from PrPSc accumulation in a mouse model for prion disease treated with simvastatin. Archives of Neurology 65:762-775.

Hawes CM, Wiemer H, Krueger SR, Karten B (2010) Pre-synaptic defects of NPC1-deficient hippocampal neurons are not directly related to plasma membrane cholesterol. Journal of Neurochemistry 114:311-322.

Hawkes DJ, Mak J (2006) Lipid membrane; A novel target for viral and bacterial pathogens. Current Drug Targets 7:1615-1621.

Hayashi H (2011) Lipid Metabolism and Glial Lipoproteins in the Central Nervous System. Biological & Pharmaceutical Bulletin 34:453-461.

Hicks MR, Gill AC, Bath IK, Rullay AK, Sylvester ID, Crout DH, Pinheiro TJ (2006) Synthesis and structural characterization of a mimetic membrane-anchored prion protein. FEBS Journal 273:1285-1299.

Hill AF, Desbruslais M, Joiner S, Sidle KC, Gowland I, Collinge J, Doey LJ, Lantos P (1997) The same prion strain causes vCJD and BSE. Nature 389:448-450, 526.

Holtta-Vuori M, Uronen RL, Repakova J, Salonen E, Vattulainen I, Panula P, Li ZG, Bittman R, Ikonen E (2008) BODIPY-Cholesterol: A New Tool to Visualize Sterol Trafficking in Living Cells and Organisms. Traffic 9:1839-1849.

Hooper NM (2011) Glypican-1 facilitates prion conversion in lipid rafts. Journal of Neurochemistry 116:721-725.

Hooper NM, Taylor DR, Watt NT (2008) Mechanism of the metal-mediated endocytosis of the prion protein. Biochemical Society Transactions 36:1272-1276.

Hope J, Morton LJ, Farquhar CF, Multhaup G, Beyreuther K, Kimberlin RH (1986) The major polypeptide of scrapie-associated fibrils (SAF) has the same size, charge distribution and N-terminal protein sequence as predicted for the normal brain protein (PrP). EMBO Journal 5:2591-2597.

Hope J, Ritchie L, Farquhar C, Somerville R, Hunter N (1989) Bovine spongiform encephalopathy: a scrapie-like disease of British cattle. Progress in Clinical Biology Research 317:659-67.

Hornemann S, Korth C, Oesch B, Riek R, Wider G, Wuthrich K, Glockshuber R (1997) Recombinant full-length murine prion protein, mPrP(23-231): purification and spectroscopic characterization. FEBS Letters 413:277-281.

Hsiao K, Baker HF, Crow TJ, Poulter M, Owen F, Terwilliger JD et al (1989) Linkage of a prion protein missense variant to Gerstmann-Straussler syndrome. Nature 338:342–345.

Hsiao KK, Cass C, Schellenberg GD, Bird TD, Devine-Gage E, Wisniewski H, Prusiner SB (1991) A prion protein variant in a family with the telencephalic form of Gerstmann-Straussler-Scheinker syndrome. Neurology 41:681-684.

Hsiao KK, Scott M, Foster D, Groth DF, DeArmond SJ, Prusiner SB (1990) Spontaneous neurodegeneration in transgenic mice with mutant prion protein. Science 250:1587-1590.

Huang P, Lian F, Wen Y, Guo C, Lin D (2013) Prion protein oligomer and its neurotoxicity. Acta Biochim Biophys Sin (Shanghai) 45(6):442-51.

Hughes TM, Rosano C, Evans RW, Kuller LH (2013) Brain Cholesterol Metabolism, Oxysterols, and Dementia. Journal of Alzheimers Disease 33:891-911.

Ikeda M, Abe K, Yamada M, Dansako H, Naka K, Kato N (2006) Different anti-HCV profiles of statins and their potential for combination therapy with interferon. Hepatology 44:117-125.

Ikonen E (2006) Mechanisms for cellular cholesterol transport: Defects and human disease. Physiological Reviews 86:1237-1261.

Ikonen E (2008) Cellular cholesterol trafficking and compartmentalization. Nature Reviews Molecular Cell Biology 9:125-138.

Issop L, Rone MB, Papadopoulos V (2013) Organelle plasticity and interactions in cholesterol transport and steroid biosynthesis. Molecular and Cellular Endocrinology 371:34-46.

Jacobson K, Mouritsen OG, Anderson RGW (2007) Lipid rafts: at a crossroad between cell biology and physics. Nature Cell Biology 9:7-14.

Jaeger S, Pietrzik CU (2008) Functional role of lipoprotein receptors in Alzheimer's disease. Current Alzheimer Research 5:15-25.

Jaiswal JK, Andrews NW, Simon SM (2002) Membrane proximal lysosomes are the major vesicles responsible for calcium-dependent exocytosis in nonsecretory cells. Journal of Cell Biology 159:625-635.

Jasmin SB, Pearson V, Lalonde D, Domenger D, Theroux L, Poirier J (2014) Differential regulation of ABCA1 and ABCG1 gene expressions in the remodeling mouse hippocampus after entorhinal cortex lesion and liver-X receptor agonist treatment. Brain Research 1562:39-51.

Jeffrey M, Goodbrand IA, Goodsir CM (1995) Pathology of the transmissible spongiform encephalopathies with special emphasis on ultrastructure. Micron 26(3):277-98.

Jen A, Parkyn CJ, Mootoosamy RC, Ford MJ, Warley A, Liu Q, Bu G, Baskakov IV, Moestrup S, McGuinness L, Emptage N, Morris RJ (2010) Neuronal low-density lipoprotein receptor-related protein 1 binds and endocytoses prion fibrils via receptor cluster 4. Journal of Cell Science 123:246-255.

Jeon JH, Kim SK, Kim HJ, Chang J, Ahn CM, Chang YS (2010) Lipid raft modulation inhibits NSCLC cell migration through delocalization of the focal adhesion complex. Lung Cancer 69:165-171.

Jiang H, Badralmaa Y, Yang J, Lempicki R, Hazen A, Natarajan V (2012) Retinoic acid and liver X receptor agonist synergistically inhibit HIV infection in CD4+T cells by up-regulating ABCA1-mediated cholesterol efflux. Lipids in Health and Disease 11:69.

Jobling MF, Stewart LR, White AR, McLean C, Friedhuber A, Maher F, Beyreuther K, Masters CL, Barrow CJ, Collins SJ, Cappai R. (1999) The Hydrophobic Core Sequence Modulates the Neurotoxic and Secondary Structure Properties of the Prion Peptide 106–126 Journal of Neurochemistry 73, 1557–1565

Jobling MG, Yang ZJ, Kam WR, Lencer WI, Holmes RK (2012) A Single Native Ganglioside GM(1)-Binding Site Is Sufficient for Cholera Toxin To Bind to Cells and Complete the Intoxication Pathway. mBio 3(6). pii: e00401-12.

Kalback W, Esh C, Castano EM, Rahman A, Kokjohn T, Luehrs DC, Sue L, Cisneros R, Gerber F, Richardson C, Bohrmann B, Walker DG, Beach TG, Roher AE (2004) Atherosclerosis, vascular amyloidosis and brain hypoperfusion in the pathogenesis of sporadic Alzheimer's disease. Neurological Research 26:525-539.

Kaneko K, Vey M, Scott M, Pilkuhn S, Cohen FE, Prusiner SB (1997) COOH-terminal sequence of the cellular prion protein directs subcellular trafficking and controls conversion into the scrapie isoform. Proceedings of the National Acadedy of Sciences USA 94:2333-2338.

Kang YS, Zhao X, Lovaas J, Eisenberg E, Greene LE (2009) Clathrin-independent internalization of normal cellular prion protein in neuroblastoma cells is associated with the Arf6 pathway. Journal of Cell Science 122(Pt 22):4062-9.

Karasinska JM, Rinninger F, Lutjohann D, Ruddle P, Franciosi S, Kruit JK, Singaraja RR, Hirsch-Reinshagen V, Fan J, Brunham LR, Bissada N, Ramakrishnan R, Wellington CL, Parks JS, Hayden MR (2009) Specific Loss of Brain ABCA1 Increases Brain Cholesterol Uptake and Influences Neuronal Structure and Function. Journal of Neuroscience 29:3579-3589.

Karten B, Campenot RB, Vance DE, Vance JE (2006) Expression of ABCG1, but not ABCA1, correlates with cholesterol release by cerebellar astroglia. Journal of Biological Chemistry 281:4049-4057.

Karten B, Peake KB, Vance JE (2009) Mechanisms and consequences of impaired lipid trafficking in Niemann-Pick type C1-deficient mammalian cells. Biochimica et Biophysica Acta-Molecular and Cell Biology of Lipids 1791:659-670.

Kawahara M, Koyama H, Nagata T, Sadakane Y (2011) Zinc, copper, and carnosine attenuate neurotoxicity of prion fragment PrP106-126. Metallomics 3(7):726-34.

Kempster S, Bate C, Williams A (2007) Simvastatin treatment prolongs the survival of scrapie-infected mice. Neuroreport 18:479-482.

Kennedy BE, Charman M, Karten B (2012) Niemann-Pick Type C2 protein contributes to the transport of endosomal cholesterol to mitochondria without interacting with NPC1. Journal of Lipid Research 53:2632-2642.

Kilsdonk EPC, Yancey PG, Stoudt GW, Bangerter FW, Johnson WJ, Phillips MC, Rothblat GH (1995) Cellular Cholesterol Efflux Mediated by Cyclodextrins. Journal of Biological Chemistry 270:17250-17256.

Kim DH, Iijima H, Goto K, Sakai J, Ishii H, Kim HJ, Suzuki H, Kondo H, Saeki S, Yamamoto T (1996) Human apolipoprotein E receptor 2 - A novel lipoprotein receptor of the low density lipoprotein receptor family predominantly expressed in brain. Journal of Biological Chemistry 271:8373-8380.

Kim MS, Song J, Park C (2009) Determining protein stability in cell lysates by pulse proteolysis and Western blotting. Protein Science 18:1051-1059.

Kimberlin RH, Walker CA (1979) Pathogenesis of mouse scrapie: dynamics of agent replication in spleen, spinal cord and brain after infection by different routes. Journal of Computational Pathology 89:551-562.

Kimberlin RH, Walker CA (1985) Competition between strains of scrapie depends on the blocking agent being infectious. Intervirology 23:74-81.

Kimberlin RH, Walker CA (1989) The role of the spleen in the neuroinvasion of scrapie in mice. Virus Research 12:201-211.

Klohn P, Stoltze L, Flechsig E, Enari M, Weissmann C (2003) A quantitative, highly sensitive cell-based infectivity assay for mouse scrapie prions. . Proceedings of the National Acadedy of Sciences USA 100:11666-11671.

Klohn PC, Farmer M, Linehan JM, O'Malley C, de Marco MF, Taylor W, Farrow M, Khalili-Shirazi A, Brandner S, Collinge J (2012) PrP Antibodies Do Not Trigger Mouse Hippocampal Neuron Apoptosis. Science 335:52-52.

Koch G, Lalley PA, Mcavoy M, Shows TB (1981) Assignment of Lipa, Associated with Human Acid Lipase Deficiency, to Human Chromosome-10 and Comparative Assignment to Mouse Chromosome-19. Somatic Cell Genetics 7:345-358.

Kocisko DA, Priola SA, Raymond GJ, Chesebro B, Lansbury PT, Jr., Caughey B (1995) Species specificity in the cell-free conversion of prion protein to protease-resistant forms: a model for the scrapie species barrier. Proceedings of the National Acadedy of Sciences USA 92:3923-3927.

Korade, Zeljka; Kenworthy, Anne K. (2008). "Lipid rafts, cholesterol, and the brain". Neuropharmacology 55 (8): 1265–73

Kordek R, Hainfellner JA, Liberski PP, Budka H (1999) Deposition of the prion protein (PrP) during the evolution of experimental Creutzfeldt-Jakob disease. Acta Neuropathologica 98:597-602.

Kosicek M, Malnar M, Goate A, Hecimovic S (2010) Cholesterol accumulation in Niemann Pick type C (NPC) model cells causes a shift in APP localization to lipid rafts. Biochemical and Biophysical Research Communications 393:404-409.

Kretzschmar HA, Stowring LE, Westaway D, Stubblebine WH, Prusiner SB, DeArmond SJ (1986) Molecular cloning of a human prion protein cDNA. DNA 5:315-324.

Kumar R, McClain D, Young R, Carlson GA (2008) Cholesterol transporter ATP-binding cassette A1 (ABCA1) is elevated in prion disease and affects PrPC and PrPSc concentrations in cultured cells. Journal of General Virology 89:1525-1532.

Kurt TD, Jiang L, Fernandez-Borges N, Bett C, Liu J, Yang T, Spraker TR, Castilla J, Eisenberg D, Kong QZ, Sigurdson CJ (2015) Human prion protein sequence elements impede cross-species chronic wasting disease transmission. Journal of Clinical Investigation 125:1485-1496.

Laszlo L, Lowe J, Self T, Kenward N, Landon M, McBride T, Farquhar C, McConnell I, Brown J, Hope J, Mayer RJ (1992) Lysosomes as key organelles in the pathogenesis of prion encephalopathies. Journal of Pathology 166:333-341.

Lawrence JC, Saslowsky DE, Edwardson JM, Henderson RM (2003) Real-time analysis of the effects of cholesterol on lipid raft behavior using atomic force microscopy. Biophysical Journal 84:1827-1832.

Lewis PA, F P, Prodromidou K, A C, J C, GS J (2006) Removal of the glycosylphosphatidylinositol anchor from PrP(Sc) by cathepsin D does not reduce prion infectivity. Biochemical Journal 395:443-448.

Lewis V, Haigh CL, Masters CL, Hill AF, Lawson VA, Collins SJ (2012) Prion subcellular fractionation reveals infectivity spectrum, with a high titre-low PrPres level disparity. Molecular Neurodegeneration 7:18.

Lewis V, Hooper NM (2011) The role of lipid rafts in prion protein biology. Frontiers in Bioscience 16:151-168.

Li H, Dhanasekaran P, Alexander ET, Rader DJ, Phillips MC, Lund-Katz S (2013) Molecular Mechanisms Responsible for the Differential Effects of ApoE3 and ApoE4 on Plasma Lipoprotein-Cholesterol Levels. Arteriosclerosis Thrombosis and Vascular Biology 33:687-U101.

Li J, Browning S, Mahal SP, Oelschlegel AM, Weissmann C (2010) Darwinian evolution of prions in cell culture. Science 327:869-872.

Li TG, Chiang JYL (2014) Bile Acid Signaling in Metabolic Disease and Drug Therapy. Pharmacological Reviews 66:948-983.

Li YH, Lu WY, He X, Schwartz AL, Bu GJ (2004) LRP6 expression promotes cancer cell proliferation and tumorigenesis by altering beta-catenin subcellular distribution. Oncogene 23:9129-9135.

Libby P, Ridker PM, Hansson GK (2011) Progress and challenges in translating the biology of atherosclerosis. Nature 473:317-325.

Liberski PP, Sikorska B, Lindenbaum S, Goldfarb LG, McLean C, Hainfellner JA, Brown P (2012) Kuru: genes, cannibals and neuropathology. Journal of Neuropathology & Experimental Neurology. 71(2):92-103.

Lin YC, Lin CH, Kuo CY, Yang VC (2009) ABCA1 modulates the oligomerization and Golgi exit of caveolin-1 during HDL-mediated cholesterol efflux in aortic endothelial cells. Biochemical and Biophysical Research Communications 382:189-195.

Linden R, Martins VR, Prado MAM, Cammarota M, Izquierdo I, Brentani RR (2008) Physiology of the Prion Protein Physiological Reviews 88:2, 673-728

Lingwood D, Simons K (2007) Detergent resistance as a tool in membrane research Nature Protocols 2:2159-2165

Liu H, Urbe S, Clague MJ (2012) Selective protein degradation in cell signalling. Seminars in Cell & Developmental Biology 23:509-514.

Liu Q, Zerbinatti CV, Zhang J, Hoe HS, Wang B, Cole SL, Herz J, Muglia L, Bu GJ (2007) Amyloid precursor protein regulates brain apolipoprotein e and cholesterol metabolism through lipoprotein receptor LRP1. Neuron 56:66-78.

Liu Y, Yu JT, Wang HF, Han PR, Tan CC, Wang C, Meng XF, Risacher SL, Saykin AJ, Tan L (2015) APOE genotype and neuroimaging markers of Alzheimer's disease: systematic review and meta-analysis. Journal of Neurology Neurosurgery and Psychiatry 86:127-134.

Loertscher R, Lavery P (2002) The role of glycosyl phosphatidyl inositol (GPI)-anchored cell surface proteins in T-cell activation. Transplant Immunology 9:93-96.

Lopez CA, de Vries AH, Marrink SJ (2011) Molecular Mechanism of Cyclodextrin Mediated Cholesterol Extraction. Plos Computational Biology 7(3):e1002020.

Lu XL, Li Y, Wang WQ, Chen SC, Liu T, Jia D, Quan XP, Sun DL, Chang AK, Gao B (2014) 3 beta-Hydroxysteroid-Delta 24 Reductase (DHCR24) Protects Neuronal Cells from Apoptotic Cell Death Induced by Endoplasmic Reticulum (ER) Stress. PLoS ONE 9(1):e86753.

Luers L, Bannach O, Stohr J, Wordehoff MM, Wolff M, Nagel-Steger L, Riesner D, Willbold D, Birkmann E (2013) Seeded fibrillation as molecular basis of the species barrier in human prion diseases. PLoS ONE 8:e72623.

Ma J (2012)The Role of Cofactors in Prion Propagation and Infectivity. PLoS Pathogens 8(4): e1002589.

Magalhaes AC, Silva JA, Lee KS, Martins VR, Prado VF, Ferguson SS, Gomez MV, Brentani RR, Prado MA (2002) Endocytic intermediates involved with the intracellular trafficking of a fluorescent cellular prion protein. Journal of Biological Chemistry 277(36):33311-8.

Mahal SP, Baker CA, Demczyk CA, Smith EW, Julius C, Weissmann C (2007) Prion strain discrimination in cell culture: The cell panel assay. Proceedings of the National Acadedy of Sciences USA 104:20908-20913.

Mahal SP, Browning S, Li J, Suponitsky-Kroyter I, Weissmann C (2010) Transfer of a prion strain to different hosts leads to emergence of strain variants. Proceedings of the National Acadedy of Sciences USA 107(52):22653-8.

Mahfoud R, Garmy N, Maresca M, Yahi N, Puigserver A, Fantini J (2002) Identification of a common sphingolipid-binding domain in Alzheimer, prion, and HIV-1 proteins Journal of Biological Chemistry 277:11292-11296.

Malnar M, Kosicek M, Lisica A, Posavec M, Krolo A, Njavro J, Omerbasic D, Tahirovic S, Hecimovic S (2012) Cholesterol-depletion corrects APP and BACE1 misstrafficking in NPC1-deficient cells. Biochimica et Biophysica Acta-Molecular Basis of Disease 1822:1270-1283.

Mange A, Nishida N, Milhavet O, McMahon HEM, Casanova D, Lehmann S (2000) Amphotericin B inhibits the generation of the scrapie isoform of the prion protein in infected cultures. Journal of Virology 74:3135-3140.

Mani K, Cheng F, Fransson LA (2006) Defective nitric oxide-dependent, deaminative cleavage of glypican-1 heparan sulfate in Niemann-Pick C1 fibroblasts. Glycobiology 16:711-718.

Marbiah MM, Harvey A, West BT, Louzolo A, Banerjee P, Alden J, Grigoriadis A, Hummerich H, Kan HM, Cai Y, Bloom GS, Jat P, Collinge J, Klohn PC (2014) Identification of a gene regulatory network associated with prion replication. EMBO Journal 33:1527-1547.

Marella M, Lehmann S, Grassi J, Chabry J (2002) Filipin prevents pathological prion protein accumulation by reducing endocytosis and inducing cellular PrP release. Journal of Biological Chemistry 227:25457-25464.

Marijanovic Z, Caputo A, Campana V, Zurzolo C (2009) Identification of an Intracellular Site of Prion Conversion. Plos Pathogens 5(5):e1000426.

Masserini M, Palestini P, Pitto M (1999) Glycolipid-enriched caveolae and caveolae-like domains in the nervous system. Journal of Neurochemistry 73(1):1-11.

Mauerer R, Ebert S, Langmann T (2009) High glucose, unsaturated and saturated fatty acids differentially regulate expression of ATP-binding cassette transporters ABCA1 and ABCG1 in human macrophages. Experimental and Molecular Medicine 41:126-132.

Maulik M, Westaway D, Jhamandas JH, Kar S (2013) Role of Cholesterol in APP Metabolism and Its Significance in Alzheimer's Disease Pathogenesis. Molecular Neurobiology 47:37-63.

May P, Woldt E, Matz RL, Boucher P (2007) The LDL receptor-related protein (LRP) family: An old family of proteins with new physiological functions. Annals of Medicine 39:219-228.

Mays CE, Kim C, Haldiman T, van der Merwe J, Lau A, Yang J, Grams J, Di Bari MA, Nonno R, Telling GC, Kong QZ, Langeveld J, McKenzie D, Westaway D, Safar JG (2014) Prion disease tempo determined by host-dependent substrate reduction. Journal of Clinical Investigation 124:847-858.

Maxfield,FR, T E Mcgraw (2004) Endocytic recycling: Nature Reviews Molecular Cell Biology 5:121-132.

McEvoy K, McMahon HEM (2009) Antiprion action of new cyclodextrin analogues. Biochimica et Biophysica Acta-General Subjects 1790:1382-1386.

Mirza R, Hayasaka S, Takagishi Y, Kambe F, Ohmori S, Maki K, Yamamoto M, Murakami K, Kaji T, Zadworny D, Murata Y, Seo H (2006) DHCR24 gene knockout mice demonstrate lethal dermopathy with differentiation and maturation defects in the epidermis. Journal of Investigative Dermatology 126:638-647.

Mok SW, Thelen KM, Riemer C, Bamme T, Gultner S, Lutjohann D, Baier M (2006) Simvastatin prolongs survival times in prion infections of the central nervous system. Biochem Biophys Res Commun 348:697-702.

Morris RJ, Parkyn CJ, Jen A (2006) Traffic of prion protein between different compartments on the neuronal surface, and the propagation of prion disease. FEBS Letters 580(23):5565-71.

Murai T, Maruyama Y, Mio K, Nishiyama H, Suga M, Sato C (2011) Low Cholesterol Triggers Membrane Microdomain-dependent CD44 Shedding and Suppresses Tumor Cell Migration. Journal of Biological Chemistry 286:1999-2007.

Nakamura S, Ono F, Hamano M, Odagiri K, Kubo M, Komatsuzaki K, Terao K, Shinagawa M, Takahashi K, Yoshikawa Y (2000) Immunohistochemical detection of apolipoprotein E within prion-associated lesions in squirrel monkey brains. Acta Neuropathologica 100:365-370.

Narita M, Bu GJ, Holtzman DM, Schwartz AL (1997) The low-density lipoprotein receptor-related protein, a multifunctional apolipoprotein E receptor, modulates hippocampal neurite development. Journal of Neurochemistry 68:587-595.

Naslavsky N, Shmeeda H, Friedlander G, Yanai A, Futerman AH, Barenholz Y, Taraboulos A (1999) Sphingolipid depletion increases formation of the scrapie prion protein in neuroblastoma cells infected with prions. Journal of Biological Chemistry 274:20763-20771.

Naslavsky N, Stein R, Yanai A, Friedlander G, Taraboulos A (1997) Characterization of detergent-insoluble complexes containing the cellular prion protein and its scrapie isoform. J Biol Chem 272:6324-6331.

Naureckiene S, Sleat DE, Lackland H, Fensom A, Vanier MT, Wattiaux R, Jadot M, Lobel P (2000) Identification of HE1 as the second gene of Niemann-Pick C disease. Science 290:2298.

Nesic I, Guix FX, Vennekens K, Michaki V, Van Veldhoven PP, Feiguin F, De Strooper B, Dotti CG, Wahle T (2012) Alterations in phosphatidylethanolamine levels affect the generation of Abeta. Aging Cell 11:63-72.

Ng EL, Gan BQ, Ng F, Tang BL (2012) Rab GTPases regulating receptor trafficking at the late endosome-lysosome membranes. Cell Biochemistry and Function 30:515-523.

Nicholson AM, Ferreira A (2009) Increased Membrane Cholesterol Might Render Mature Hippocampal Neurons More Susceptible to beta-Amyloid-Induced Calpain Activation and Tau Toxicity. Journal of Neuroscience 29:4640-4651.

Nordstrom E, Fisone G, Kristensson K (2009) Opposing effects of ERK and p38-JNK MAP kinase pathways on formation of prions in GT1-1 cells. FASEB Journal 23:613-622.

Norman AW, VANDEENE.LL, Dekruyff B, Demel RA (1972) Studies on Biological Properties of Polyene Antibiotics - Evidence for Direct Interaction of Filipin with Cholesterol. Journal of Biological Chemistry 247:1918-&.

Nurenberg G, Volmer DA (2012) The analytical determination of isoprenoid intermediates from the mevalonate pathway. Analytical and Bioanalytical Chemistry 402:671-685.

Nygaard HB, Strittmatter SM (2009) Cellular prion protein mediates the toxicity of beta-amyloid oligomers: implications for Alzheimer disease. Archives of Neurology 66:1325-1328.

Obrig TG, Culp WJ, Mckeehan WL, Hardesty B (1971) Mechanism by Which Cycloheximide and Related Glutarimide Antibiotics Inhibit Peptide Synthesis on Reticulocyte Ribosomes. Journal of Biological Chemistry 246:174-&.

Oesch B, Westaway D, Walchli M, McKinley MP, Kent SBH, Aebersold R, Barry RA, Tempst P, Teplow DB, Hood LE, Prusiner SB, Weissmann C (1985) A Cellular Gene Encodes Scrapie Prp 27-30 Protein. Cell 40:735-746.

Ogundare M, Theofilopoulos S, Lockhart A, Hall LJ, Arenas E, Sjovall J, Brenton AG, Wang YQ, Griffiths WJ (2010) Cerebrospinal Fluid Steroidomics: Are Bioactive Bile Acids Present in Brain? Journal of Biological Chemistry 285:4666-4679.

Onodera R, Motoyama K, Okamatsu A, Higashi T, Kariya R, Okada S, Arima H (2013) Involvement of cholesterol depletion from lipid rafts in apoptosis induced by methyl-beta-cyclodextrin. International Journal of Pharmaceutics 452:116-123.

Onodera T, Sakudo A, Tsubone H, Itohara S (2014) Review of studies that have used knockout mice to assess normal function of prion protein under immunological or pathophysiological stress. Microbiology and Immunology 58:361-374.

Oram JF, Heinecke JW (2005) ATP-binding cassette transporter A1: A cell cholesterol exporter that protects against cardiovascular disease. Physiological Reviews 85:1343-1372.

Owen DM, Magenau A, Williamson D, Gaus K (2012) The lipid raft hypothesis revisited - New insights on raft composition and function from super-resolution fluorescence microscopy. Bioessays 34:739-747.

Pan KM, Baldwin MA, Nguyen J, Gasset M, Serban A, Groth D, Mehlhorn I, Huang Z, Fletterick RJ, Cohen FE, Prusiner SB (1993) Conversion of α-helices into β-sheets features in the formation of the scrapie prion proteins. Proceedings of the National Academy of Sciences USA 90:10962-10966.

Panza G, Luers L, Stohr J, Nagel-Steger L, Weibeta J, Riesner D, Willbold D, Birkmann E (2010) Molecular Interactions between Prions as Seeds and Recombinant Prion Proteins as Substrates Resemble the Biological Interspecies Barrier In Vitro. PLoS ONE 5:e14283.

Parkin ET, Watt NT, Hussain I, Eckman EA, Eckman CB, Manson JC, Baybutt HN, Turner AJ, Hooper NM (2007) Cellular prion protein regulates beta-secretase cleavage of the Alzheimer's amyloid precursor protein. Proceedings of the National Academy of Sciences USA 104:11062-11067.

Parkyn CJ, Vermeulen EG, Mootoosamy RC, Sunyach C, Jacobsen C, Oxvig C, Moestrup S, Liu Q, Bu G, Jen A, Morris RJ (2008) LRP1 controls biosynthetic and endocytic trafficking of neuronal prion protein. Journal of Cell Science 121(Pt 6):773-83.

Passet B, Halliez S, Beringue V, Laude H, Vilotte JL (2013) The prion protein family Looking outside the central nervous system. Prion 7:127-130.

Paulick MG, Bertozzi CR (2008) The Glycosylphosphatidylinositol Anchor: A Complex Membrane-Anchoring Structure for Proteins. Biochemistry 47(27):6991-7000.

Pauly PC, Harris DA (1998) Copper stimulates endocytosis of the prion protein. Journal of Biological Chemistry 273:33107-33110.

Pawar A, Botolin D, Mangelsdorf DJ, Jump DB (2003) The role of liver X receptor-alpha in the fatty acid regulation of hepatic gene expression. Journal of Biological Chemistry 278:40736-40743.

Peet DJ, Janowski BA, Mangelsdorf DJ (1998) The LXRs: a new class of oxysterol receptors. Current Opinion in Genetics & Development 8:571-575.

Peretz D, Scott MR, Groth D, Williamson RA, Burton DR, Cohen FE, Prusiner SB (2001) Strain-specified relative conformational stability of the scrapie prion protein. Protein Science 10:854-863.

Peri A, Serio M (2008) Neuroprotective effects of the Alzheimer's disease-related gene seladin-1. Journal of Molecular Endocrinology 41:251-261.

Persaud-Sawin DA, Lightcap S, Harry GJ (2009) Isolation of rafts from mouse brain tissue by a detergent-free method. Journal of Lipid Research 50:759-767.

Peters PJ, Mironov A, Jr., Peretz D, Van Donselaar E, Leclerc E, Erpel S, DeArmond SJ, Burton DR, Williamson RA, Vey M, Prusiner SB (2003) Trafficking of prion proteins through a caveolae-mediated endosomal pathway. Journal of Cell Biology 162:703-717.

Pfrieger FW (2003) Cholesterol homeostasis and function in neurons of the central nervous system. Cellular and Molecular Life Sciences 60:1158-1171.

Pfrieger FW, Ungerer N (2011) Cholesterol metabolism in neurons and astrocytes. Progress in Lipid Research 50:357-371.

Pillay CS, Elliott E, Dennison C (2002) Endolysosomal proteolysis and its regulation. Biochemical Journal 363:417-429.

Pitas RE, Boyles JK, Lee SH, Hui D, Weisgraber KH (1987) Lipoproteins and Their Receptors in the Central-Nervous-System - Characterization of the Lipoproteins in Cerebrospinal-Fluid and Identification of Apolipoprotein-B,E(Ldl) Receptors in the Brain. Journal of Biological Chemistry 262:14352-14360.

Plinston C, Hart P, Chong A, Hunter N, Foster J, Piccardo P, Manson JC, Barron RM (2011) Increased Susceptibility of Human-PrP Transgenic Mice to Bovine Spongiform Encephalopathy Infection following Passage in Sheep. Journal of Virology 85:1174-1181.

Plummer PJ (1946) Scrapie-A Disease of Sheep: A Review of the literature. Canadian journal of comparative medicine and veterinary science 10(2):49-54.

Plump AS, Azrolan N, Odaka H, Wu L, Jiang X, Tall A, Eisenberg S, Breslow JL (1997) ApoA-I knockout mice: Characterization of HDL metabolism in homozygotes and identification of a post-RNA mechanism of apoA-I up-regulation in heterozygotes. Journal of Lipid Research 38:1033-1047.

Plump AS, Scott CJ, Breslow JL (1994) Human Apolipoprotein-A-I Gene-Expression Increases High-Density-Lipoprotein and Suppresses Atherosclerosis in the Apolipoprotein E-Deficient Mouse. Proceedings of the National Academy of Sciences of the United States of America 91:9607-9611.

Poirier J, Minnich A, Davignon J (1995) Apolipoprotein E, synaptic plasticity and Alzheimer's disease. Annals of Medicine 27:663-670.

Portilho DM, Soares CP, Morrot A, Thiago LS, Butler-Browne G, Savino W, Costa ML, Mermelstein C (2012) Cholesterol depletion by methyl-beta-cyclodextrin enhances cell proliferation and increases the number of desmin-positive cells in myoblast cultures. European Journal of Pharmacology 694:1-12.

Prčina M, Kontseková E, Novák M (2015) Prion protein prevents heavy metals overloading of cells and thus protects them against their toxicity Acta Virology 59 (2): 179–84.

Prinz M, Montrasio F, Furukawa H, van der Haar ME, Schwarz P, Rulicke T, Giger OT, Hausler KG, Perez D, Glatzel M, Aguzzi A (2004) Intrinsic resistance of oligodendrocytes to prion infection. Journal of Neuroscience 24:5974-5981.

Prior M, Lehmann S, Sy MS, Molloy B, McMahon HE (2007) Cyclodextrins inhibit replication of scrapie prion protein in cell culture. Journal of Virology 81(20):11195-207.

Provansal M, Roche S, Pastore M, Casanova D, Belondrade M, Alais S, Leblanc P, Windl O, Lehmann S (2010) Proteomic consequences of expression and pathological conversion of the prion protein in inducible neuroblastoma N2a cells. Prion 4:292-301.

Prusiner SB (1982) Novel proteinaceous infectious particles cause scrapie. Science 216:136-144.

Prusiner SB (1998) Prions. Proceedings of the National Academy of Sciences USA 95:13363-13383.

Prusiner SB, Gabizon R, McKinley MP (1987) On the biology of prions. Acta Neuropathology (Berlin) 72:299-314.

Qi X, Moore RA, McGuirl MA (2012) Dissociation of Recombinant Prion Protein Fibrils into Short Protofilaments: Implications for the Endocytic Pathway and Involvement of the N-Terminal Domain. Biochemistry 51(22):4600-8.

Qi YP, Wang JKT, McMillian M, Chikaraishi DM (1997) Characterization of a CNS cell line, CAD, in which morphological differentiation is initiated by serum deprivation. Journal of Neuroscience 17:1217-1225.

Ramasamy I, Law M, Collins S, Brooke F (2003) Organ distribution of prion proteins in variant Creutzfeldt-Jakob disease. Lancet Infectious Disease 3:214-222.

Ramos MC, Sierra S, Ramirez C, Velasco J, Burgos JS (2012) Simvastatin Modulates the Alzheimer's Disease-Related Gene seladin-1. Journal of Alzheimers Disease 28:297-301.

Rapp A, Gmeiner B, Huttinger M (2006) Implication of apoE isoforms in cholesterol metabolism by primary rat hippocampal neurons and astrocytes. Biochimie 88:473-483.

Raymond GJ, Race B, Hollister JR, Offerdahl DK, Moore RA, Kodali R, Raymond LD, Hughson AG, Rosenke R, Long D, Dorward DW, Baron GS (2012) Isolation of Novel Synthetic Prion Strains by Amplification in Transgenic Mice Coexpressing Wild-Type and Anchorless Prion Proteins. Journal of Virology 86:11763-11778.

Re L, Rossini F, Re F, Bordicchia M, Mercanti A, Fernandez OSL, Barocci S (2006) Prion protein potentiates acetylcholine release at the neuromuscular junction. Pharmacological Research 53:62-68.

Refolo LM, Pappolla MA, Malester B, LaFrancois J, Bryant-Thomas T, Wang R, Tint GS, Sambamurti K, Duff K (2000) Hypercholesterolemia accelerates the Alzheimer's amyloid pathology in a transgenic mouse model. Neurobiology of Disease 7:321-331.

Ren SY, Johnson BG, Kida Y, Ip C, Davidson KC, Lin SL, Kobayashi A, Lang RA, Hadjantonakis AK, Moonc RT, Duffield JS (2013) LRP-6 is a coreceptor for multiple fibrogenic signaling pathways in pericytes and myofibroblasts that are inhibited by DKK-1. Proceedings of the National Academy of Sciences of the United States of America 110:1440-1445.

Rietveld A, Simons K (1998) The differential miscibility of lipids as the basis for the formation of functional membrane rafts Biochimica et Biophysica Acta - Reviews on Biomembranes 1376 (3): 467–79

Robinson SJ, Samuel MD, O'Rourke KI, Johnson CJ (2012). The role of genetics in chronic wasting disease of North American cervids. Prion. 6(2):153-62.

Runz H, Rietdorf J, Tomic I, de Bernard M, Beyreuther K, Pepperkok R, Hartmann T (2002) Inhibition of intracellular cholesterol transport alters presenilin localization and amyloid precursor protein processing in neuronal cells. Journal of Neuroscience 22:1679-1689.

Rushworth JV, Griffiths HH, Watt NT, Hooper NM (2013) Prion protein-mediated toxicity of amyloid-beta oligomers requires lipid rafts and the transmembrane LRP1. Journal of Biological Chemistry 288(13):8935-51.

Russell DW, Halford RW, Ramirez DMO, Shah R, Kotti T (2009) Cholesterol 24-Hydroxylase: An Enzyme of Cholesterol Turnover in the Brain. Annual Review of Biochemistry 78:1017-1040.

Saborio GP, Permanne B, Soto C (2001) Sensitive detection of pathological prion protein by cyclic amplification of protein misfolding. Nature 411:810-813.

Saher G, Brugger B, Lappe-Siefke C, Mobius W, Tozawa R, Wehr MC, Wieland F, Ishibashi S, Nave KA (2005) High cholesterol level is essential for myelin membrane growth. Nature Neuroscience 8:468-475.

Sandberg MK, Al Doujaily H, Sharps B, Clarke AR, Collinge J (2011) Prion propagation and toxicity in vivo occur in two distinct mechanistic phases. Nature 470:540-542.

Sankaranarayanan S, Kellner-Weibel G, Llera-Moya M, Phillips MC, Asztalos BF, Bittman R, Rothblat GH (2011) A sensitive assay for ABCA1-mediated cholesterol efflux using BODIPY-cholesterol. Journal of Lipid Research 52:2332-2340.

Sarkar S, Carroll B, Buganim Y, Maetzel D, Ng AHM, Cassady JP, Cohen MA, Chakraborty S, Wang HY, Spooner E, Ploegh H, Gsponer J, Korolchuk VI, Jaenisch R (2013) Impaired Autophagy in the Lipid-Storage Disorder Niemann-Pick Type C1 Disease. Cell Reports 5:1302-1315.

Sarnataro D, Campana V, Paladino S, Stornaiuolo M, Nitsch L, Zurzolo C (2004) PrPC association with lipid rafts in the early secretory pathway stabilizes its cellular conformation. Molecular Biology of the Cell 15:4031-4042.

Sarnataro D, Caputo A, Casanova P, Puri C, Paladino S, Tivodar SS, Campana V, Tacchetti C, Zurzolo C (2009) Lipid Rafts and Clathrin Cooperate in the Internalization of PrPC in Epithelial FRT Cells. PLoS ONE 4(6): e5829.

Saunders SE, Bartelt-Hunt SL, Bartz JC (2012) Occurrence, transmission, and zoonotic potential of chronic wasting disease. Emerging Infectious Diseases 18(3):369-76.

Schnitzer JE, Oh P, Pinney E, Allard J (1994) Filipin-Sensitive Caveolae-Mediated Transport in Endothelium - Reduced Transcytosis, Scavenger Endocytosis, and Capillary-Permeability of Select Macromolecules. Journal of Cell Biology 127:1217-1232.

Schroeder F, Holland JF, Bieber LL (1971) Fluorometric Evidence for Binding of Cholesterol to Filipin Complex. Journal of Antibiotics 24:846.

Schweitzer JK, Pietrini SD, D'Souza-Schorey C (2009) ARF6-Mediated Endosome Recycling Reverses Lipid Accumulation Defects in Niemann-Pick Type C Disease. PLoS ONE 4(4): e5193.

Shi Q, Zhang BY, Gao C, Zhang J, Jiang HY, Chen C, Han J, Dong XP (2012) Mouse-adapted scrapie strains 139A and ME7 overcome species barrier to induce experimental scrapie in hamsters and changed their pathogenic features. Virology Journal 9:63.

Shyng,SL, J E Heuser, D A Harris, 1994, A glycolipid-anchored prion protein is endocytosed via clathrin-coated pits: Journal of Cell Biology, v. 125, p. 1239-1250.

Shyng SL, Moulder KL, Lesko A, Harris DA (1995) The N-terminal domain of a glycolipid-anchored prion protein is essential for its endocytosis via clathrin-coated pits. Journal of Biological Chemistry 270:14793-14800.

Simons K, Ikonen E (1997) Functional rafts in cell membranes. Nature 387:569-572.

Simons K, Ikonen E (2000) Cell biology - How cells handle cholesterol. Science 290:1721-1726.

Simons K, Van Meer G (1988) Lipid Sorting in Epithelial-Cells. Biochemistry 27:6197-6202.

Sinensky M, Lutz RJ (1992) The Prenylation of Proteins. Bioessays 14:25-31.

Singh A, Haldar S, Horback K, Tom C, Zhou L, Meyerson H, Singh N (2013) Prion Protein Regulates Iron Transport by Functioning as a Ferrireductase. Journal of Alzheimers Disease 35(3):541-52.

Smith JD (2010) Apolipoprotein A-I and its mimetics for the treatment of atherosclerosis. Current Opinion in Investigational Drugs 11:989-996.

Sonnino S, Prinetti A (2013) Membrane domains and the "lipid raft" concept. Current Medical Chemistry 20(1):4-21.

Spann NJ, Garmire LX, McDonald JG, Myers DS, Milne SB, Shibata N, Reichart D, Fox JN, Shaked I, Heudobler D, Raetz CRH, Wang EW, Kelly SL, Sullards MC, Murphy RC, Merrill AH, Brown HA, Dennis EA, Li AC, Ley K, Tsimikas S, Fahy E, Subramaniam S, Quehenberger O, Russell DW, Glass CK (2012) Regulated Accumulation of Desmosterol Integrates Macrophage Lipid Metabolism and Inflammatory Responses. Cell 151:138-152.

Stahl N, Borchelt DR, Hsiao K, Prusiner SB (1987) Scrapie prion protein contains a phosphatidylinositol glycolipid. Cell 51:229-240.

Strickland DK, Kounnas MZ, Argraves WS (1995) Ldl Receptor-Related Protein - A Multiligand Receptor for Lipoprotein and Proteinase Catabolism. FASEB Journal 9:890-898.

Strittmatter WJ, Saunders AM, Schmechel D, Pericak Vance M, Enghild J, Salvesen GS, Roses AD (1993) Apolipoprotein E: high-avidity binding to beta-amyloid and increased frequency of type 4 allele in late-onset familial Alzheimer disease. . Proceedings of the National Acadedy of Sciences USA 90:1977-1981.

Sturley SL, Patterson MC, Balch W, Liscum L (2004) The pathophysiology and mechanisms of NP-C disease. Biochimica et Biophysica Acta-Molecular and Cell Biology of Lipids 1685:83-87.

Sugimoto Y, Ninomiya H, Ohsaki Y, Higaki K, Davies JP, Ioannou YA, Ohno K (2001) Accumulation of cholera toxin and GM1 ganglioside in the early endosome of Niemann-Pick C1-deficient cells. Proceedings of the National Academy of Sciences of the United States of America 98:12391-12396.

Sunyach C, Jen A, Deng J, Fitzgerald KT, Frobert Y, Grassi J, McCaffrey MW, Morris R (2003) The mechanism of internalization of glycosylphosphatidylinositol-anchored prion protein. EMBO Journal 22:3591-3601.

Suzuki KGN, Fujiwara TK, Sanematsu F, Iino R, Edidin M, Kusumi A (2007) GPI-anchored receptor clusters transiently recruit Lyn and G alpha for temporary cluster immobilization and Lyn activation: single-molecule tracking study 1. Journal of Cell Biology 177:717-730.

Tabas I (1995) The Stimulation of the Cholesterol Esterification Pathway by Atherogenic Lipoproteins in Macrophages. Current Opinion in Lipidology 6:260-268.

Taguchi Y, Shi ZD, Ruddy B, Dorward DW, Greene L, Baron GS (2008) Specific Biarsenical Labeling of Cell Surface Proteins Allows Fluorescent- and Biotin-tagging of APP and Prion Proteins. Molecular Biology of the Cell 20(1):233-44.

Tahir SA, Yang G, Goltsov A, Song KD, Ren CZ, Wang JX, Chang WJ, Thompson TC (2013) Caveolin-1-LRP6 Signaling Module Stimulates Aerobic Glycolysis in Prostate Cancer. Cancer Research 73:1900-1911.

Tanaka M, Collins SR, Toyama BH, Weissman JS (2006) The physical basis of how prion conformations determine strain phenotypes. Nature 442:585-589.

Taraboulos A, Scott M, Semenov A, Avraham D, Laszlo L, Prusiner SB (1995) Cholesterol depletion and modification of COOH-terminal targeting sequence of the prion protein inhibit formation of the scrapie isoform. Journal of Cell Biology 129:121-132.

Taylor DR, Hooper NM (2006) The prion protein and lipid rafts (Review). Molecular Membrane Biology 23:89-99.

Taylor DR, Hooper NM (2007) The low-density lipoprotein receptor-related protein 1 (LRP1) mediates the endocytosis of the cellular prion protein. Biochemical Journal 402:17-23.

Taylor DR, Whitehouse IJ, Hooper NM (2009) Glypican-1 mediates both prion protein lipid raft association and disease isoform formation. PLoS Pathogens 5:e1000666.

Thanh NX, Chuck AW, Ohinmaa A, Jacobs P (2012) Benefits of Pharmaceutical Innovation: the Case of Simvastatin in Canada. International Journal of Technology Assessment in Health Care 28:390-397.

Thellung S, Gatta E, Pellistri F, Corsaro A, Villa V, Vassalli M, Robello M, Florio T (2013) Excitotoxicity Through NMDA Receptors Mediates Cerebellar Granule Neuron Apoptosis Induced by Prion Protein 90-231 Fragment. Neurotoxicity Research 23:301-314.

Timmes AG, Moore RA, Fischer ER, Priola SA (2013) Recombinant prion protein refolded with lipid and RNA has the biochemical hallmarks of a prion but lacks in vivo infectivity. PLoS ONE 8:e71081.
Torres JM, Espinosa JC, Aguilar-Calvo P, Herva ME, Relano-Gines A, Villa-Diaz A, Morales M, Parra B, Alamillo E, Brun A, Castilla J, Molina S, Hawkins SAC, Andreoletti O (2014) Elements Modulating the Prion Species Barrier and Its Passage Consequences. PLoS ONE 9(3):e89722.
Tzaban S, Friedlander G, Schonberger O, Horonchik L, Yedidia Y, Shaked G, Gabizon R, Taraboulos A (2002) Protease-sensitive scrapie prion protein in aggregates of heterogeneous sizes. Biochemistry 41:12868-12875.
Ulven M, Dalen KT, Gustafsson JA, Nebb HI (2004) Tissue-specific autoregulation of the LXR alpha gene facilitates induction of apoE in mouse adipose tissue. Journal of Lipid Research 45:2052-2062.
Urist MR, Behnam K, Kerendi F, Bagga D, Adkisson HD, Nevenzel J, Malinin T (1997) Neutral lipids facilitate transfer of bone morphogenetic proteins and other noncollagenous proteins. Medical Hypotheses 49:465-475.
Vance JE (2006) Lipid imbalance in the neurological disorder, Niemann-Pick C disease. FEBS Letters 580:5518-5524.
Vance JE (2010) Transfer of Cholesterol by the NPC Team. Cell Metabolism 12:105-106.
Vandyke RW (1993) Acidification of Rat-Liver Lysosomes - Quantitation and Comparison with Endosomes. American Journal of Physiology 265:C901-C917.
Vanheyningen S (1976) Subunits of Cholera Toxin - Structure, Stoichiometry, and Function. Journal of Infectious Diseases 133:S5-S13.
Vanik DL, Surewicz KA, Surewicz WK (2004) Molecular basis of barriers for interspecies transmissibility of mammalian prions. Molecular Cell 14:139-145.
Verot L, Chikh K, Freydiere E, Honore R, Vanier MT, Millat G (2007) Niemann-Pick C disease: functional characterization of three NPC2 mutations and clinical and molecular update on patients with NPC2. Clinical Genetics 71:320-330.
Vey M, Pilkuhn S, Wille H, Nixon R, DeArmond SJ, Smart EJ, Anderson RGW, Taraboulos A, Prusiner SB (1996) Subcellular colocalization of the cellular and scrapie prion proteins in caveolae-like membranous domains. Proceedings of the National Academy of Science USA 93:14945-14949.
Vieira TCRG, Cordeiro Y, Caughey B, Silva JL (2014) Heparin binding confers prion stability and impairs its aggregation. FASEB Journal 28:2667-2676.
Waheed AA, Jones TLZ (2002) Hsp90 interactions and acylation target the G protein G alpha(12) but not G alpha(13) to lipid rafts. Journal of Biological Chemistry 277:32409-32412.
Wang F, Wang X, Yuan CG, Ma J (2010) Generating a prion with bacterially expressed recombinant prion protein. Science 327:1132-1135.
Warner M, Gustafsson JA (2015) Estrogen receptor beta and Liver X receptor beta: biology and therapeutic potential in CNS diseases. Molecular Psychiatry 20:18-22.
Waterham HR, Koster J, Romeijn GJ, Hennekam RCM, Vreken P, Andersson HC, Fitzpatrick DR, Kelley RI, Wanders RJA (2001) Mutations in the 3 beta-hydroxysterol Delta(24)-reductase gene cause desmosterolosis, an autosomal recessive disorder of cholesterol biosynthesis. American Journal of Human Genetics 69:685-694.
Watt NT, Griffiths HH, Hooper NM (2014) Lipid rafts: linking prion protein to zinc transport and amyloid-beta toxicity in Alzheimer's disease. Frontiers in Cellular Developmental Biology 2:41.
Watt NT, Taylor DR, Kerrigan TL, Griffiths HH, Rushworth JV, Whitehouse IJ, Hooper NM (2012) Prion protein facilitates uptake of zinc into neuronal cells. Nature Communications 3:1134.
Watts JC, Giles K, Patel S, Oehler A, DeArmond SJ, Prusiner SB (2014) Evidence That Bank Vole PrP Is a Universal Acceptor for Prions. Plos Pathogens 10(4):e1003990.
Weber T, Aguzzi A (1997) The spectrum of transmissible spongiform encephalopathies. Intervirology 40:198-212.
Wechsler A, Brafman A, Shafir M, Heverin M, Gottlieb H, Damari G, Gozlan-Kelner S, Spivak I, Moshkin O, Fridman E, Becker Y, Skaliter R, Einat P, Faerman A, Bjorkhem I, Feinstein E (2003) Generation of viable cholesterol-free mice. Science 302:2087-2087.

Weissmann C, Bueler H (2004) A mouse to remember. Cell 116:S111-113, 112.
Wollmer MA (2010) Cholesterol-related genes in Alzheimer's disease. Biochimica et Biophysica Acta-Molecular and Cell Biology of Lipids 1801:762-773.
Wu CW, Miloslavskaya I, Demontis S, Maestro R, Galaktionov K (2004) Regulation of cellular response to oncogenic and oxidative stress by Seladin-1. Nature 432:640-645.
Yang YT, Liao JD, Lin CCK, Chang CT, Wang SH, Ju MS (2012) Characterization of cholesterol-depleted or -restored cell membranes by depth-sensing nano-indentation. Soft Matter 8:682-687.
Ye ZJ, Go GW, Singh R, Liu WZ, Keramati AR, Mani A (2012) LRP6 Protein Regulates Low Density Lipoprotein (LDL) Receptor-mediated LDL Uptake. Journal of Biological Chemistry 287:1335-1344.
Yeganeh B, Wiechec E, Ande SR, Sharma P, Moghadam AR, Post M, Freed DH, Hashemi M, Shojaei S, Zeki AA, Ghavami S (2014) Targeting the mevalonate cascade as a new therapeutic approach in heart disease, cancer and pulmonary disease. Pharmacology & Therapeutics 143:87-110.
Yim YI, Park BC, Yadavalli R, Zhao XH, Eisenberg E, Greene LE (2015) The multivesicular body is the major internal site of prion conversion. Journal of Cell Science 128:1434-1443.
Yusa S, Oliveira-Martins JB, Sugita-Konishi Y, Kikuchi Y (2012) Cellular prion protein: from physiology to pathology. Viruses 4:3109-3131.
Zeng LF, Liao HL, Liu Y, Lee TS, Zhu MJ, Wang X, Stemerman MB, Zhu Y, Shyy JYJ (2004) Sterol-responsive element-binding protein (SREBP) 2 down-regulates ATP-binding cassette transporter A1 in vascular endothelial cells - A novel role of SREBP in regulating cholesterol metabolism. Journal of Biological Chemistry 279:48801-48807.
Zerbinatti CV, Bu GJ (2005) LRP and Alzheimer's disease. Reviews in the Neurosciences 16:123-135.
Zerenturk EJ, Sharpe LJ, Ikonen E, Brown AJ (2013) Desmosterol and DHCR24: Unexpected new directions for a terminal step in cholesterol synthesis. Progress in Lipid Research 52:666-680.
Zha XH, Gauthier A, Genest J, McPherson R (2003) Secretory vesicular transport from the golgi is altered during ATP-binding cassette protein A1 (ABCA1)-mediated cholesterol efflux. Journal of Biological Chemistry 278:10002-10005.
Zhou F, Millhauser GL (2012) The Rich Electrochemistry and Redox Reactions of the Copper Sites in the Cellular Prion Protein. Coordinated Chemistry Reviews 256:2285-2296.
Zhu D, Xiong WC, Mei L (2006) Lipid rafts serve as a signaling platform for nicotinic acetylcholine receptor clustering. Journal of Neuroscience 26:4841-4851.
Zhu YZ, Cao MM, Wang WB, Wang W, Ren H, Zhao P, Qi ZT (2012) Association of heat-shock protein 70 with lipid rafts is required for Japanese encephalitis virus infection in Huh7 cells. Journal of General Virology 93:61-71.
Zuliani G, Donnorso MP, Bosi C, Passaro A, Dalla Nora E, Zurlo A, Bonetti F, Mozzi AF, Cortese C (2011) Plasma 24S-hydroxycholesterol levels in elderly subjects with late onset Alzheimer's disease or vascular dementia: a case-control study. British Medical Council Neurology 11:121.

Appendix 1 – Abstract and citation for 'Identification of a gene regulatory network associated with prion replication.'

During my PhD I was privileged to work closely with the others in our research group, leading to publication of research not shown in this thesis in EMBO Journal. The abstract and publication information are presented here to support my PhD candidacy and to acknowledge the fantastic contributions made by my co-authors in this study.

Identification of a gene regulatory network associated with prion replication

Masue M Marbiah† Anna Harvey†, Billy T West†, Anais Louzolo, Priya Banerjee, Jack Alden, Anita Grigoriadis, Holger Hummerich, Ho-Man Kan, Ying Cai, George S Bloom, Parmjit Jat, John Collinge & Peter-Christian Klöhn

†Authors contributed equally to this work.

DOI 10.15252/embj.201387150 | Received 14 October 2013 | Revised 13 March 2014 | Accepted 15 April 2014

Abstract

Prions consist of aggregates of abnormal conformers of the cellular prion protein (PrP^C). They propagate by recruiting host-encoded PrP^C although the critical interacting proteins and the reasons for the differences in susceptibility of distinct cell lines and populations are unknown. We derived a lineage of cell lines with markedly differing susceptibilities, unexplained by PrP^C expression differences, to identify such factors. Transcriptome analysis of prion-resistant revertants, isolated from highly susceptible cells, revealed a gene expression signature associated with susceptibility and modulated by differentiation. Several of these genes encode proteins with a role in extracellular matrix (ECM) remodelling, a compartment in which disease-related PrP is deposited. Silencing nine of these genes significantly increased susceptibility. Silencing of *Papss2* led to undersulphated heparan sulphate and increased PrP^C deposition at the ECM, concomitantly with increased prion propagation. Moreover, inhibition of fibronectin 1 binding to integrin α8 by RGD peptide inhibited metalloproteinases (MMP)-2/9 whilst increasing prion propagation. In summary, we have identified a gene regulatory network associated with prion propagation at the ECM and governed by the cellular differentiation state.